Progress Report 1989-1990

[unknown], [unknown]

1990

BIENNIAL REPORT
1989-90

Division of Atomic Physics
Lund Institute of Technology
P.O. Box 118
S-221 00 Lund
SWEDEN

Lund Reports on Atomic Physics
LRAP-119

CONTENTS

TEACHING PROGRAM:

INTRODUCTION

The Division of Atomic Physics, Lund Institute of Technology (LTH), is responsible for the basic physics teaching at all sections of LTH and for specialised teaching in Optics, Atomic Physics, Atomic and Molecular Spectroscopy and Laser Physics. The Division has research activities in basic and applied optical spectroscopy, to a large extent based on lasers. It is also part of the Physics Department, Lund University, where it forms one of seven divisions. Since the beginning of 1980 the research activities of our division have been centred around the use of lasers. The activities during the 1980 - 1988 period have been described in previous Biennial Progress Reports (Lund Reports on Atomic Physics LRAP-20, LRAP-43, LRAP-85 and LRAP-90). During the last two years the research programme has been further expanded.

Some important developments have occurred which will have a profound effect on the Atomic Physics Division. The formation of the "Lund Laser Center" has been proposed with a strengthening of existing fields of research and the establishment of additional activities in the field of lasers and spectroscopy. Several new professorships have also been proposed. The proposal of a Laser Center has been supported by the University Administration and the building-up process is in progress. A new professorship in Atomic Physics (especially optical spectroscopy with technical applications) has been established and Dr Willy Persson has been appointed to the position. A new professorship in Combustion Diagnostics with Laser Techniques has been funded by the Swedish Board for Technical Development (STU) and the Swedish Energy Authority (SEV) for a 5-year period, later to be taken over by the University. A dedicated governmental annual allocation of 1 million SEK has been approved for the operation of the Lund Laser Center. Very recently, the Knut and Alice Wallenberg Foundation allocated 7 million SEK as a first investment for a proposed high-power laser facility in Lund.

The Atomic Physics Division is also co-founder of two new "non-material" centers for the coordination of research in the environmental measurements area and in medical laser utilization. The Environmental Measurement Techniques Center (CENTEC), which was proposed jointly with 4 other divisions at the Lund Institute of Technology, has now been established, while the Lund University Medical Laser Center, proposed jointly with 18 clinical departments, is presently under consideration. The Combustion Center (FTC) was established 5 years ago. Basic atomic- and laser physics in Lund is now efficiently interacting through three centers; in the fields of energy, the environment and medicine, respectively. This structure is illustrated in the figure.

The High-Power Laser Facility, including a planned terawatt system, is also indicated with its National Steering Group. The high-power activities will be connected both to our basic atomic physics research section and to a proposed section for Quantum Electronics, headed by a new professor. Current planning also includes a professorship in Medical Laser Physics and, at some future date, also a professorship in Chemical Laser Physics.

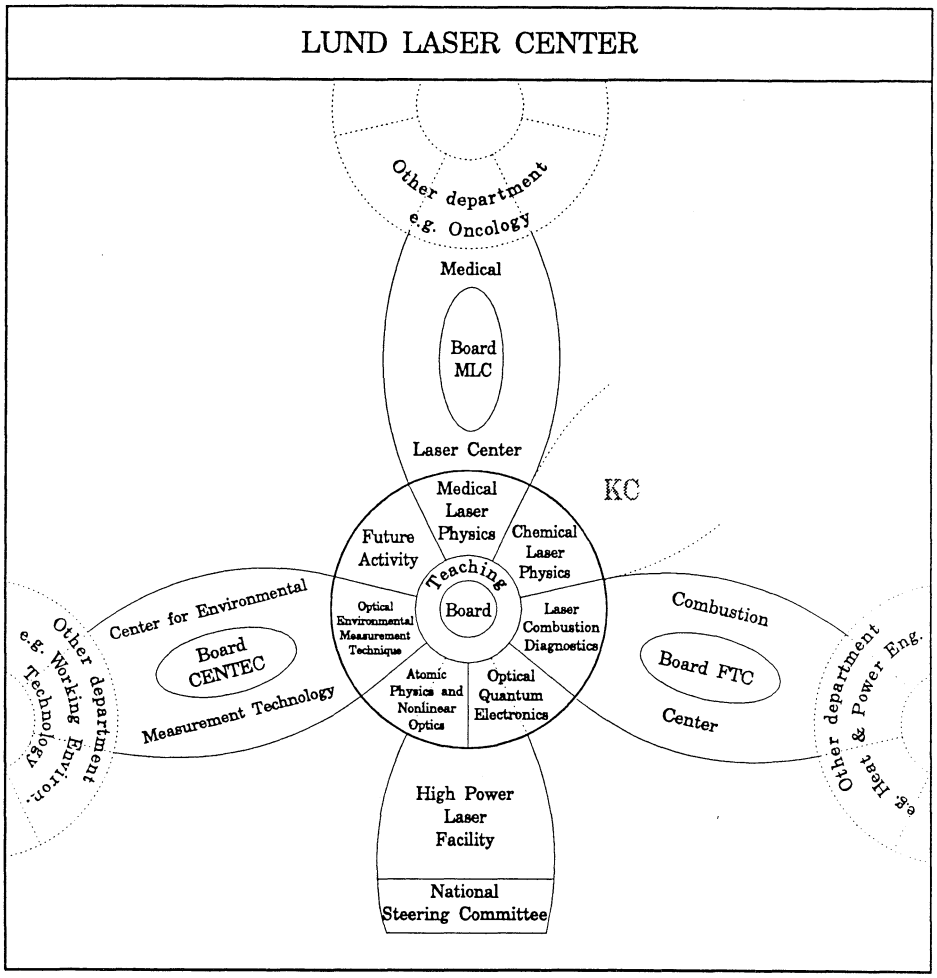

Two major issues related to the Lund Laser Center remain to be solved. The most important one is the financing of a dedicated new laboratory building, and the vice chancellor's office of Lund University is actively seeking solutions. The second issue is the establishment of an appropriate departmental structure in view of the expanding activities.

After this brief sketch of the structural developments related to the Atomic Physics Division, our ongoing research activities will be briefly commented upon.

Research on emission spectroscopy and term analysis, a classical field for atomic physics in Lund, is being pursued with emphasis on the analysis of the spectra of multiply ionized inert gases. The study of such ions is strongly motivated by their importance in laser and collisional physics and for interesting interplay with theory in the interpretation of the spectra. This programme is supported by the Swedish Natural Science Research Council (NFR).

In the basic atomic laser spectroscopy group the experimental activities employing CW high-resolution techniques and time-resolved methods are well integrated with a theoretical atomic physics programme. The activities are supported by the Swedish Natural Science

Research Council. During the last two years the activities have concentrated on light non-metallic elements, such as nitrogen and silicon, the light alkali atoms lithium and sodium, and, very extensively, the copper and silver atoms.

A precision method for lifetime measurements using a mode-locked dye laser in conjunction with photon counting techniques has been further refined to allow critical tests of accurate theoretical calculations. Pulsed level-crossing, optical-double-resonance and quantum-beat spectroscopy have been used extensively to attain new accurate data using pulsed lasers at very short excitation wavelengths. In particular, the copper, silver and ytterbium atoms have been studied. A programme for studying light elements, normally occurring as molecules, has been initiated. Simultaneous photodissociation production of free atoms and spectroscopic investigation is performed using pulsed lasers. Static and dynamic properties of saturation spectroscopy have also been studied.

In a project supported by the Research Council of the Swedish Board for Technical Development (STUF) gain in CO molecules has been investigated experimentally and theoretically. Gain has also been observed at short wavelengths in a recombining Al plasma.

In the field of theoretical atomic physics work has been focused on the application of the multi-configuration Hartree-Fock method for the calculation of radiative properties and hyperfine structure. The development of a general hyperfine structure calculation code constitutes a highlight in this work.

The Division is expanding its activities in the field of optical quantum electronics. An experiment demonstrating coherent harmonic generation at the MAX synchrotron undulator has been performed using a Nd:YAG laser. Studies of terawatt laser generation techniques have been made in preparation for the establishment of such techniques at the Lund Laser Center. A new STUF-supported project concerning optical photon echo techniques for information storage has been initiated in cooperation with the Stanford Research Institute. In another new project, supported by NFR and STU, new microscopy techniques are being developed based on soft X-rays, tomography and gradient imaging.

Several projects within applied laser spectroscopy are being pursued. For several years, a major project concerned with combustion diagnostics using lasers has been pursued in Lund, supported by STU and the Swedish Energy Board (STEV). Most of these activities are now being pursued within the Combustion Center headed by Dr M. Aldén. Most of the graduate students active within the Centre are enrolled in the Division of Atomic Physics. Many aspects of flame kinetics, NO_x and soot formation, turbulence and spark ignition are being studied using laser-induced fluorescence, Raman and CARS spectroscopy. Theoretical work on kinetics and spark ignition supplements the extensive programme. A close coupling to industry is maintained through special projects and the Center participates in several joint European programmes.

An additional STU-funded combustion spectroscopy programme is being pursued at the Division in coordination with our other spectroscopic programmes. Methods for combustion diagnostics based on multicolour imaging, degenerate four-wave mixing and diode-laser frequency-modulation spectroscopy are being developed.

Environmental remote sensing using optical techniques is another applied spectroscopy project. The programme includes the development of new optical measurement techniques for air pollution monitoring and field experiments to facilitate the transfer of technology to practical applications in industry and air quality management. Our mobile lidar system has been extensively used for range-resolved mapping of atomic mercury. The work includes studies of emissions from industries and crematoria, but have their main focus on geophysical aspects. Extensive field experiments were performed in Italian geothermal fields and mining areas in close cooperation with Italian researchers.

A vertically sounding ozone lidar system has been constructed and tested. The system, which provides vertical profiles for the troposphere, was developed within the framework of the EUREKA project EUROTRAC. This project also includes the development of powerful techniques for differential optical absorption spectroscopy (DOAS). A research doas system overlooking the city of Lund is providing data over three different paths which are selected under computer control. Celestial objects can also be tracked and used as natural light-sources.

A fluorescence lidar system has been tested which provides remote data on vegetation and water. Our project is part of the EUROMAR and the LASFLEUR cooperations within EUREKA. Successful field tests were performed in Italian beech forests and at the Arno river.

Basic research in remote sensing is supported by the Swedish Board for Space Activities (DFR) while applied work is supported by the Swedish Environmental Protection Board (SNV). Close cooperation with the Swedish Environmental Research Institute (IVL) in Göteborg is maintained. Environmental measurement techniques have been made practically available through a spin-off company, OPSIS AB, under the directorship of two former group members.

In a further spectroscopic project of industrial interest optical diagnostics techniques in connection with ore smelting and processing are being developed. The techniques may have a major impact on the metal industry. Geogas studies, including mercury vapour monitoring, are also being pursued with an interesting potential for mineral prospecting. Through a spin-off company (SEMTECH AB) with participation of division members these new developments can be made practically available.

During the last two years our activities in the medical field have increased. A research programme on cancer tumour detection and treatment using lasers is being pursued jointly with the Lund University Hospital. A multi-colour fluorescence imaging system for cancer detection has been developed using the spectroscopic information provided by endogenous chromophores and added photosensitizers, such as hemato-

porphyrin derivatives. A powerful laser system for photodynamic cancer treatment has been acquired for joint work with clinical departments.

Work on spectroscopic diagnostics of atherosclerotic plaque is also being actively pursued, aiming at spectroscopic guidance in fibre-optic plaque ablation using excimer laser radiation. Measurements have been performed during open-heart surgery. Time-resolved measurements using fast pulse techniques are being increasingly more utilized. In this context the MAX synchrotron radiation facility in Lund has also been used. The time-resolved techniques are also being employed for gated optical transillumination of tissue eliminating the traditional multiple-scattering problems. The medical spectroscopy programme is supported by the Swedish Cancer Foundation (RmC), The Swedish Medical Research Council (MFR) and STU. These techniques are made practically available for clinical work through a new spin-off company, Spectraphos AB.

In our report series "Lund Reports on Atomic Physics" (LRAP) material which is not published in international journals is presented. The reports include dissertations, diploma papers and special investigations. So far about 120 papers have appeared. At the end of the period covered by this progress report the staff of the Division totalled 51. This number includes 20 graduate students and 13 supporting personnel. In addition about 10 diploma students perform their projects within our division every year. It is through the dedicated work of these people that the research and teaching accomplishments reported here have been made.

We are very grateful for the support of various funding agencies, in particular the Swedish Natural Science Research Council (NFR), the Swedish Board for Technical Development (STU and STUF), the Swedish Energy Authority (SEV), the Swedish Board for Space Activities (DFR), the Swedish Environmental Protection Board (SNV), the Swedish Cancer Society (RmC), the Swedish Medical Research Council (MFR) and the Knut and Alice Wallenberg Foundation.

Special thanks are due to Dr Hans Hertz, who has invested a great deal of time, patience and skill in serving as the editor of this progress report.

Sune Svanberg

Head of the Division of Atomic Physics

STAFF

Head of Division:
Prof. Sune Svanberg

Emeritus Prof. Lennart Minnhagen

Deputy Head:
Prof. Willy Persson

Adjoint Professor:
Prof. Thure Högberg
(Head, Combustion Centre) - June 1990

University lecturers:
Docent Elvir Andersson, dean
Dr Stig Borgström
Dr Bodil Jönsson
Docent Gilbert Jönsson
Docent Göran Jönsson
Docent Rune Kullberg
Dr Sven-Göran Pettersson

Senior scientists:
Docent Marcus Aldén (Head, Combustion Centre) July 1990 -
Docent Stefan Kröll
Docent Hans Lundberg

Post-doctoral researchers:
Dr Stefan Andersson-Engels
Dr Hans Edner
Dr Hans Hertz
Dr Claes-Göran Wahlström

Graduate students:
Sara Agrup, M.Sc.(Tech.)
Jonas Bengtsson, M.Sc. (Tech.)
Per-Erik Bengtsson, M.Sc.(Tech.)
Roger Berg, M.Sc.(Tech.)
Håkan Bergström, M.Sc.(Tech.)
Jörgen Carlsson, M.Sc.(Tech.)
Bo Galle[a], M.Sc.(Tech.)
Jonas Johansson, M.Sc.(Tech.)
Per Jönsson, M.Sc.
Peter Kauranen, M.Sc.(Tech.)
Jörgen Larsson, M.Sc. (Tech.)
Lars Martinsson, M.Sc. (Tech.)
Hans Neij, M.Sc. (Tech.)
Anders Persson, M.Sc.(Tech.)
Pär Ragnarson, M.Sc.(Tech.)
Lennart Sturesson, M.Sc.(Tech.)
Svante Wallin[b], M.Sc.(Tech.)
Eva Wallinder, M.Sc.(Tech.)
Wilhelm Wendt[c], M.Sc.(Tech.)
Ulf Westblom, M.Sc.(Tech.)

Diploma and project students:
Roger Berg
Lars Eyrich
Magnus Haake
Tomas Karlsson
Olof Lindblad
Lars Malmqvist
Hans Neij
Anders Nilsson
Johan Olsson
Lars Rymell
Stefan Spännare
Johan Sääw
Ola Widlund
Sven Andrae

Technical staff:

Margareta Arnwald
Åke Bergqvist
Lars Gramstad
Bertil Hermansson
Carin Holmqvist
Jan Hultqvist
Gunnel Mattsson
Lennart Nilsson
Jan Olsson
Per Olsson
Georg Romerius
Göran Werner

Guest researchers:

Prof. Jiang Zhankui (Jilin University)
Dr Wang Dadi (Acad. Sci. Beijing)
Prof. Ma Bao Zhang (Shanghai Med. Univ.)
Dr Wolfgang Schade (Kiel University)

Ph.D. Theses:

Stefan Andersson-Engels	1990-01-26	Laser-Induced Fluorescence for Medical Diagnostics.
Jörgen Carlsson	1990-09-28	Excited States of Free Atoms in the Dimension of Time.
Anders Persson	1990-11-09	Laser Spectroscopic Techniques Applied to the Study of Excited States of Free Atoms, Ions and Molecules.

Licenciat Examination:

Hans Hallstadius	1989-04-14	Studies of Laser Generated Vacuum Ultraviolet Radiation and Spectroscopic Investigations of Light Elements in Laser-Produced Plasmas.

a) External student. Address: Swedish Environmental Research Institute, P.O. Box 47086, S-402 58 Göteborg
b) External student. Address: OPSIS AB, Idéon, S-223 70 Lund.
c) External student. Address: Semtech AB, Idéon, S-223 70 Lund

FIELDS OF RESEARCH - PERSONNEL
DECEMBER 1990

DIVISION OF ATOMIC PHYSICS
LUND INSTITUTE OF TECHNOLOGY
Head: S. Svanberg
Deputy head: W. Persson

EMISSION SPECTROSCOPY	ATOMIC LASER SPECTROSCOPY	COMBUSTION DIAGNOSTICS	ATMOSPHERIC OPTICAL REM. SENSING	MEDICAL AND INDUSTRIAL SPECTR. APPL.
W. PERSSON	H. LUNDBERG	M. ALDÉN	H. EDNER	S. ANDERSSON-E.
L. MINNHAGEN	C-G WAHLSTRÖM	T. HÖGBERG	B. GALLE	R. BERG
S-G PETTERSSON	G. JÖNSSON	S. KRÖLL	E. WALLINDER	J. JOHANSSON
	J. CARLSSON	S. AGRUP	S. WALLIN	S. BORGSTRÖM
	G. J. BENGTSSON	P-E BENGTSSON	P. RAGNARSON	H. HERTZ
	H. BERGSTRÖM	L. MARTINSSON		W. WENDT
	P. JÖNSSON	H. NEIJ		(W. PERSSON)
	J. LARSSON	U. WESTBLOM		
	A. PERSSON			
	L. STURESSON			
	P. KAURANEN			
	D. WANG			

35 Research Personnel (14 Ph.D., 20 Grad. Students, 1 Visitor)
14 Ext. Positions
7 Post-graduate Fellowships
Total Personnel, Div. of Atomic Physics: 50

1. EMISSION SPECTROSCOPY

Lennart Minnhagen, Willy Persson, Sven-Göran Pettersson, Claes-Göran Wahlström

Studies of the emission spectra of low and intermediate ionization stages of the rare gases, discussed in preceding progress reports, have been continued. The investigation of the spectrum of doubly ionized neon has been completed [1.1]. In the longlasting collaboration with the spectroscopy groups in La Plata (Argentina) and Campinas (Brazil) interest has been directed towards the spectra of various ionization stages of krypton. Since the preceding progress report the main efforts of the emission spectroscopy group have been directed towards novel applications of emission spectroscopy in natural and industrial processes. This work will be discussed separately in sections 7A and 7B.

The spectra of krypton in the VUV region were recorded in Lund using a theta-pinch discharge and in La Plata using a discharge tube with inner electrodes. The sources have provided spectra from Kr III to Kr VIII. The analysis of the data recorded is in progress. So far, results have been reported for Kr VIII [1.2], Kr VII [1.3] and Kr V [1.4].

The analysis of the spectrum of singly ionized oxygen, O II, discussed in the preceding progress report, has now been completed and published [1.5].

References

1.1. W. Persson, C.-G. Wahlström, L. Jönsson and H.O. Di Rocco, The Spectrum of Doubly Ionized Neon, submitted.

1.2. M. Gallardo, F. Bredice, M. Raineri, J. Reyna Almandos, S.-G. Pettersson and A.G. Trigueiros, New Spectroscopic Results in Kr VIII, Appl. Opt. **28**, 5088 (1989).

1.3. A.G. Trigueiros, S.-G. Pettersson, J.G. Reyna Almandos and M. Gallardo, A Study of the Configurations 4s5s and 4s5p in Six Times Ionized Krypton (Kr VII), Phys. Lett. A **141**, 135 (1989).

1.4. A.G. Trigueiros, C.J.B. Pagan, S.-G. Pettersson and J.G. Reyna Almandos, Transitions and Energy Levels in the n=4 complex of Kr V, Phys. Rev. A **40**, 3911 (1989).

1.5. S.-G. Pettersson and I. Wenåker, Vacuum-ultraviolet Lines in the Spectrum of O II, Physica Scripta **42**, 187 (1990).

2. BASIC ATOMIC PHYSICS

Jonas Bengtsson, G. Jonas Bengtsson, Håkan Bergström, Jörgen Carlsson, Hans Hallstadius, Jiang Zhankui*, Per Jönsson, Jörgen Larsson, Hans Lundberg, Anders Persson, Lennart Sturesson, Sune Svanberg, Claes-Göran Wahlström, Wang Dadi*

* visiting scientist

Many different research activities in the field of basic atomic physics are pursued within the division, including laser spectroscopic studies of excited atomic states, studies using laser-produced plasmas and theoretical calculations. The investigation of radiative properties - such as lifetimes - and hyperfine structures of free atoms is an important aspect of the work. During the last few years much of our interest has been directed towards alkali atoms and copper and silver atoms. These all have one electron outside closed shells but they also show interesting correlation effects between the valence electron and the electrons in the closed shells. These effects can be quite subtle, as in lithium and sodium, or totally dominating as in copper. In either case, it is necessary to combine accurate experiments and *ab initio* theory to gain an understanding of the atom. Another group of atoms that has been studied are the light, non-metallic elements. These are of general theoretical interest, since they allow accurate calculations. On the experimental side our main efforts have been aimed at making more accurate time-resolved measurements and at spectroscopy at shorter wavelengths. The simultaneous generation of free non-metallic atoms and the spectroscopy is another point of focus. The experiments are supported by *ab initio* calculations using the multi-configuration Hartree-Fock method.

During the last two-year period our work has resulted in two Ph.D. theses [2.1-2.2]. Much of the work has been presented at international conferences for atomic physics and spectroscopy [2.3-9]. The basic and applied spectroscopic work of the Atomic Physics Division has been exposed in a newly published book [2.10].

In order to promote new projects, two of the group members have spent longer periods at other laboratories. Dr Claes-Göran Wahlström has spent a year working with Professor Hutchinson's group at the high-power laser facility at Imperial College, London. The main emphasis was put at the experimental and theoretical study of high harmonic generation. Per Jönsson has spent half a year at Professor Charlotte Froese Fischer's department in Nashville, working with the MCHF atomic structure theory.

2A. Theoretical atomic physics

For several years much of the theoretical activities of the group have been concerned with lifetimes of excited states; lifetimes which have been calculated with the multi-configuration Hartree-Fock method. Parallel to these activities an increasing interest has lately been focused on the calculation of hyperfine structures. There are two reasons for this. One is, of course, that atomic hyperfine structure

is extensively experimentally studied in the group. A second reason is that the potential of the MCHF method in calculating hyperfine structures has not before been properly examined.

Under high resolution, the fine-structure levels of an isotope with non-zero nuclear spin are each split into a set of hyperfine structure levels. This effect is attributed to the interaction between the electrons and the electromagnetic multipole moments of the nucleus. The contribution to the electronic Hamiltonian can be represented by an expansion in multipoles of order k,

$$H_{hfs} = \sum_{k>0} T^k \cdot M^k$$

where T^k and M^k are spherical tensor operators of rank k in the electronic and nuclear space, respectively. The k=1 term accounts for the interaction of the nuclear magnetic dipole moment with the magnetic field created at the nucleus by the atomic electrons. The k=2 term accounts for the interaction of the nuclear electric quadrupole moment with the inhomogeneous electric field produced by the electrons. Higher order terms are much smaller and can often be neglected.

When the hyperfine contribution is included in the Hamiltonian, the wavefunction representation for which the Hamiltonian is diagonal is $|\gamma_I \gamma_J IJFM_F>$, where **F = I + J**. In this representation, first-order perturbation theory gives the following hyperfine energy correction to the fine-structure level

$$E_{hfs}(J) = \frac{1}{2} A_J C + B_J \frac{\frac{3}{4} C(C+1) - I(I+1)J(J+1)}{2I\,(2I-1)J\,(2J-1)}$$

where

$$A_J = <\gamma_J JJ|T^1_0|\gamma_J JJ><\gamma_I II|M^1_0|\gamma_I II>/IJ,$$

$$B_J = 4<\gamma_J JJ|T^2_0|\gamma_J JJ><\gamma_I II|M^2_0|\gamma_I II>$$

and

$$C = F(F+1) - J(J+1) - I(I+1).$$

Since the hyperfine structure depends on properties of both the nucleus and the electrons, investigations can give information on nuclear properties as well as on atomic structure. In order to evaluate nuclear quantities from hyperfine structure measurements the electronic parts of the interaction must be calculated. This can be done with a newly written hyperfine structure program [2A.1]. The program is a part of the MCHF atomic structure package of Charlotte Froese Fischer [U.S. Department of Energy Report No. DOE/ER/10618-11, 1983 (unpublished)] and adheres to the structure and constraints underlying the package.

A special feature of the program is that it allows for a limited degree of non-orthogonality between orbitals in the configuration state expansion. The use of non-orthogonal orbitals has been shown to be effective for the study of electron correlation where relativistic effects are small. Since correlation effects, in many cases, have an appreciable effect on the hyperfine structure, the MCHF method should

be an effective method in these cases. Relativistic corrections may be included through the Breit-Pauli (BP) approximation. A large group of atomic structure problems has been studied with the MCHF and MCHF+BP method. Together with the hyperfine program this should provide a versatile general purpose method for the study of hyperfine structures.

An interesting and difficult problem, which has been studied with the aid of these programs, is the hyperfine structure of the odd states of ^{63}Cu [2A.2]. The hyperfine structure of the 4p $^2P_{1/2,3/2}$ states has previously been studied using many-body perturbation theory [J-L. Heully, Z. Phys. **A319,** 253 (1984)] giving $A(^2P_{1/2})$ = 440 MHz, in good agreement with the experimental value of 507 MHz. The result $A(^2P_{3/2})$ = 83 MHz, however, is far from the experimental value of 195 MHz. No explanation was found for the discrepancy. Using the MCHF method with non-orthogonal orbitals in a 28 configuration wave function expansion we obtained $A(^2P_{1/2})$ = 480 MHz and $A(^2P_{3/2})$ = 157 MHz, showing that the core-polarization effects and the important configuration interaction with the $3d^9$4s4p states had been handled in an effective way. Further up in the ^2P sequence this configuration interaction has a drastic effect on the hyperfine structure. Such effects have already been pointed out in our study of the lifetimes and fine-structure splittings of the copper atom [Phys. Rev. **A38,** 1702 (1988)] and the effects on the hyperfine structure are equally pronounced.

2B. Saturation spectroscopy

Hyperfine structure and isotope shifts have been measured in the two isotopes of copper [2B.1]. The aim of this work was to compare two different high-resolution techniques utilizing a hollow-cathode discharge for the production of copper atoms in the metastable $3d^94s^2\ ^2D$ states. The methods compared were Doppler-free saturation spectroscopy on a hollow-cathode discharge and fluorescence spectroscopy on a collimated atomic beam produced by a hollow-cathode discharge. In Figure 2B.1 hyperfine spectra recorded from the same transition using the two methods are shown. During these experiments a program package was developed [2B.2]. This has been used for data collection, curve fitting and evaluation of the spectra shown in Figure 2B.1.

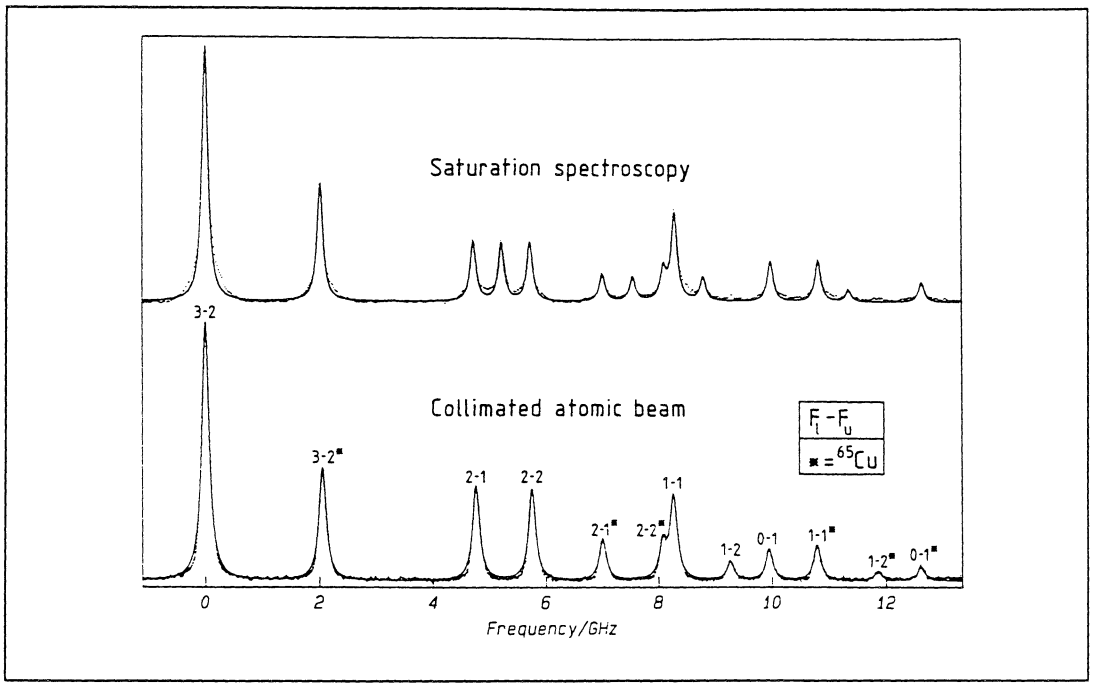

Fig. 2B.1. Experimental recordings of a transition in copper using two different high-resolution techniques.

Recently, the high-contrast transmission version of saturated absorption laser spectroscopy was introduced [S. Svanberg *et al.*, Opt. Lett. **10**, 597 (1986), S. Svanberg *et al.*, J. Opt. Soc. Am. **B4**, 462 (1987)]. In normal saturated absorption spectroscopy a gaseous sample of moderate absorption is used and a rather weak pumping beam is used to avoid power broadening of the Doppler-free signal. Correspondingly, only relatively small changes in the transmission of the probe beam are observed, giving rise to a need for techniques based on lock-in detection, since dye lasers are rather noisy light sources. A different approach is to use the high-contrast transmission spectroscopy method, where the probe beam is normally totally blocked by a very dense sample, only to be transmitted at the line centre, where a strong, saturating beam bleaches a path straight through the otherwise opaque sample. Since the wings of the Doppler-free signal are more strongly attenuated than the central part, narrow, even sub-natural linewidths can be obtained at the same time as extreme contrast (background rejection) is attainable.

A study of systematic shifts in high-contrast transmission spectroscopy has been performed on the D_1 line of sodium [2B.3]. The experimental set-up is illustrated in Figure 2B.2. The cell containing sodium vapour was placed in a simple oven. A thermometer with a resolution of 0.1 °C was attached to the coldest part of the cell. The laser beam was given a top-hat intensity distribution passing an aperture. After traversing the cell the transmitted pump beam was reflected by a mirror and used as a probe beam.

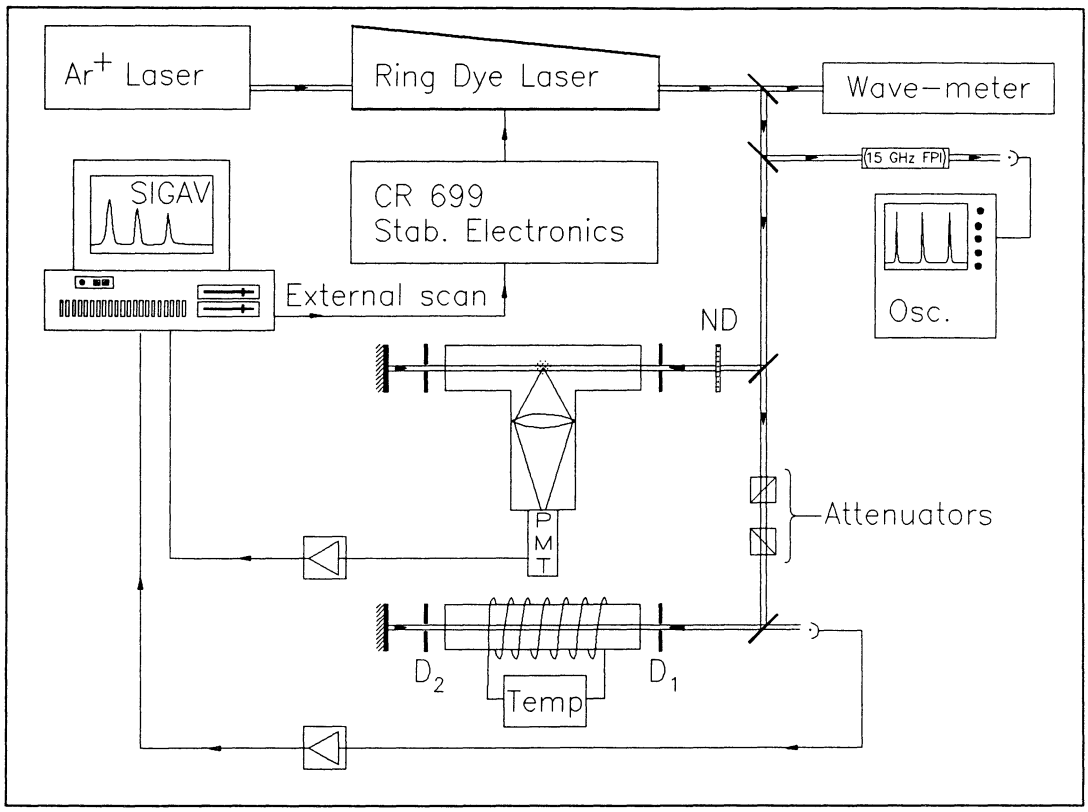

Fig. 2B.2. Experimental set-up for the determination of systematic shifts in high-contrast saturation spectroscopy.

The need for a precise reference became obvious in early measurements and we decided to use a well collimated atomic beam for this purpose. To eliminate any influence from the first-order Doppler effect in the interaction between the atomic beam and the exciting laser beam, the latter was reflected back onto itself. An angle offset was deliberately chosen and each component of the Doppler-free spectra was thus recorded twice. The unperturbed signal position then corresponded to the mean value of the two signal positions. The observed shifts are plotted in Figure 2B.3.

Theoretical models describing the "hole burning" effect for overlapping signal components have been developed and computer simulations have been performed.

Experiments on the dynamic properties of the pump-probe interaction in saturation spectroscopy have also been initiated [2.3]. An acousto-optic modulator was used to pulse-modulate the pump beam, giving it a rise time of the order of 10 ns. As we performed the experiment on the D-lines of sodium, the lifetimes of the excited states were 16.4 ns and the atoms were excited many times as they travelled through the region of interaction. The time of flight through the pump and probe beams, with diameters of 1 mm, was roughly 1 μs. Such a long transit time gives rise to a strong optical pumping effect, so both the rise time and the fall time can be expected to depend strongly on the experimental conditions. An experimental recording of the temporal

behaviour of the cell transmission of the probe beam is shown in Figure 2B.4 for the case of a 10 μs long rectangular pump beam pulse.

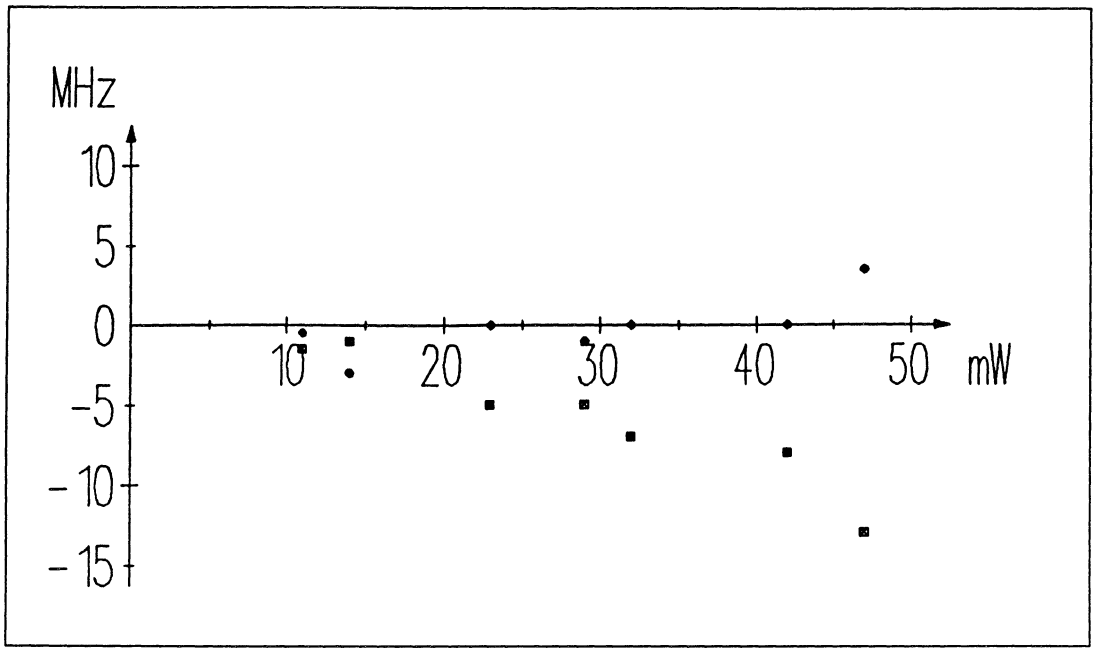

Fig. 2B.3. Observed shifts for two different components.

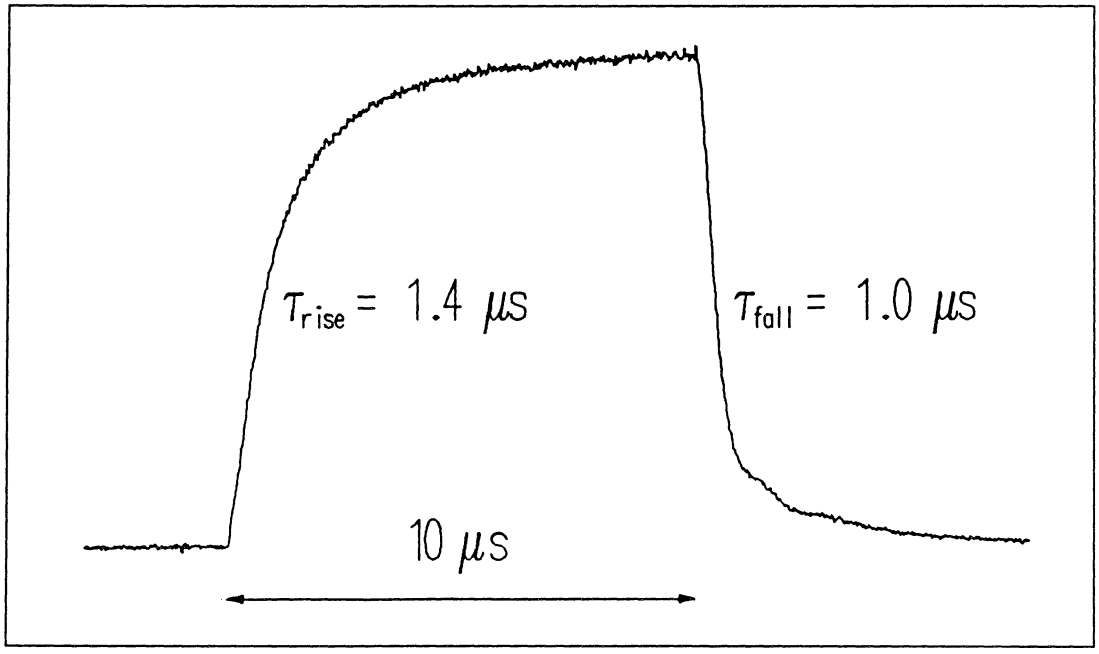

Fig. 2B.4. Temporal behaviour of the transmitted probe beam.

2C. High-resolution laser spectroscopy in the short-wavelength region using pulsed lasers

New techniques for measurement of hyperfine structures and Lande' g_J factors have been developed by our group. By combining the well-known level-crossing (LC) and optical double resonance (ODR) techniques with pulsed laser excitation, powerful tools are obtained for high-resolution spectroscopy at "difficult" wavelengths. These methods and the quantum-beat technique have been used to obtain new spectroscopic data for a number of atoms. A paper covering different aspects of resonance spectroscopy has been published. [2C.1]

The hyperfine structure of the strongly perturbed $5\,^2P_{3/2}$ state of copper provides a sensitive test for data obtained from theoretical calculations currentlly being performed [2A.2]. An accurate measurement of the hyperfine structure parameters could be performed using pulsed LC spectroscopy following excitation at 202 nm [2C.2]. The experimental set-up is shown in Figure 2C.1.

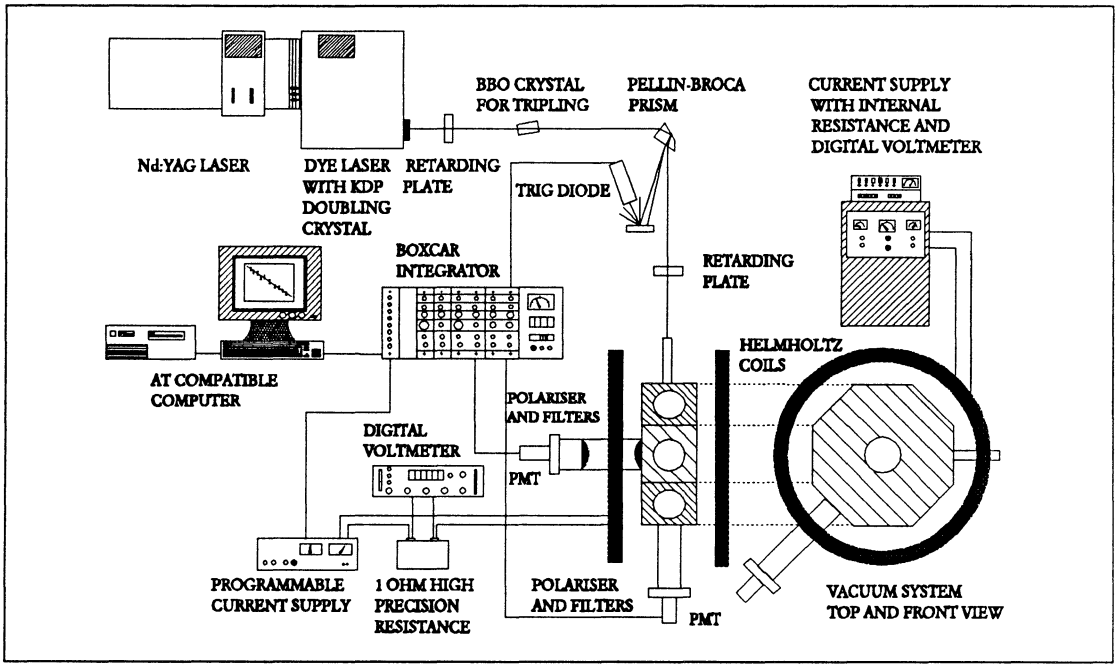

Fig. 2C.1. Experimental set-up for pulsed level crossing spectroscopy.

In Figure 2C.2 an experimental curve and a theoretical fit yielding the magnetic dipole interaction constant a, the electric quadrupole interaction constant b and the natural lifetime are given.

For the $6\,^2P_{3/2}$ state of neutral silver, all three above mentioned techniques were used [2C.3]. The ODR method was found to yield the highest precision in this case. Using delayed detection, a resolution betted than the Heisenberg limit could be obtained. ODR signals for "old" silver atoms are shown in Figure 2C.3.

The effectiveness of QBS was found to be greatly improved when a new fast transient recorder was made available to us. Using this technique, the hfs of

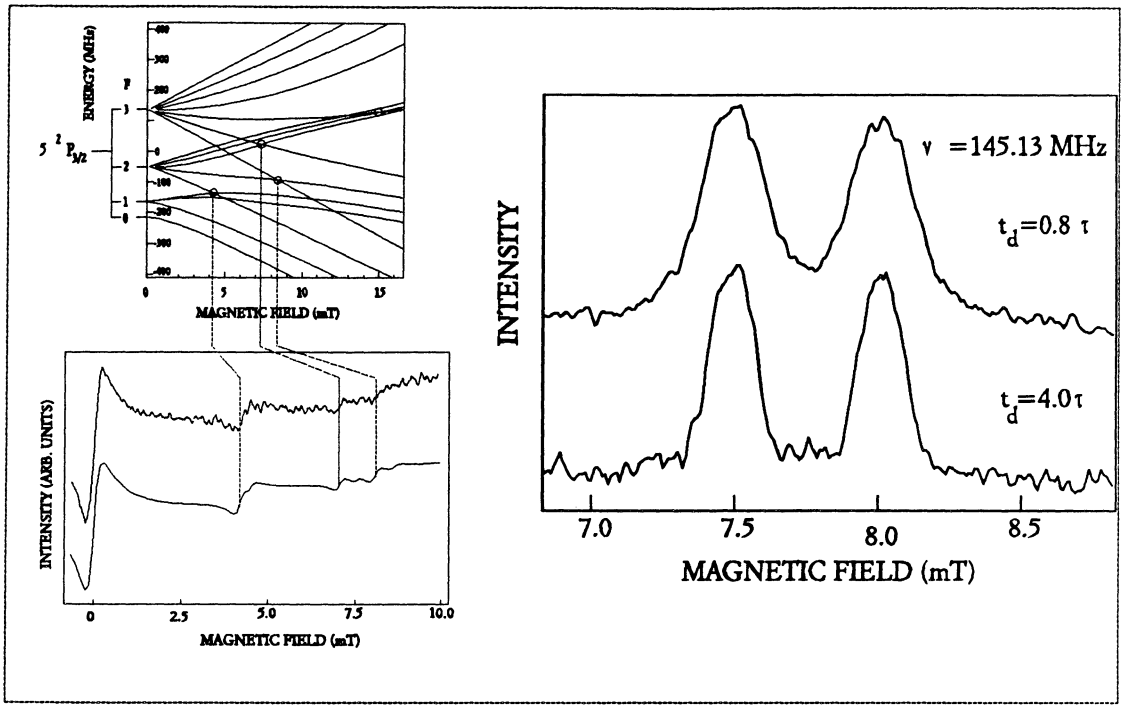

Fig. 2C.2. Energy-level structure for the 5 $^2P_{3/2}$ state of ^{63}Cu and the fluorescence as a function of magnetic field for both isotopes.

Fig. 2C.3. ODR recording from the 6 $^2P_{3/2}$ state of silver. One of the recordings was obtained after a considerable time delay, yielding a spectral resolution below the Heisenberg

the 6 $^2P_{1/2}$ [2C.3] and 7$^2P_{3/2}$ [2C.4] states could be measured. For the excitation of the 7 $^2P_{3/2}$ state, VUV radiation at 185 nm was used. This radiation was obtained by dye laser frequency tripling in BBO (β-barium borate) and subsequent stimulated Raman shifting in a Raman converter adapted for VUV work. A recording is shown in Figure 2C.4.

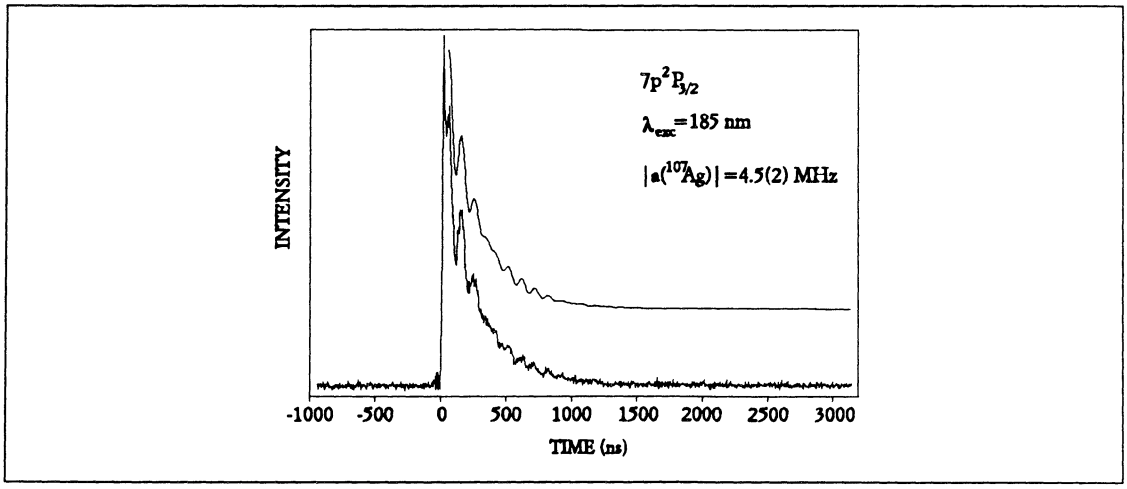

Fig. 2C.4. Time-resolved fluorescense from the 7$^2P_{3/2}$ state of silver with quantum beats. A theoretical curve is also given.

The QBS technique was also used for measurements of g_J factors in the 6snp ^1P and 6snp ^3P Rydberg sequences of ytterbium [2C.5]. This experiment yields new information of the configuration mixing in the high-lying states. Excitation wavelengths in the region of 200 nm were used. This is a collaboration between the Jilin University (PRC) and our group. An extensive MQDT analysis of our data is now being performed in China. In Figure 2C.5 an experimental recording is given and in Figure 2C.6 the g_J factor as a function of the principal quantum number of the ^1P and ^3P sequences is shown.

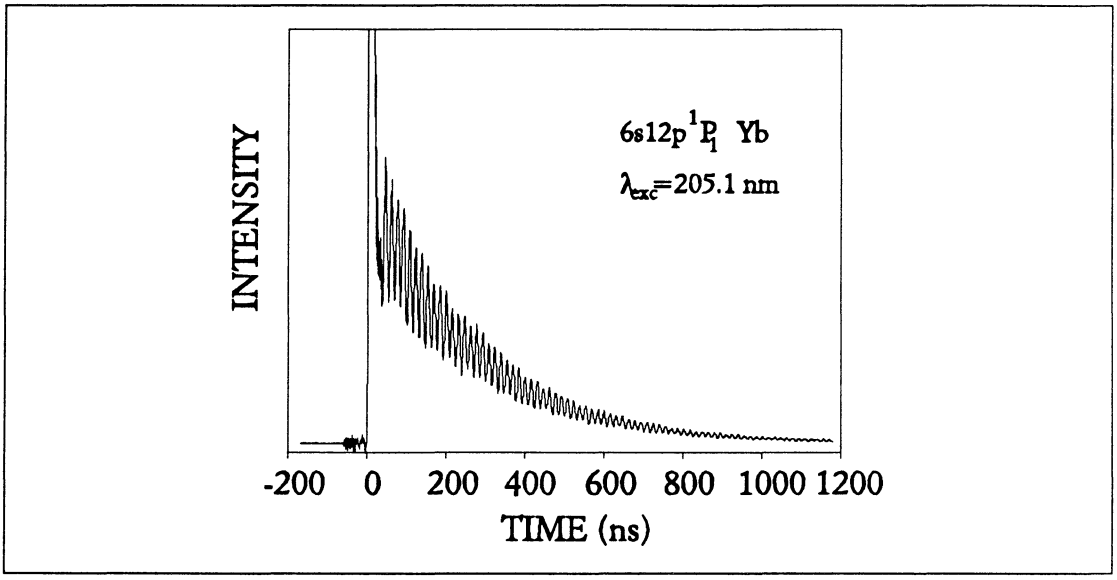

Fig. 2C.5. Experimental recording of Zeeman quantum-beats from the 6s12p $^1P_1$ state of ytterbium. The beat frequency gives information on the g_J factor

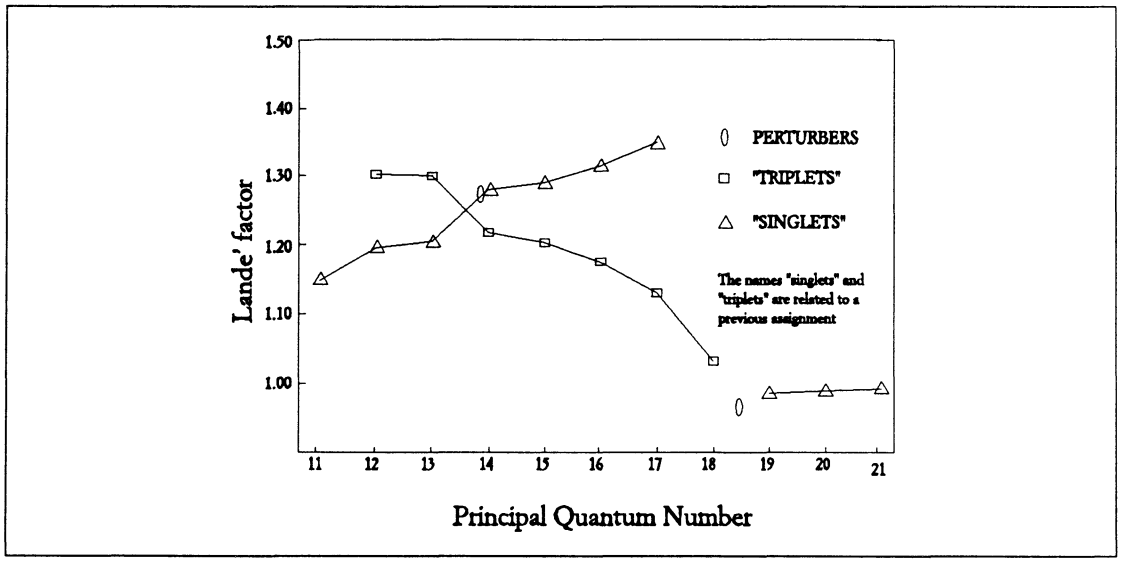

Fig . 2C.6. The g_J factor as a function of the principal quantum number for the

A powerful method for producing light elements has recently been applied to the study of natural lifetimes in nitrogen atoms [2C.6]. As in previous experiments on oxygen, [Phys. Rev. Lett. **55**, 284 (1985)] atoms were produced by photodissociation. In the present experiments nitreous oxide (N_20) is photodissociated by laser radiation which is in two-photon resonance with the transition to either the $3p\ ^4D_{7/2}$ or to the $3p\ ^4S_{3/2}$ state of nitrogen. The decay of these states, or of higher lying states, following excitation by a second laser pulse is recorded with a transient digitizer. An example of a Stern-Volmer plot leading to a natural lifetime determination is shown in Figure 2C.7.

Many of the light elements have odd isotopes in small abundances. Experiments on isotope-enriched samples in sealed cells, giving information about the hyperfine structure of these states, are planned as well as experimens on other light elements.

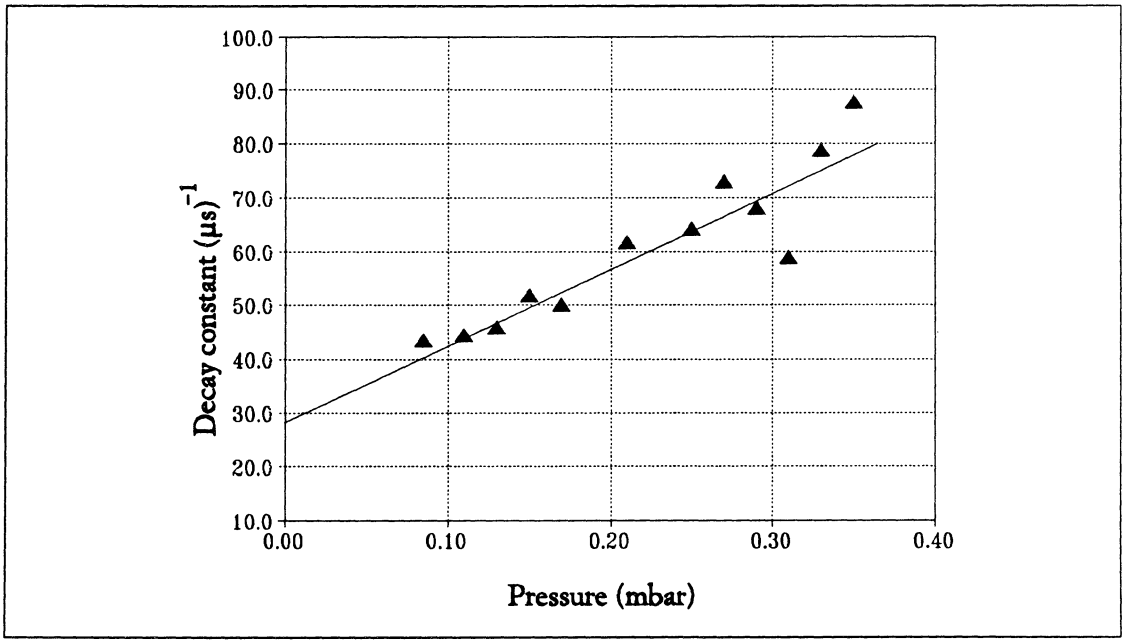

Fig. 2C.7. Stern-Volmer plot for the $6s\ ^4P_{5/2}$ state of neutral nitrogen

As a part of the study of the copper and silver atoms, the lifetimes of the states in the silver $4d^{10}ns\ ^2S$ and $4d^{10}nd\ ^2D$ series have been determined using pulsed laser excitation [2C.7]. An extended MCHF calculation could well reproduce the experimental results.

Two reviews covering our work in the field of high resolution laser spectroscopy in the short wavelength region have been published [2C.8, 2C.9].

2D. Accurate time-resolved spectroscopy

Two different techniques are available to perform accurate time-resolved measurements on atoms. One is the fast-beam laser technique, which was introduced by H. J. Andrä *et al.* in the 1970's. During the last few years also another technique has proven capable of giving lifetime values with uncertainties well below 1 %, namely the delayed coincidence technique with a continuous mode-locked dye laser as the source of the excitation light. A set-up for this type of experiment is illustrated in Figure 2D.1.

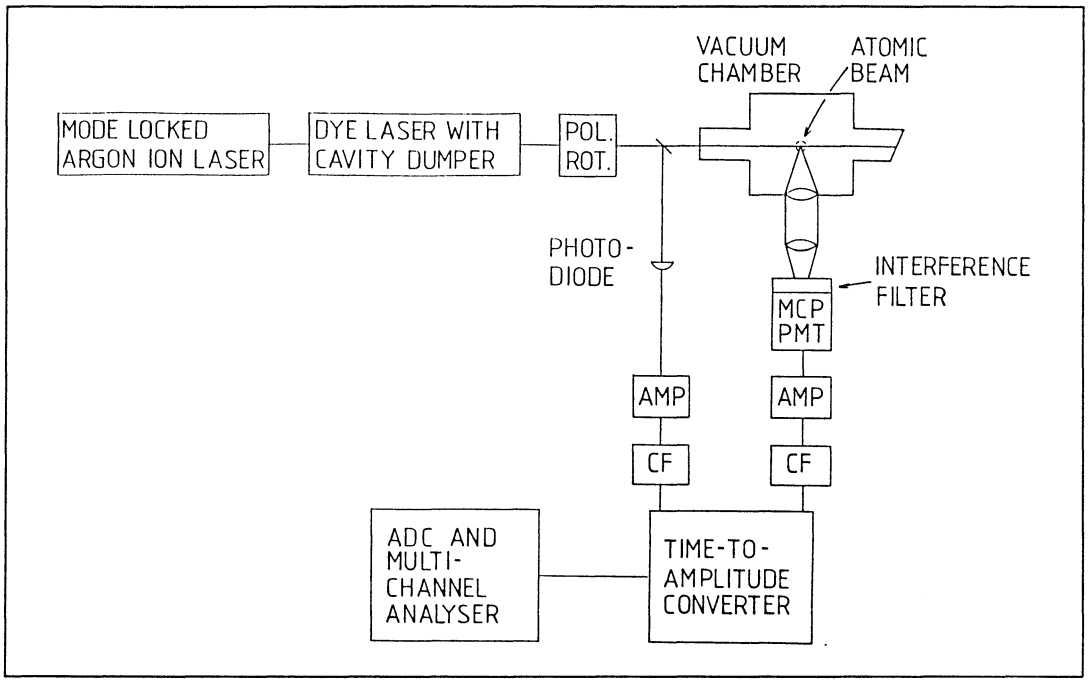

Fig. 2D.1. Set-up used for delayed coincidence experiments on the lithium 2p ^2P states.

The time resolution of these experiments is limited mainly by the transit time scattering in the photomultiplier tube. Using a photo-multiplier tube with microchannel plates and stabilizing the signals with constant fraction discriminators, a response function with a full width at half maximum of 75 ps is obtained, as illustrated in Figure 2D.2.

The first measurements using this technique, on sodium, bismuth, copper and iron, were described in our report for 1987-1988. Measurements could also be performed at elements for which free atoms were obtained in a discharge [2D.1]. This accurate technique has since been used to determine the lifetimes of the lowest ^2P states in lithium [2D.2] and in silver [2D.3].

Lithium, with its three electrons, allows one of the most important tests of atomic theory and for the lifetime of the 2p ^2P states there is a difference of about 1 % between the most accurate experimental lifetime values and values calculated with different *ab initio* methods

such as multi-configuration Hartree-Fock and many-body perturbation theory. A similar difference is found for the 3p ^{2}P states of sodium. An experimental recording from the study of lithium is shown in Figure 2D.3.

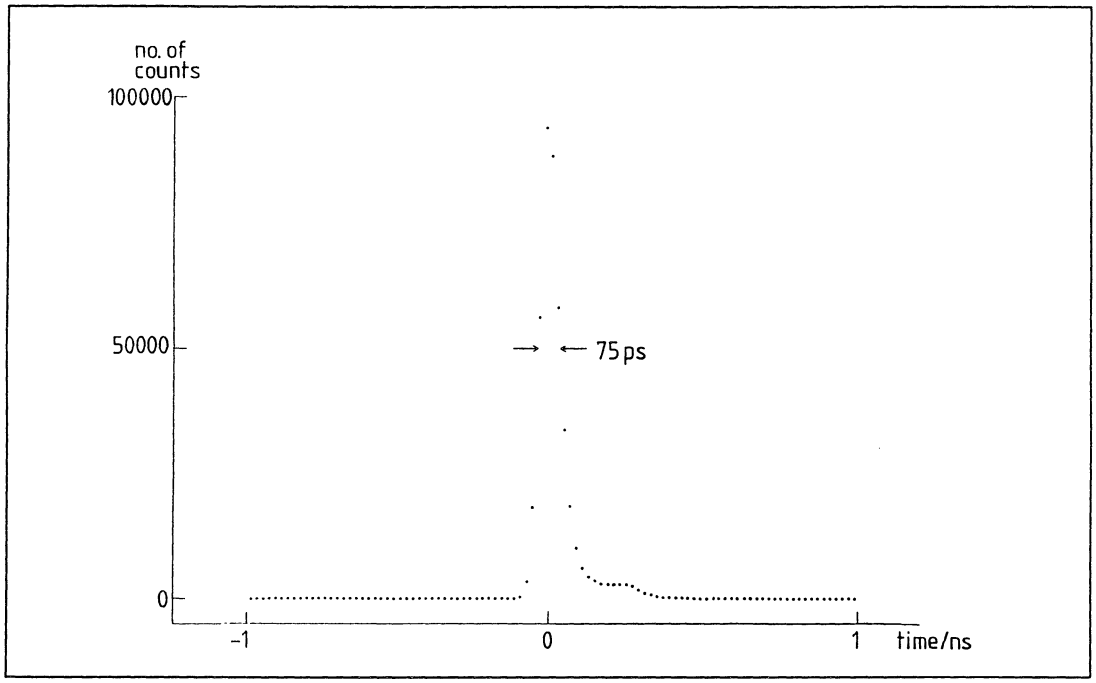

Fig. 2D.2. Response function from the delayed coincidence experiments.

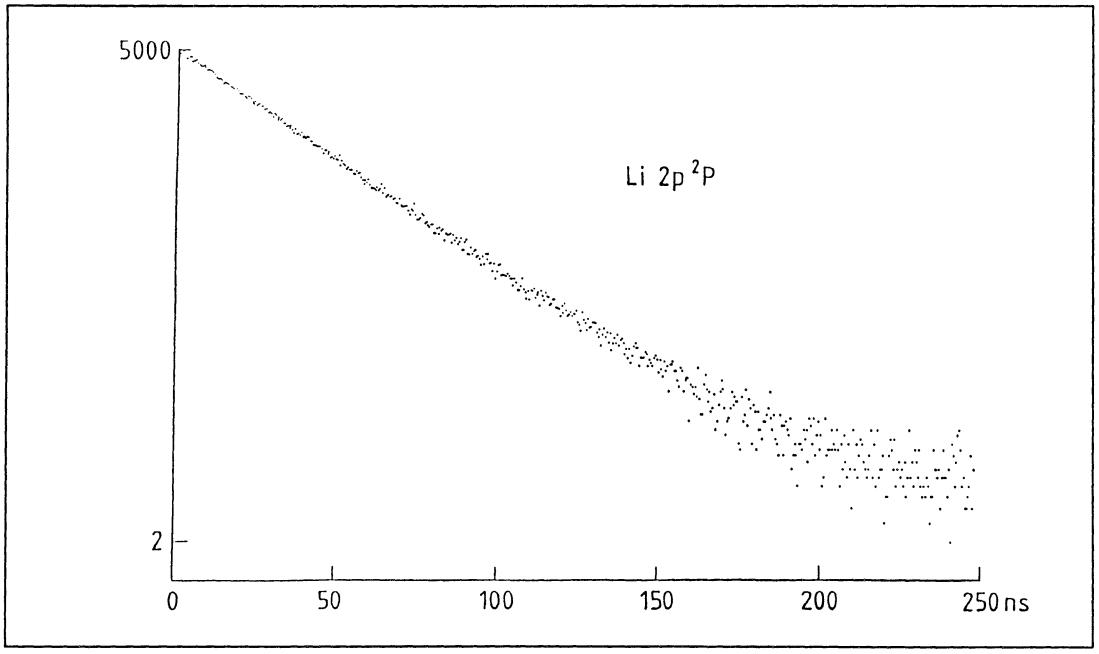

Fig. 2D3. Experimental decay curve for the 2p ^{2}P states of lithium, in a logarithmic scale. The curve was recorded with an angle of 54.7° between the polarizations of the excitation and detection light, in order to avoid quantum beats.

The silver atom has been studied at the 328 nm and 338 nm resonance lines and the lifetimes of the $4d^{10}5p\ ^2P$ states have been accurately determined.

The length of the pulses from the mode-locked dye laser is 6 ps. This gives a Heisenberg limited bandwidth of 70 GHz and the pulses can thus be used to achieve coherent excitation of large structures (fine- or hyperfine structures) among the excited states. This will induce quantum beats in the decay and from these beats the magnitude of the energy separations in the excited state can be obtained. The time resolution of the detection system is high enough to record beat frequencies of several gigahertz. Quantum beats have been used to determine the hyperfine structure parameters of the lithium $2p\ ^2P_{3/2}$ and sodium $3p\ ^2P_{3/2}$ states [2D.2] and of the silver $4d^{10}5p\ ^2P_{1/2}$ and $4d^{10}5p\ ^2P_{3/2}$ states [2D.3]. In favourable cases, such as the sodium $3p\ ^2P$ states, the accuracy in the determination of hyperfine structure splittings with this technique can be even better than for the corresponding lifetimes.

Recently, the use of this technique has been extended to states which, because of their parity, cannot be reached directly from the ground state. This has been achieved by two-step excitation with a continuous dye laser for the first step. The first application of this was a measurement on the $3d\ ^2D$ states of lithium for which the lifetime was determined with an uncertainty of 0.8 % [2D.4]. Apart from the $2p\ ^2P$ states, these are the only states in lithium for which the lifetime is known with such a good accuracy and this provides a new test for atomic theory.

2E. VUV spectroscopy, laser plasmas and stimulated emission

A wavelength scale with designation of spectral regions is given in Figure 2E.1. Conventional laser systems with dyes and frequency-doubling crystals produce radiation down to about 200 nm. Shorter wavelengths in the VUV region have been generated from laser radiation using non-linear optical mixing processes in noble gases and metal vapours, and soft X-ray radiation has been produced from laser-induced plasmas. Amplified radiation due to stimulated emission has been investigated in recombining plasmas and in two-photon-pumped atoms and molecules.

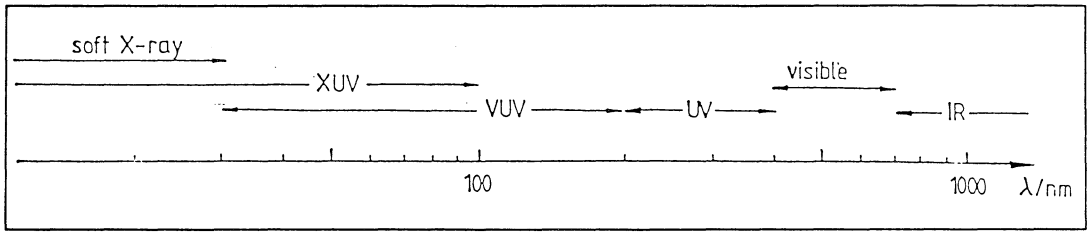

Fig. 2E.1. Designation of spectral regions.

Electron density measurements have been performed in an expanding laser-produced plasma using a two-wavelength beam-deflection technique [2E.1]. The examined plasma was formed in a vacuum chamber by using a 250 mm lens to focus 25 to 50 mJ of 1.06 μm radiation from a Q-switched Nd:YAG laser (corresponding to 10^{10} W/cm^2) onto a rotating target. The target materials investigated were boron, graphite, silicon, iron, tantalum and tungsten. The beam-deflection apparatus consisted of a HeNe laser and a HeCd laser which were carefully overlapped and focused to equal beam sizes of 250 μm. The deflections of these two beams were measured using a fast quadrant detector connected to a transient recorder. The system had a spatial resolution of 250 μm, a temporal resolution of 25 ns and a dynamic range of 1000. Figure 2E.2 shows electron density profiles for a laser-produced plasma with a graphite target. The curves were obtained by tomographic reconstruction from single temporal beam-deflection curves. By using a two-wavelength technique the contributions from the electrons could be separated from other components (ions, neutral atoms, molecules and particles) since the refractive index of the electrons is less than one and varies rapidly with wavelength, which is not the case for the other components (if not close to a resonance).

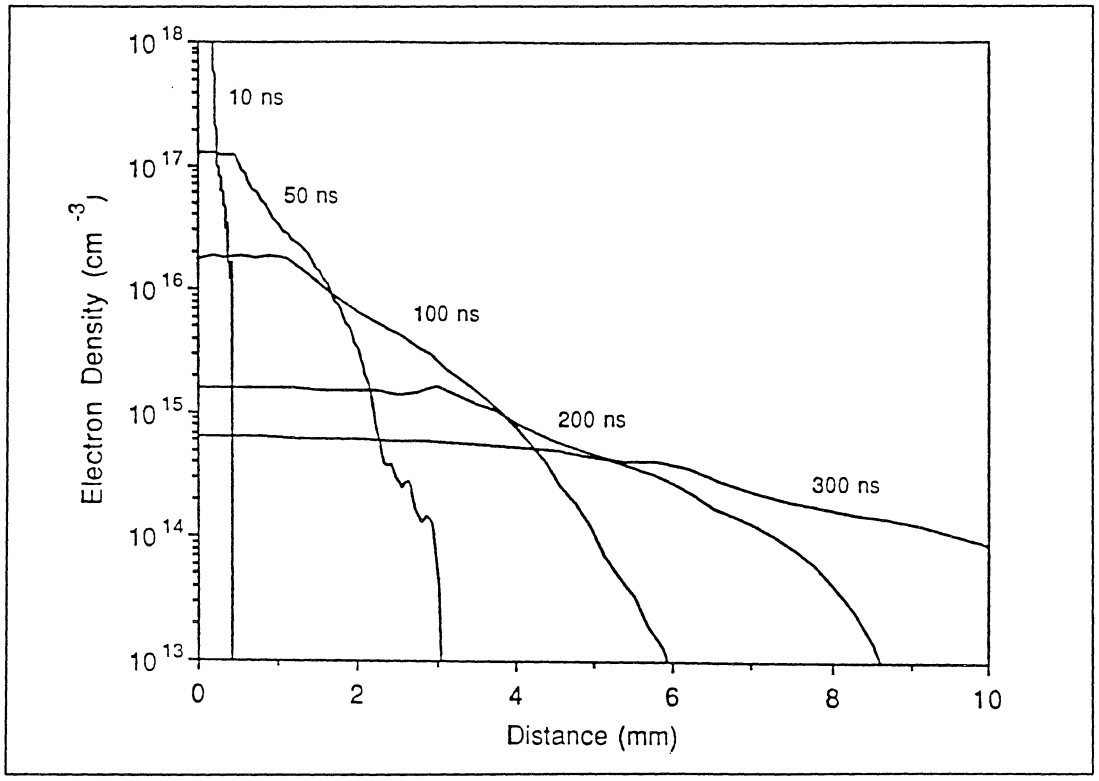

Fig. 2E.2. Electron density profiles for a laser-produced plasma with a graphite target. The curves were obtained by tomographic reconstruction from single temporal beam-deflection curves.

Amplification of VUV radiation has been studied in an expanding laser-produced Al plasma [2.7, 2E.2]. The investigations were performed for wavelengths longer than 1200 Å and the shortest wavelength with gain was the 5f-3d transition in Al III at 1353 Å. Measurements were made using a two-plasma technique with a power

§density at the Al target of 10^9 W/cm^2. Population inversions were created in the plasma due to recombination during expansion in a buffer gas. Amplification was observed in a limited region of the plasma. Figure 2E.3 shows the change in probe pulse intensity when passing through the plasma at different distances from the target. A peak small-signal gain of 0.5 cm^{-1} was obtained for the 1353 Å line.

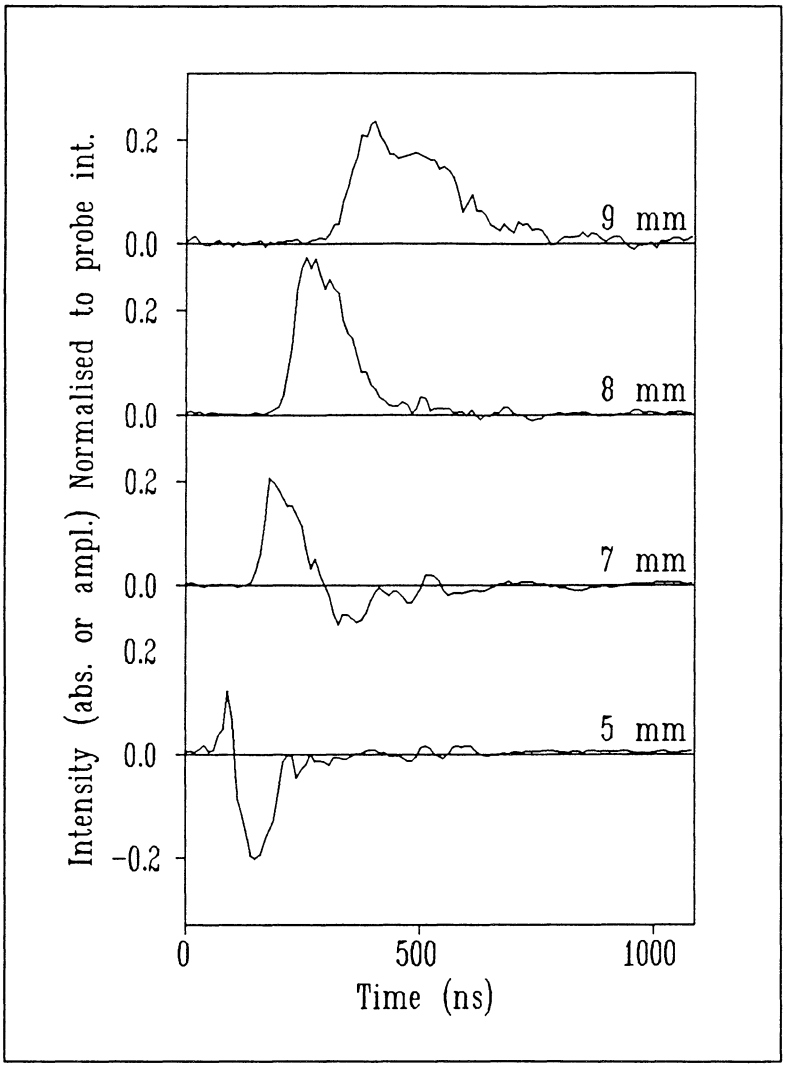

Fig. 2E.3. Amplification and absorption of a probe pulse in an expanding plasma. The recordings were made on the 1353 Å line in Al III and the curves have been normalized to the probe pulse intensity.

For several materials it is very difficult to produce free atoms with standard methods, such as evaporation from an oven. Among these elements are the theoretically interesting light elements silicon and carbon. We have made measurements of radiative lifetimes in silicon and studied amplified laser-induced fluorescence in carbon using plasmas as a source of free atoms.

The silicon atoms were produced by focusing one of two synchronously triggered Nd:YAG lasers (with a power of 25 mJ and a duration of 7 ns), using a 25 cm lens, onto a rotating silicon target in a high-vacuum chamber (10^{-6} mbar) [2E.3]. The other Nd:YAG laser was used to pump two dye lasers. The fluorescence from the rapidly expanding plasma lasted for about one microsecond after which it was possible to perform the step-wise excitation without cascade effects in the fluorescence light using the two dye lasers. The first step from the $3p^2\ ^3P$ ground state to the 3p4s ^3P state was performed by frequency doubling and Raman shifting the output from a dye laser operating on Rhodamine 6G, while the second-step laser, a home-built Littman-cavity dye laser, also operating on R6G, performed the excitation to the 3p5p $^3S_1$, $^3P_{0,1,2}$ and $^3D_{1,2,3}$ states. The laser-induced fluorescence was filtered through a monochromator, detected in a photomultiplier tube and recorded by a transient recorder with sampling period of 10 ns. The obtained experimental lifetimes were compared with theoretical values obtained using multi-configuration Hartree-Fock wavefunctions.

The same procedure as that described above was also used to produce excited carbon atoms and molecules. Two-photon excitation from the ground state was used to reach the excited 2p3p ^3P and ^3D states as well as some vibrational levels of the A $^3\Pi_g$ state of the C_2 molecule. Radiative lifetimes were measured for these excited states [2E.4]. The stimulated emission on the infrared 2p3p to 2p3s emission lines in carbon was investigated. The possibility to use the stimulated emission for absolute concentration measurements as well as the influence on laser-induced fluorescence measurements used for concentration or lifetime measurements were discussed. Calculations of the densities were performed using rate equations to support the measurements. However, because of difficulties encountered in calculating the stimulated emission in the rapidly expanding plasma we switched to the study of two-photon induced stimulated emission in carbon monoxide which could be performed in a cell experiment.

The stimulated emission on the Ångström band ($B^1\Sigma^+$ to $A^1\Pi$) was investigated after populating the upper laser level by two-photon pumping from the $X^1\Sigma^+$ state [2E.5-6]. The spectroscopic data required for a "complete" rate equation analysis of the amount of stimulated emission obtained were collected. These include measurements of quenching rates, lifetimes, two-photon absorption and ionization cross-sections. Figure 2E.4 shows a Stern-Vollmer plot for the B state giving the A factors for the B-A and B-X transition arrays as well as the quenching factor. This was possible since the very strong multiple scattering totally closed the decay channel to the ground state for sufficiently high pressures.

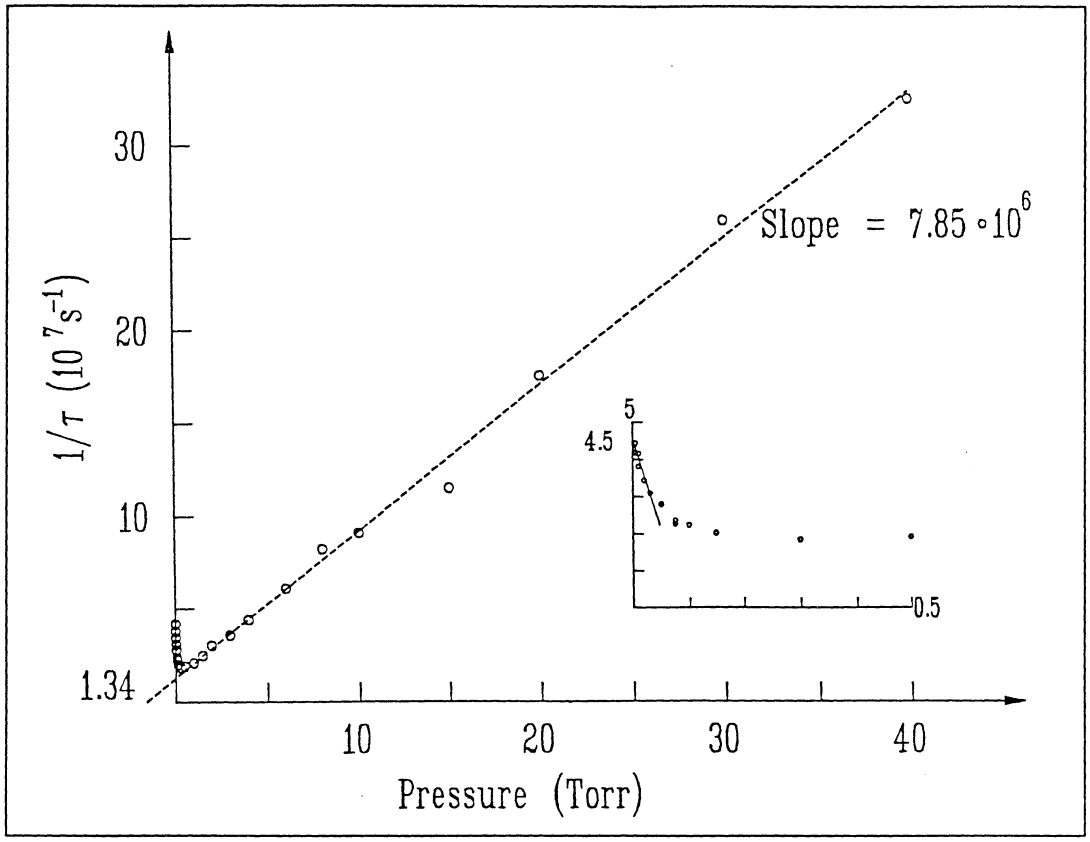

Fig. 2E.4. A Stern-Vollmer plot of lifetimes in the CO B $^1\Sigma$ state.

The measurements and evaluations of the two-photon and ionization cross-sections were simplified by implementing an extra nonresonant ionization channel. This was achieved by using the residual radiation after doubling a Nd:YAG laser (used to pump the dye laser in the two-photon pumping process). This residual Nd:YAG radiation was doubled and mixed to the third harmonic at 355 nm which will be energetic enough to ionize the B state molecules in one step. The advantage is then the possibility of calibrating the fluorescence yield absolutely by comparing the fluorescence with the ion signals with and without the extra ionization channel.

The stimulated emission was investigated both in the forward and backward directions, as well as the effects of introducing feedback. A rate equation analysis was performed to check the potential and accuracy of density measurements based on stimulated emission measurements.

A system for generating VUV radiation using 4-wave-mixing techniques has been constructed [2E.7]. Using laser beams in the visible and UV, shorter wavelengths are generated through non-linear processes in noble gases and metal vapours. Using such radiation, spectroscopic investigations have been performed on the $A^1\Pi$ $v=13$ level in the CO molecule [2E.8].

2F. Atomic physics at high optical field strengths

Within the last few years techniques have become available which enable one to construct laboratory-scale lasers with output powers of terawatts and intensities of the order of 10^{19} W/cm^2. This has led to a very rapid development in the exciting fields of research dealing with atomic physics at ultra-high field strengths.

At the peak intensities available with these lasers the electric field is in excess of 10^{10} V/cm. For a hydrogen atom the Coulomb field at one Bohr radius from the nucleus is about $5 \cdot 10^9$ V/cm. It follows that, provided the atom can survive the rapidly increasing intensity of an ultra-short pulse from a terawatt laser, the electrons may be exposed to electric fields higher than that due to the nucleus. New and unexpected observations are constantly being reported, observations which have attracted considerable interest amongst theoreticians. The key to these developments is the production and amplification of ultra-short pulses. Pulse energies of about 1 Joule and pulse durations of the order of a picosecond are typical data for a terawatt laser.

Experimental research in the above mentioned field of atomic physics will be carried out within the Atomic Physics Division during the forthcoming years. During the two-year period covered by the present progress report, substantial preparatory work has been carried out to set the stage for this new field of activity.

An extensive survey [2F.1] has been made over the latest trends in high-power laser developments, including new solid state materials and novel short pulse amplification techniques. Visits to several laboratories and topical conferences in Europe and in the USA have been made. The survey also covered a wide range of commercially available components and systems for terawatt pulse generation.

A major step in the realization of a high-power laser facility was taken very recently, when 7 million SEK were donated by the Knut and Alice Wallenberg Foundation to cover the cost of the initial investment required. This opened the doors wide open for the operation, within the next two-year period, of a terawatt laser in Lund. Pulses of ultra-high intensity will be delivered for fundamental research.

As a part in the preparation for this new field of research in Lund, Dr C.-G. Wahlström spent a year with the Laser Optics and Spectroscopy Group at Imperial College in London. There, under the leadership of Professor Henry Hutchinson, a high-power laser facility has been built. Research activities within the fields of multi-photon physics, laser produced plasmas and X-ray lasers have been initiated, involving researchers with several different specialities. The main investigation carried out during Dr Wahlström's stay at the facility was on the temporal dependence of the radiation created through high harmonic generation in free atoms.

It has been found, especially by the Saclay group, that very high (>50) order harmonic radiation is produced during the interaction of infra-red laser radiation with rare gases. Interesting intensity

dependencies on harmonic order have been reported. After a pronounced drop from the third to the fifth harmonic, the harmonic generation rate remains practically constant over a broad energy range from the seventh harmonic to a high-order harmonic before falling abruptly and becoming undetectable. The plateau region is longer for Ar than for Xe and Kr, though the conversion efficiency is lower. These observations have been made at intensities of the order of 10^{13} W/cm^2, the same order of magnitude as the saturation intensity for photo-ionization of the neutral gases. The interpretation of the results is not an easy task since it involves both the single-atom response to the laser interaction and the many-atom response, the capability of the medium to ensure proper phase matching between the incident field and the generated radiation.

The aim of the time-resolved investigations being carried out in London, is to obtain complementary data which can be used to deduce more about the fundamental processes involved in high harmonic generation. Operating the laser in a mode where the pulses were as long as 50-100 ps, harmonic radiation was generated in a low density pulsed jet of Xe gas from a nozzle. The radiation generated in individual laser pulses, for a given harmonic order, was recorded using a vacuum monochromator and an XUV-sensitive streak camera. The peak intensity and the temporal profile of the corresponding infra-red (1.053 μm) laser pulses were simultaneously recorded using an IR-sensitive streak camera.

Depending on focusing geometry and pulse shape, spatially and temporally dependent ionization occurs in the interaction region. This affects the intensity of the generated radiation in two ways. Firstly, the single-atom response changes as the density of neutrals is reduced and different ionization stages are produced and further ionized. The neutral atoms and the different ions are expected to have quite different nonlinear responses to the driving field. However, there are no data in the literature regarding this for the rare gas ions. Secondly, the many-atom response, the phase matching, is drastically affected by the change in refractive index which follows upon the ionization. The dominant contribution is the dispersion in the free electron gas produced.

A theoretical model for the harmonic generation process has been developed, including single- as well as many-atom responses. The model uses experimental data concerning the density and distribution of the target gas, temporal and spatial profiles for the IR laser pulses and the focusing parameters as input data. Numerically calculated harmonic intensity for a large number of grid points in time, can be compared with the experimentally recorded profiles obtained using the XUV-sensitive streak camera [2F.2, 2F.3].

Studies of these temporal features, using different gas densities, pulse energies and focusing geometry and comparisons between the model and the observed data are expected to produce novel information about, e.g., the ionic responses and free electron dynamics in the presence of high optical field strengths.

The above described investigation of high harmonic generation is an on-going project and there will be continued engagement from Lund [2F.4]. Several future projects are also being planned in a close

collaboration between the high power laser facilities in London and Lund. This will most certainly give rise to many interesting and stimulating results to report on in the next progress report.

References

2.1. J. Carlsson, Excited states of free atoms in the dimension of Time, Ph.D. thesis, Lund, 1990

2.2. A. Persson, Laser spectroscopic techniques applied to the study of excited states of free atoms, ions and molecules, Ph.D. thesis, Lund, 1990

2.3. J. Bengtsson, J. Larsson, A. Persson, L. Sturesson and S. Svanberg, Saturation spectroscopy for dense atomic samples studied with time-integrated and time-resolved techniques, 3rd ECAMP, Bordeaux, April 3-7, 1989

2.4. J. Carlsson, L. Sturesson and S. Svanberg, Accurate lifetime measurements on copper and iron atoms, 3rd ECAMP, Bordeaux, April 3-7, 1989

2.5. J. Bengtsson, J. Larsson, S. Svanberg and C-G. Wahlström, High-resolution atomic spectroscopy in the UV/VUV spectral region using pulsed lasers, 2nd EQEC, Dresden, August 28 - September 1, 1989

2.6. G. J. Bengtsson, J. Bengtsson, J. Larsson, S. Svanberg and C-G. Wahlström, High-resolution laser spectroscopy in the UV/VUV region, 22nd EGAS, Uppsala, July 10-13, 1990

2.7. H. Bergström and H. Lundberg, Amplification of VUV radiation in a recombining plasma, 22nd EGAS, Uppsala, July 10-13, 1990

2.8. J. Carlsson, P. Jönsson and L. Sturesson, Time-resolved studies of the resonance transitions in lithium and silver, 22nd EGAS, Uppsala, July 10-13, 1990

2.9. J. Bengtsson, J. Carlsson, P. Jönsson, J. Larsson, L. Sturesson and S. Svanberg, Laser spectroscopy on copper and silver atoms, 12th ICAP, Ann Arbor, July 29 - August 3, 1990

2.10. S. Svanberg, Atomic and molecular spectroscopy - Fundamental aspects and practical applications, Springer series in atoms and plasmas, Vol. 6, Springer-Verlag, Heidelberg, 1990

2A.1. P. Jönsson, C-G.Wahlström and C. Froese Fischer, A general program for computing magnetic dipole and electric quadrupole hyperfine constants for atoms, manuscript in preparation for Computer Physics Communications

2A.2. J. Carlsson and P. Jönsson, Hyperfine structure of the copper atom, manuscript in preparation

2B.1. H. Bergström, W. X. Peng and A. Persson, Two different types of hollow-cathode discharges used for high resolution laser spectroscopy on copper, Z. Phys **D13**, 203 (1989)

2B.2. A. Persson and H. Bergström, SIGAV, a program for signal averaging and evaluation in high-resolution laser spectroscopy experiments, Lund Reports on Atomic Physic, **LRAP-98** (1989)

2B.3. Jiang Zhankui, A. Persson, L. Sturesson and S. Svanberg, Investigation of shifts and interaction of signals in high-contrast transmission spectroscopy, manuscript in preparation for Z. Phys. **D**

2C.1. J. Larsson, L. Sturesson and S. Svanberg, Manipulation of level crossing signals using narrow-band or pulsed laser excitation, Phys. Scr. **40**, 165 (1989)

2C.2. J. Bengtsson, J. Larsson, S. Svanberg and C-G. Wahlström, Hyperfine-structure study of the $3d^{10}5p\ ^2P_{3/2}$ level of neutral copper using pulsed level crossing spectroscopy at short laser wavelengths, Phys. Rev. **A41**, 233 (1990)
2C.3. J. Bengtsson, J. Larsson, and S. Svanberg, Hyperfine structure and radiative lifetime determination for the $4d^{10}6p\ ^2P$ states of neutral silver using pulsed laser spectroscopy, Phys. Rev. **A42**, 5457 (1990)
2C.4. G. J. Bengtsson, P. Jönsson, J. Larsson and S. Svanberg, Time-resolved spectroscopy studies of the $7p\ ^2P$ states of neutral silver following VUV-excitation, manuscript in preparation
2C.5. J. Larsson and Jiang Zhankui, manuscript in preparation
2C.6. G. J. Bengtsson, J. Larsson, S. Svanberg and Wang Dadi, Radiative lifetimes for nitrogen atoms, manuscript in preparation
2C.7. Jiang Zhankui, P. Jönsson, J. Larsson, and S. Svanberg, Studies of radiative lifetimes in the $4d^{10}ns\ ^2S$ and $4d^{10}nd\ ^2D$ sequences of neutral silver, Z. Phys. **D17**, 1 (1990)
2C.8. J. Bengtsson, J. Larsson, C-G. Wahlström and S. Svanberg, High resolution pulsed laser spectroscopy in the UV/VUV spectral region, in Laser Spectroscopy IX, Academic Press, New York, 1990
2C.9. S. Svanberg, High-resolution laser spectroscopy in the UV/VUV spectral region, in Applied laser spectroscopy, eds. M. Inguscio and W. Demtröder, Plenum, New York, to appear
2D.1. J. Carlsson, L. Sturesson and S. Svanberg, Accurate time-resolved laser spectroscopy on sputtered metal atoms, Z. Phys. **D11**, 287 (1989)
2D.2. J. Carlsson and L. Sturesson, Accurate time-resolved laser spectroscopy on lithium atoms, Z. Phys. **D14**, 281 (1989)
2D.3. J. Carlsson, P. Jönsson and L. Sturesson, Accurate time-resolved laser spectroscopy on silver atoms, Z. Phys. **D16**, 87 (1990)
2D.4. J. Carlsson, P. Jönsson and L. Sturesson, Accurate determination of the lithium $3d\ ^2D$ lifetime, manuscript in preparation
2E.1. G. Faris and H. Bergström, Two-wavelength beam-deflection technique for electron density measurements in laser-produced plasmas, submitted to Appl. Optics (1990)
2E.2. H. Bergström and H. Lundberg, Amplification of VUV radiation in a recombining Al plasma, manuscript in preparation
2E.3. H. Bergström, G. W. Faris, H. Hallstadius, H. Lundberg and A. Persson, Investigations of radiative lifetimes in the 3p5p configuration of neutral silicon, Z. Phys. **D13**, 29 (1989)
2E.4. H. Bergström, H. Hallstadius, H. Lundberg and A. Persson, Detection of carbon using amplified laser-induced fluorescence, Chem. Phys. Lett. **155**, 27 (1989)
2E.5. H. Bergström, H. Lundberg and A. Persson, Investigations of stimulated emission on the B-A lines in CO, submitted for publication
2E.6. H. Bergström, Calculations on stimulated emission induced by two-photon pumping, LRAP in preparation
2E.7. H. Hallstadius, Studies on vacuum ultraviolet radiation and spectroscopic investigations of light elements in laser-produced plasmas, Lic. avhandling, **LRAP-101**, Lund (1989)

2E.8. H. Hallstadius and H. Lundberg, Investigation of the $A^1\Pi$ v'=13 level in CO using VUV radiation generated by resonant sum frequency mixing in Hg vapour, Phys. Scr. **40**, 652 (1989)
2F.1. A. Persson, S. Svanberg: Högeffektlaserfacilitet vid Laser-centrum Lund, Lund Reports on Atomic Physics, **LRAP-109**, Lund (1990)
2F.2. M. E. Faldon, M. H. R. Hutchinson, S. Luan, J. P. Marangos, R. A. Smith and C.-G. Wahlström: Studies of high harmonic generation with intense lasers, on Multiphoton Processes, ICOMP V, Paris, September 24-28, 1990
2F.3. M. E. Faldon, M. H. R. Hutchinson, S. Luan, J. P. Marangos, R. A. Smith and C.-G. Wahlström: Studies of temporal dependence of high harmonic generation, manuscript in preparation
2F.4. C.-G. Wahlström, J. Muffett and M. H. R. Hutchinson: Intensity-dependent susceptibilities for high harmonic generation, work in progress

3. QUANTUM ELECTRONICS

Håkan Bergström, Stefan Kröll, Jörgen Larsson, Anders Persson, Sven-Göran Pettersson, Sune Svanberg

3A. Photon echoes in rare-earth-ion-doped crystals

In a photon echo experiment energy from some arbitrary input sequence may be stored as a phase grating and/or as a population grating in the irradiated sample. Rare-earth-ion-doped crystals at liquid helium temperatures have the ability to preserve such gratings for extended times (from μs to days) and also to "remember" very complicated input sequences. Their ability to efficiently store and recall energy (=information) at high data transfer rates constitutes interesting possibilities for areas such as optical data storage, optical image processing and optical computing. Further, by storing and recalling energy, the photon echo technique enables us to study relaxation, interaction and energy transfer processes taking place in these crystals. An experimental set-up for photon echo investigations of rare-earth-ion-doped crystals is presently under construction at the Division of Atomic Physics in Lund. The work described below has, however, been performed during two visits to the Molecular Physics Laboratory at SRI International, CA, USA.

Relaxation processes in rare-earth-ion-doped crystals at liquid helium temperatures - The period of time for which a sample can "remember" the phase of a coherent interaction is a crucial parameter in the context of optical data storage or processing using the photon echo technique. This dephasing time limits both the number of bits which can be stored in any single location and the data transfer rate that can be obtained. The photon echo technique is an optical analogue of nuclear magnetic resonance (NMR) and electron spin echoes. For NMR, as well as electron spin echoes, it was known already in the sixties that excitation caused by the second pulse in a two-pulse excitation sequence could modify the local environment (field) around the atoms/ions/nuclei excited by the first pulse, and thereby changing their transition frequency and destroying the rephasing process (Klauder & Anderson, Phys. Rev. **125**, 912 (1962)). This mechanism was called instantaneous spectral diffusion (ISD). As a result of ISD the phase memory time, therefore, decreases as a function of the excitation energy of the second pulse. ISD in photon echoes would therefore be of importance for optical memory/ processing type applications. ISD was predicted for photon echoes in the middle of the seventies but no excitation pulse energy-dependent photon echo decays were observed until recently, when three groups reported such an effect. In one of these cases (in Pr-doped YAG) the ISD mechanism was not sufficient to explain the observed decay times [3A.1] and in subsequent measurements on Pr-doped $YAlO_3$ the discrepancy was even more pronounced [3A.2, 3A.3,3A.4]. The physical mechanism governing the intensity dependence in these two cases has not yet been identified. Some possible explanations, such as optical density effects and resonant or non-resonant laser heating, could be excluded based on experimental data [3A.2, 3A.5]. From measurements in magnetic fields it has been possible to separate the decay rate γ(total) into γ(total) = γ(radiative) + γ(magnetic dipole interactions) + γ(excitation energy-dependent), where γ(excitation energy-dependent) is caused by non-magnetic interactions, and at low excitation densities is approximately inversely

proportional to the average distance between excited Pr ions. A mechanism which could be consistent with the observed behaviour is a direct (long-range) energy exchange mechanism between excited Pr ions. An explicit mechanism has, however, not yet been identified.

A crucial factor in recording the low energy data was that the signal-to-noise ratio could be increased by more than two orders of magnitude by inserting an extra Pockels' cell in the beam path [3A.5]. The importance of using low excitation energies can be seen in Fig. 3A.1 where a resonance in the photon echo decay time is clearly seen at low energies (plus signs) but barely discernible at higher excitation energies (squares). Attempts had previously been ade to observe such resonances at magnetic field strengths causing Zeeman-induced anti-crossings between hyperfine levels in the Pr ion but were not successful (Wokaun, Rand, DeVoe & Brewer, Phys. Rev. B **23**, 5733 (1981)). At the magnetic field strength and crystal orientation utilized when obtaining the data in Fig. 1 no Zeeman-induced anti-crossings are expected, however, and the physical origin of the resonance is still unclear.

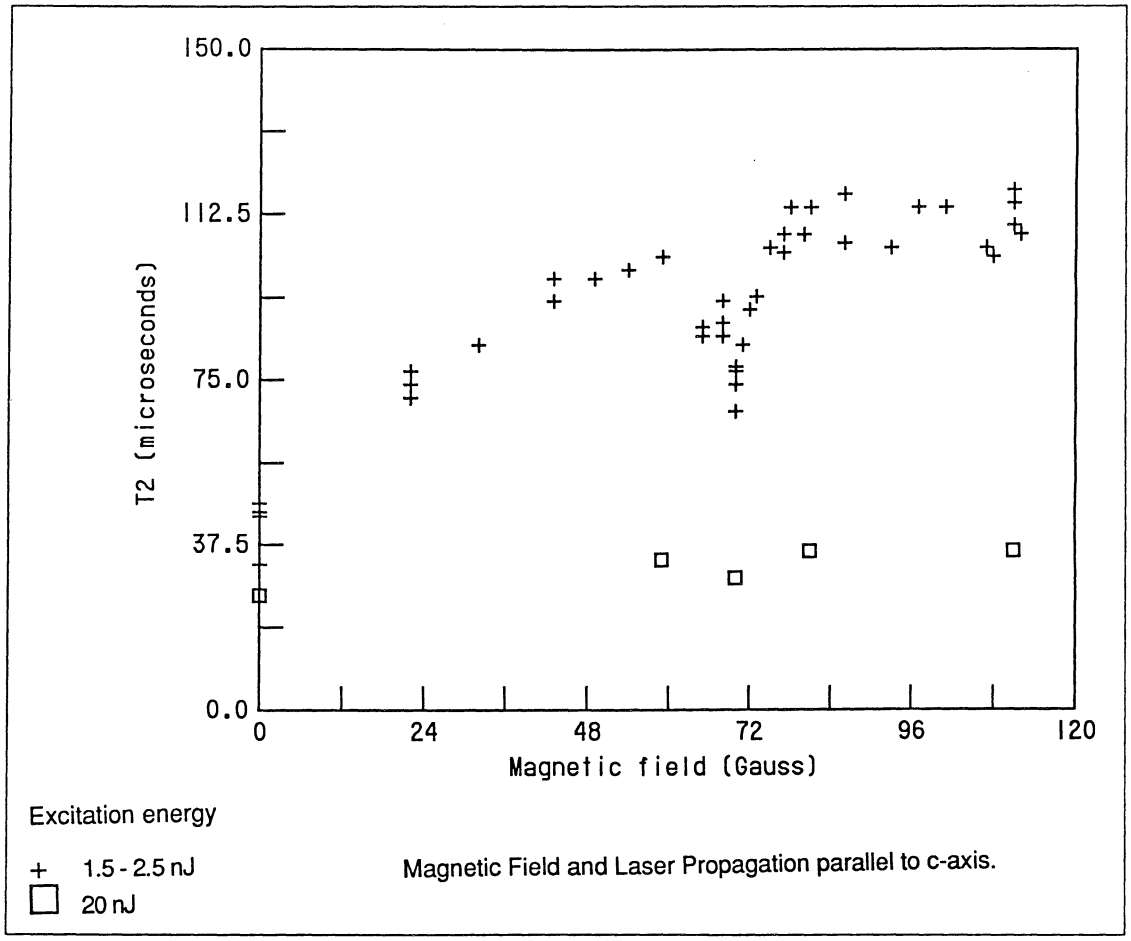

Fig. 3B.1. Photon echo decay time vs magnetic field for two different excitation pulse energies.

Multibit data storage and image processing using the photon echo technique - Briefly, in multi-bit storage at a single spatial location using stimulated photon echoes, a set of weak data pulses is transmitted into the sample and stored as a phase grating. A stronger

"write pulse" converts the phase grating into a longer-lived population grating. A later "read pulse" triggers a coherent re-emission of the stored data sequence. If all pulses are collinear the data output will be transmitted collinearly with the other pulses [3A.6] but if the read and write pulses propagate in opposite directions, the output sequence will be the phase conjugate of the input sequence [3A.4, 3A.7]. About 50 data bits were stored and recalled using a continuous-wave laser system in the co-propagating configuration. Single-shot input and output data sequences are shown in Fig. 3A.2. The 25 MHz data rate was limited by the electronics driving the acousto-optic modulator. The input energy in each data bit was about 200 pJ [3A.6].

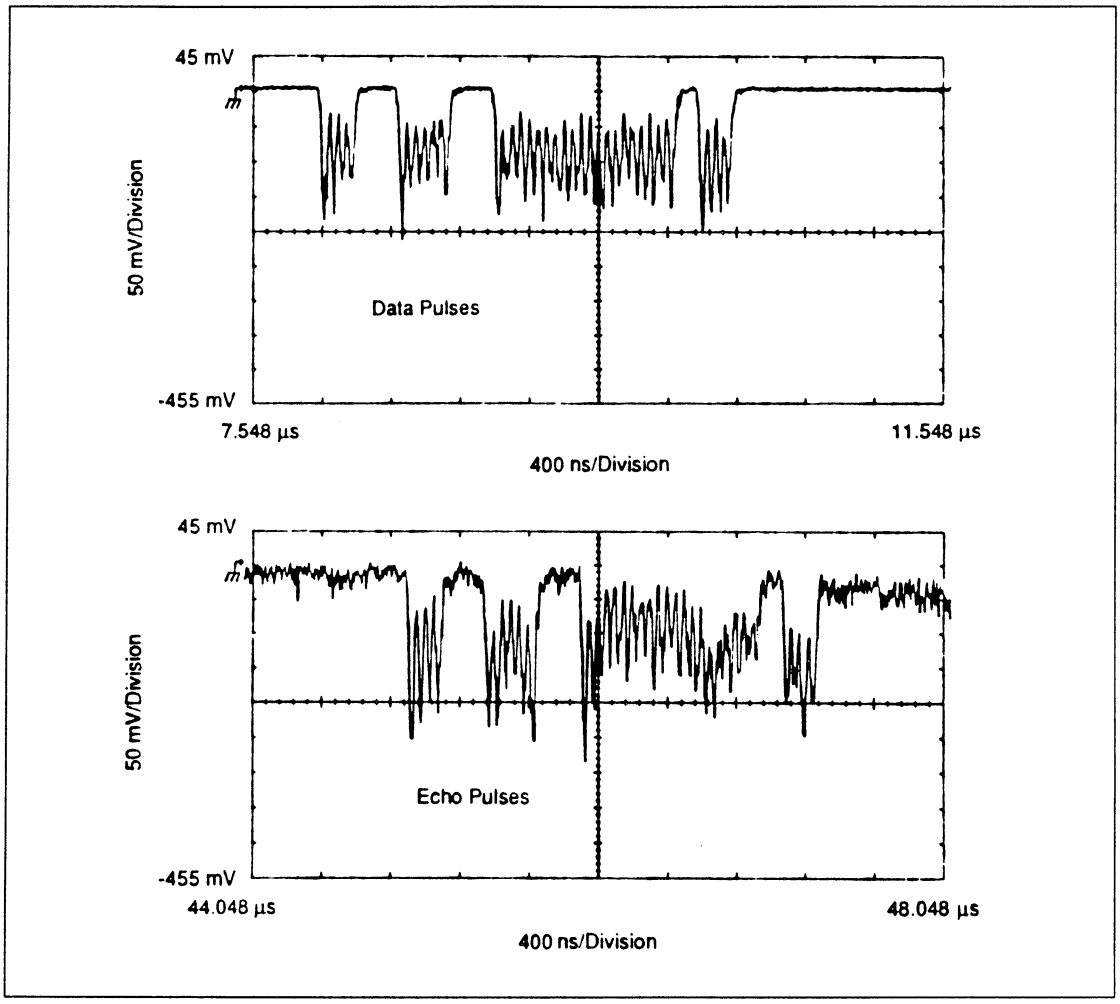

Fig. 3A.2. Multi-bit storage in a single spatial point; input data sequence (above) and output data sequence (below).

By focusing the three input beams (data, read & write) into the crystal and encoding them with image information, image processing (convolution and correlation of images) may be performed [3A.4,3A.7, 3A.8]. In particular, a whole series of pictures (corresponding to the data sequence above) may be stored in the crystal and the correlation between each of these and a read image may be the basis of a very high-speed image processing or pattern recognition system [3A.7,3A.9].

The continuation of this work in Lund will focus on fundamental as well as applied aspects of photon echoes in rare-earth-doped crystals.

3B. Optical harmonic generation at the MAX synchrotron radiation facility

Synchrotron radiation is an excellent source of intense, directed and polarized light covering wavelengths down to the extreme ultraviolet. However, the spectral brightness and coherence are much below that of laser sources. Lasers, on the other hand, offer a limited wavelength range in the UV. One way of overcoming the problem of low brightness in synchrotron radiation is to use a free electron laser (FEL). A FEL is basically a wiggler/undulator within a cavity. The useful operational time of a FEL is, however, limited due to the fast deterioration of the cavity mirrors in the intense synchrotron radiation field. We have investigated a method of producing coherent light from an undulator in the MAX electron storage ring. This method does not depend on cavity mirrors or on any absorbing nonlinear medium. The experiment was performed in two periods (of one week each) in 1989 [3B.1-3B.4]. The experimental set-up consisted of standard equipment readily available at our laboratory and the MAX facility, see Fig. 3B.1.

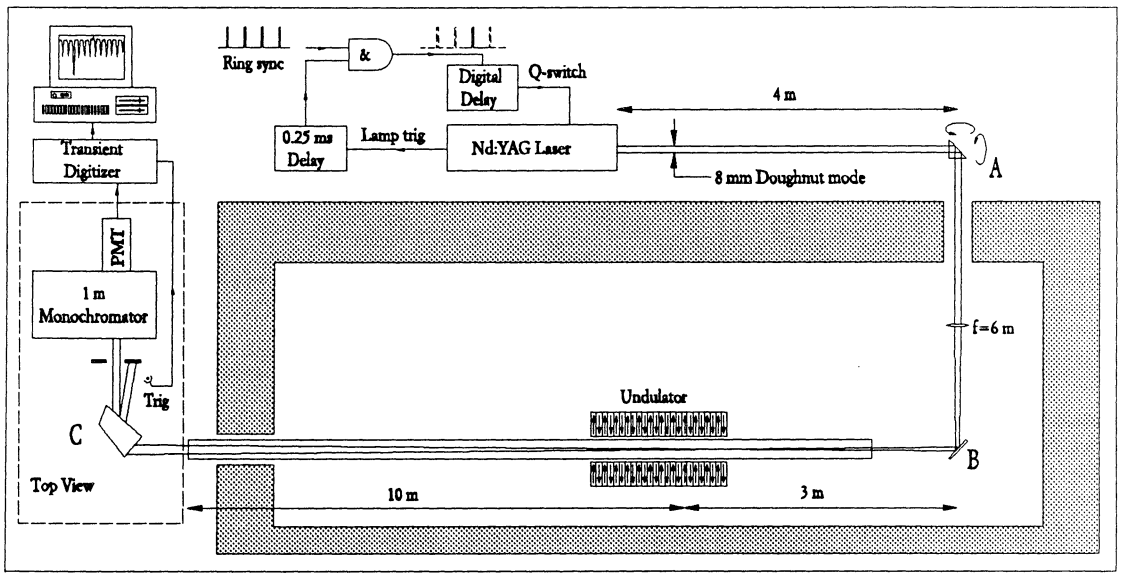

Fig. 3B.1 Overall view of the set-up of the laser harmonic generation experiment at the MAX lab. The laser was placed on the roof of the radiation shield.

The current in the storage ring is carried by electrons in (macro) bunches. The duration of one bunch is approximately 80 ps which makes the temporal characteristics of the synchrotron light well suited for time-resolved spectroscopy. The ring can be operated in a multi- or single-bunch mode. We used the single-bunch mode in our experiments. The light sources (electrons) in one bunch are not correlated. A laser field can, however, induce correlation in the electron positions. A much simplified view of the physics in the undulator is as follows. In the first part of the undulator the electrons and the laser field interact, creating an energy spread in the bunch (see Fig. 3B.2).

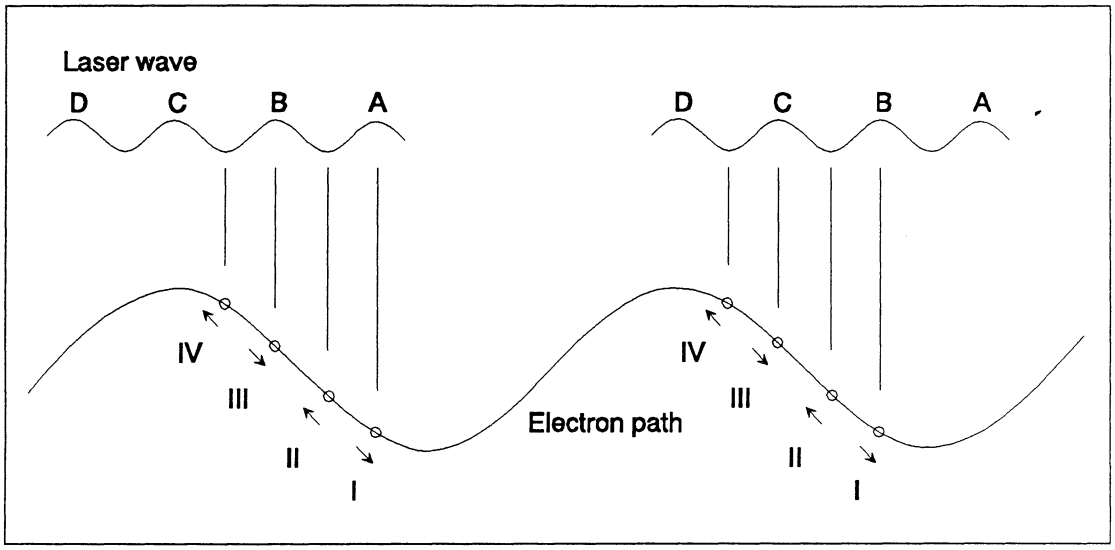

Fig. 3B.2 Schematic view of the energy exchange in the undulator with the laser beam present.

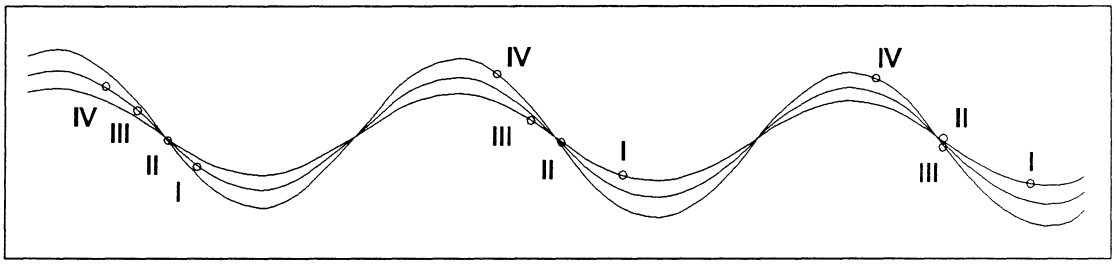

Fig. 3B.3 The micro-bunching process due to the energy spread induced by the laser.

The electrons gain or loose energy depending on the phase of the laser field at the position where the electrons are located. The electron energy is thus modulated with a wavelength equal to that of the laser. The electrons in the bunch that have increased their energy will take a slightly straighter path in the (dispersive) middle part of the undulator and vice versa (see Fig. 3B.3).

The difference in path length will result in a micro-bunching of the electrons with a period equal to the laser wavelength. In the third and last part of the undulator (there are of course no sharp boundaries between the three processes in the undulator but this provides a useful picture when discussing the interactions) the electrons will radiate with a coherent part at the fundamental wavelength of the laser and at every odd harmonic such as the third, fifth and so on. In the experiment at the MAX the third harmonic at 355 nm was detected and in future experiments higher harmonics and the feasibility of using a tunable dye laser source will be investigated. The generation of 355 nm light was not critically dependent on the pulse energy from the laser, which implies that the generation of tunable radiation for atomic physics can be attained with a dye laser. Fig. 3B.4 shows the generation of coherent (and incoherent) light for different experimental situations.

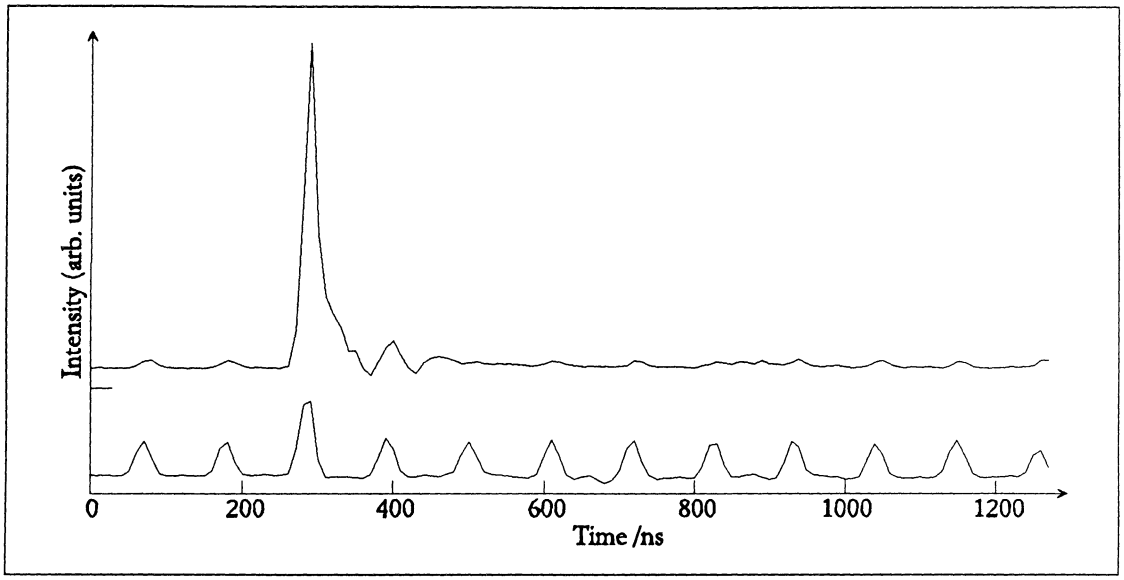

Fig. 3B.4 Intensity of coherent and incoherent radiation at 355 nm as a function of time. Each peak represents radiation from one pass of the electron bunch. The distance between two peaks is 108 ns; one revolution of the electrons in the ring. The laser was strobed on the third peak.

Table 3B1. Number of photons and FWHM at the third harmonic (355 nm) of the Nd:YAG laser

	Measured	Theory
Coherent photons/bunch	$4.5\ 10^4$	$9.8\ 10^7$
Incoherent photons/bunch	$9.3\ 10^2$	$2.8\ 10^3$
Ratio	48	$3.9\ 10^4$
FWHM	≤ 0.015 nm	≤ 0.003 nm

The number of photons/bunch, the ratio between incoherent and coherent photons and the bandwidth of the radiation was measured and compared with the results of theoretical calculations. There is a rather large discrepancy between theory and experiment, as can be seen in Table 3B.1 but the difference can be explained by the poorly known initial parameters, such as energy spread, in the storage ring and the time structure of the laser pulse.

3C. Holography and phase conjugation

Experiments with light-in-flight holography (LIFH) using a picosecond system consisting of a mode-locked argon laser synchronously pumping a cavity-dumped dye laser have been performed in cooperation with Prof. N. Abramson, Royal Institute of Technology, Sweden.

Illustration of pulse front propagation - The light-in-flight technique is suitable for studying light itself and we have, in various ways, studied how light propagates through different optical components, e.g. for educational purposes. Using a block of material, with large Mie scattering, we were able to make holograms of pulse fronts that show such relativistic effects as the apparent rotation of a pulse front.

Experiments with view-time expansion - In two experiments we have demonstrated the possibility of increasing the viewing time in LIFH. In the first experiment [3C.1] we used a skew reference wave. In normal LIFH the greatest exposure time over the photographic plate will be obtained when the reference beam falls nearly parallel to the plate. This means that the time scale on the plate is given by the speed of light. The time required for the pulse to travel over the plate can then obviously be increased by using a skew reference wave with the pulse front leaning backwards. One way to achieve this is described in Ref. [3C.2] where a grating was used to tilt the wave-front, thereby increasing the timescale over the plate by more than a factor of two compared with the maximum achievable value using normal pulses with the pulse front perpendicular to the direction of propagation.

In the second experiment, a Fabry-Perot interferometer was placed in the reference beam to produce a coherent pulse train [3C.3]. This resulted in a number of images recorded at different moments in time. One obvious advantage with this method is that the geometrical distortions seen when the observers moves sideways in front of the holographic plate are reduced.

LIFH in dispersive media - Some experiments with LIF through turbid media have also been performed. The aim is to be able to detect an absorbing object inside a highly scattering sample. Pico-second laser pulses are used to irradiate the sample and by allowing the transmitted light and a reference beam to interfere on a photographic plate a hologram is created. A time shutter is created on the hologram when there is an angle between the two beams. And by observing only the first transmitted light an image of the hidden absorbing object can be obtained. For further information about applications see section 6D.

Various experiments have been performed with BSO crystals used as phase-conjugating optical components. In this material the photo-refractive effect is responsible for the phase conjugation. With green light from an argon-ion laser of low intensity it was possible to obtain phase compensation in real time through a phase-distorting glass plate. This crystal has also been used for real-time holographic experiments. Further experiments will be performed to increase image quality and image brightness. In two-beam coupling these crystals will be used in combination with LIFH.

References

3A.1. S. Kröll, E.Y. Xu, M.K. Kim, M. Mitsunaga and R. Kachru, "Intensity dependent photon echo relaxation in rare earth doped crystals", Phys. Rev. B**41**, 11568-11571 (1990).

3A.2. S. Kröll, E.Y. Xu and R. Kachru, "Influence of excited state Pr^{3+} on the relaxation of the Pr^{3+}:$YAlO_3$ $^3H_4$-$^1D_2$ transition", submitted to Phys Rev B.

3A.3. E.Y. Xu, S. Kröll, M.K. Kim, M. Mitsunaga and R. Kachru, "Intensity dependent photon echo relaxation in solids", poster presentation at the Interdisciplinary Laser Science V Conference, Stanford, CA, USA, august 27-31, 1989.

3A.4. S. Kröll, E.Y. Xu, R. Kachru and D.L. Huestis, "Optical data storage and image processing in rare earth ion doped crystals using stimulated photon echo", p. 342-345 in *Nonlinear Optics in Solids*, Ed. O. Keller, Springer-Verlag 1990.

3A.5. S. Kröll, E.Y. Xu and R. Kachru, "Influence of magnetic field on the relaxation of the Pr^{3+}:$YAlO_3$ $^3H_4$-$^1D_2$ transition", manuscript in preparation.

3A.6. S. Kröll, L.E. Jusinski and R. Kachru, "Frequency chirped copropagating multiple bit stimulated echo storage and retrieval in Pr^{3+}:$YAlO_3$", submitted to Opt. Lett.

3A.7. E.Y. Xu, S. Kröll, D.L. Huestis, R. Kachru and M.K. Kim, "Nano-second image processing using stimulated photon echoes", Optics Lett. **15**, 562-564 (1990).

3A.8. E.Y. Xu, S.Kröll, M.K. Kim, D.L. Huestis and R. Kachru, "Nano-second spatial image processing using stimulated echo in solids", Invited talk (R Kachru) at the Interdisciplinary Laser Science V Conference, Stanford, CA, USA, august 27-31, 1989.

3A.9. R. Kachru, E.Y. Xu, S. Kröll, D.L. Huestis and M.K. Kim, "All optical image processing and pattern recognition using optical stimulated echo", patent application.

3B.1. S. Werin, M. Eriksson, H. Hallstadius, A. Persson, S. Svanberg, Experiments Towards Achieving Laser Harmonic Generation at the MAX Undulator., Memorandum MAX-Lab (1989).

3B.2. S. Werin, J. Larsson, A. Persson, S. Svanberg, M. Eriksson, Report of the First Results in Coherent Harmonic Generation Using the MAX Undulator, Svenska fysikersamfundets sektionsmöte Atom och Molekylfysik, nov. 16, 1990. Linköping

3B.3. S. Werin, M. Eriksson, J. Larsson, A. Persson, S. Svanberg, First Results in Coherent Harmonic Generation Using the Undulator at the MAX-Lab Electron Storage Ring., Nucl. Instr. and Meth. A290, 589, (1990)

3B.4. S. Werin, M. Eriksson, J. Larsson, A. Persson, S. Svanberg, Harmonic Generation at the MAX-lab Undulator - Report of the First Results, Twelfth International Free Electron Laser Conference (FEL 90), Sept. 17-21, 1990. Paris.

3C.1. N. Abramson, S.-G. Pettersson, and H. Bergström, Light-in-flight recording. 5: Theory of slowing down the faster than-light motion of the light shutter, Appl. Opt. **28**, 759 (1989).

3C.2. S.-G. Pettersson, H. Bergström, and N. Abramson, Light-in-flight recording. 6: Experiment with view-time expansion using a skew reference wave, Appl. Opt. **28**, 766 (1989).

3C.3. S.-G. Pettersson, H. Bergström, and N. Abramson, Proceedings of the International Symposium on Display Holography **III**, 315 (1988).

4. COMBUSTION DIAGNOSTICS

Sara Agrup, Marcus Aldén Per-Erik Bengtsson, Per Cederbalk, Hans Hertz, Thure Högberg, Peter Kauranen, Stefan Kröll, Christer Löfström, Lars Martinsson, Anders Nilsson, Göran Olson, Sune Svanberg and Ulf Westblom.

The current environmental situation in combination with the desire for optimized energy utilization have over recent years, made research concerning combustion processes a very important field. To, among other things, facilitate and initiate collaborations in Lund within this highly interdisciplinary area, a Combustion Centre where several departments at Lund Institute of Technology participate, has been formed. The Division of Atomic Physics is one of these participants. Its activities within the Centre, which mainly lie in the area of laser combustion diagnostics, are described below.

4A. Laser-induced fluorescence

In the field of laser-induced fluorescence several different experiments have been performed. As a continuation of the work on simultaneous, multiple-species detection in flames using spectral coincidences [4A.1], an investigation of the photo- chemical effects described were made. In Ref. A1 it was found that the OH fluorescence intensity detected at 310 nm and induced at 287 nm could be enhanced in the reaction zone by simultaneously exciting NO at 226 nm. By using two different dye laser systems which allow the use of two independently tunable wavelengths, and investigating the different parts of the flame spectrally, it could be deduced that the additional OH was due to the dissociation of nitrous oxide by a 226 nm photon into N_2 and $O(^1D)$ followed by the reaction: $O(^1D) + H_2O - 2\,OH$ [4A.2].

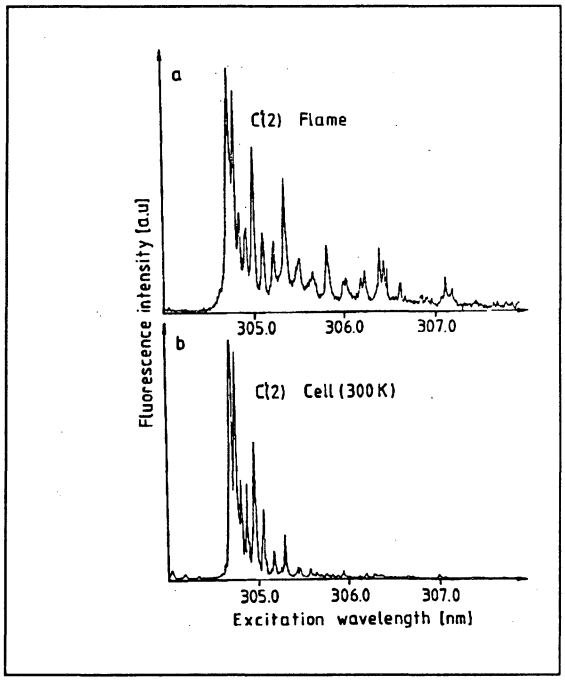

Fig. 4A.1.
Laser excitation spectra from the C'(2) of NH_3 state: a) in a NH_3 /O_2 flame; b) in a cell at room temperature.

A molecule of interest in combustion that has so far not been detected in a flame environment using laser-induced fluorescence is ammonia, NH_3 . In Ref. A3, it was shown that a newly discovered, two-photon, allowed transition could be used to induce fluorescence in flame environments.

Fig. 4A.1 shows fluorescence excitation scanns from ammonia recorded in a flame (a) and in a cell (b). The highest fluorescence intensity was induced at around 305 nm

but there were also weaker bands at around 285 nm. Investigations of spectral coincidences revealed that ammonia could be simultaneously excited with OH at around 305 nm and with NO, O and OH at around 226 nm and 287 nm, respectively. In this experiment the same frequency generation scheme as in Ref. A1 was used, doubling to 287 nm, followed by mixing with the residual IR from the Nd:YAG laser to 226 nm, the wavelength used to excite NO and O. In these experiments it has thus been shown that it is possible using one laser system, to excite simultaneously,the species OH, NO, O_2 , NH_3 and O.

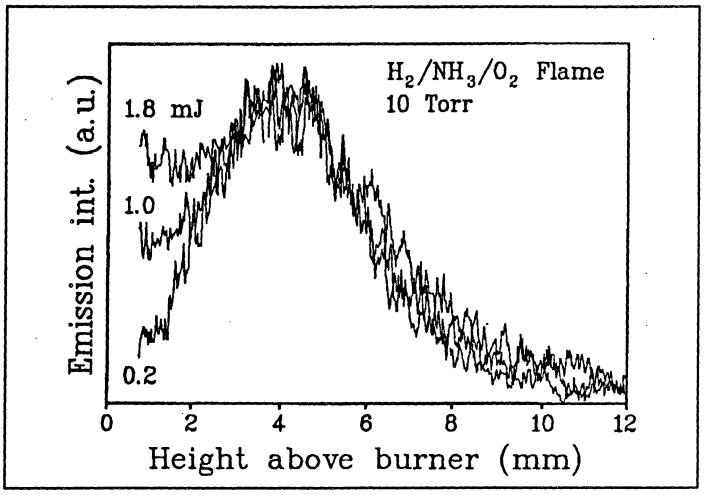

Fig. 4A.2.
Height profiles of the atomic nitrogen signal at 870 nm in a low pressure ammonia/hydrogen/oxygen flame recorded using different laser power.

The possibility to detect nitrogen [4A.4-6] and carbon [4A.7] atoms in flames has been investigated using two-photon, laser-induced fluorescence. The N atoms were excited at 211, nm followed by detection in the 700-800 nm spectral region, while the C atoms were excited at 280 nm and detected at around 910 nm. During the course of the N atom work it was realized that photo-chemical effects were present, producing nitrogen atoms from, e.g. NH_3 , N_2O and N_2 . In addition to these photo- induced signals, fluorescence from oxygen and hydrogen atoms was also detected, which were resonant with the two-photon atomic nitrogen resonance (see Fig. 4A.5 in the next section). Fig. 4A.2 shows height scans recorded at different laser powers in a low pressure flame, indicating a contribution from photo-chemically created N atoms in the early part of the scan. In the C atom work strong fluorescence from the C_2 molecule was also detected. Power dependence measurements, height scans in acetylene/oxygen and ethylene/oxygen flames and time-resolved studies showed that the C atom fluorescence and the C_2 fluorescence exhibited similar behaviour, indicat-

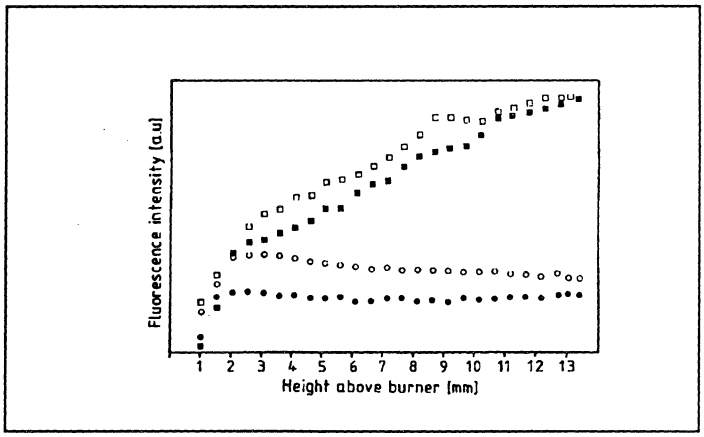

Fig. 4A.3.
Height profiles of the C atom fluorescence (filled symbols) and of the C_2 molecule fluorescence (open symbols) recorded for two different C/O ratios. Circles: C/O = 0.72, squares: C/O = 0.84.

ing a common photo-chemical origin. Fig. 4A.3 shows height scans in an atmospheric ethylene/oxygen/ nitrogen flame for both C atom and C_2 molecule fluorescence. This work is at the present time being pursued in more detail in our laboratory [4A.7].

In cooperation with Arne Rosén and Erik Fridell at the Chalmers University the hydroxyl radical has been detected above a catalytic surface [4A.8]. In this work it was found that the OH fluorescence intensity falls off continuously outside the surface at pressures around 10 mTorr, indicating that the creation of OH in the gaseous phase does not occur.

Studies to determine the possibility of two-dimensional velocity measurements using a single mode YAG have been made. A more detailed description of the principle of the technique has been described elsewhere [4A.9] and so will not be reviewed here. The principle is based on the utilization of a narrow bandwidth laser fixed in the wing of some absorbing seed species in the studied gas, in our experiment I_2. The tests performed showed that the YAG laser could be temperature-tuned onto different resonances in iodine and could induce a strong fluorescence signal. In the near future more work will be carried out within this project directed towards time-resolved, two-dimensional velocity measurements.

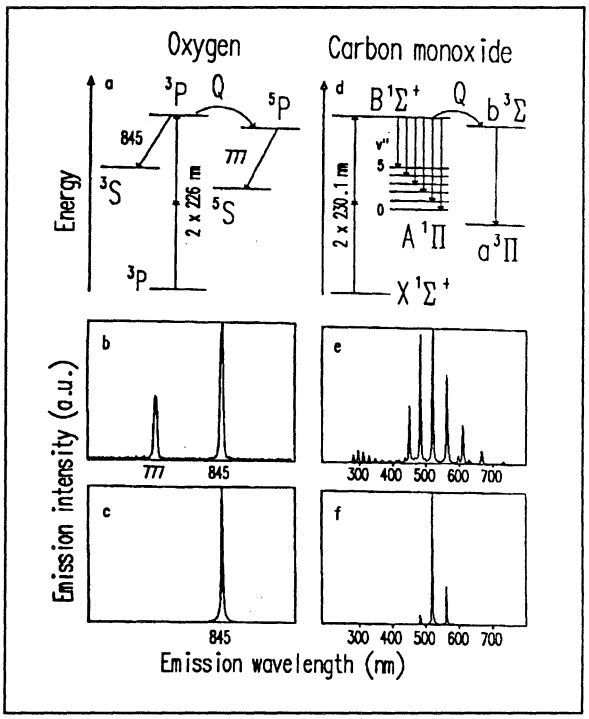

Fig. 4A.4.
a) atomic energy levels; b) dispersed fluorescence spectrum of atomc oxygen; c) dispersed SE spectrum of atomic oxygen;d) CO energy levels;e) dispersed fluorescence spectrum of CO;

Stimulated Emission - We have recently investigated the physics and the diagnostic capabilities of stimulated emission (SE). Although not as sensitive as laser induced fluorescence (LIF) for the detection of minor species, it could be a diagnostic tool of preference in, for instance, high pressure environments with limited optical access. A particular advantage of SE is that the emitted light goes into a coherent beam so that all of it can be collected. Because of the collection efficiency and the fact that the rate of stimulated emission can compete more effectively with the rate of quenching than can spontaneous emission, the SE signal can be several orders of magnitude stronger than the LIF signal.

The first experiments with SE concerned atomic oxygen [4A.10]. In this work LIF detection was also carried out for comparison. The elementary building blocks of all fuel molecules, i. e. the light atoms O, C, H, N, and S are of great importance and,

using SE, the first optical detection of atomic carbon in a flame was performed [4A.11, 4A.16]. A separate investigation of SE as such and of SE for diagnostic purposes was made on O and CO [4A.12, 4A.14, 4A.15]. The spectral emission characteristics of these species compared with those of LIF detection are displayed in Fig. 4A.4.

Our most recent study is of atomic nitrogen in a flame, also for the first time ever, by SE [4A.13] and LIF [4A.4] detection. Experiments were performed in order to establish the circumstances under which the detection is possible and what the restraints due to photochemical effects are. The presence of such effects is indicated in Fig. 4A.5, representing the LIF emission from an NH_3 /O_2 flame after nitrogen excitation, where O and H atom emission is seen in addition to the N atom signal.

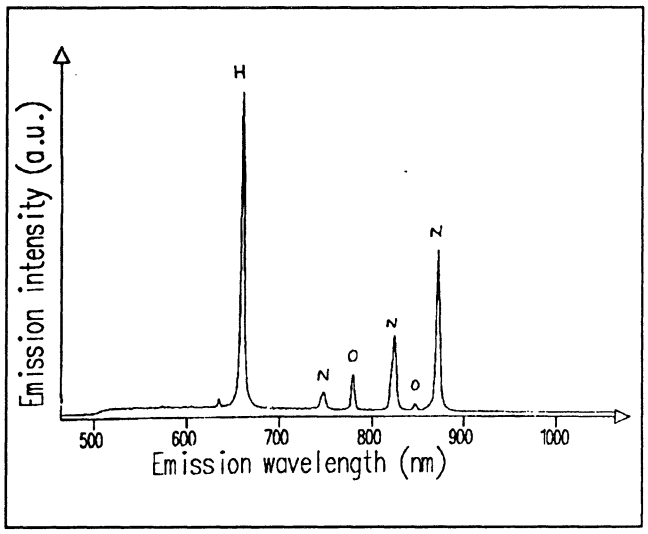

Fig. 4A.5.
LIF emission of an NH_3 /O_2 flame upon two-photon atomic nitrogen excitation

The flame profiles measured under similar experimental conditions by the LIF and SE techniques respectively, were found to be in close agreement. However, a large amount of theoretical work on the description of the SE process remains to be done before the SE method can give quantitative results.

Pico-Second Laser-Induced Fluorescence - In flames at atmospheric pressure, the collisional quenching rate is much higher than the emission rate. In order to get absolute atomic and molecular number densities from the LIF measurements, it is therefore necessary to know the quenching cross-section. The experimental scheme used by Bergano et al. (Opt Lett 8 (1983) 443), for the measurement of this quantity, has been set up at the Combustion Centre.

The two main parts of the experimental set-up are a pico-second pulsed Nd:YAG laser and a streak camera. To be able to control the amount of initially excited species, one has to use a laser pulse which is so short that there is small probability for quenching to take place during the excitation. This is achieved by a laser pulse of a few ps. The decay of the fluorescence light after the laser pulse, gives the fluorescence rate plus the quenching rate coefficient. The time resolution required, in the order of ps, is given by the streak camera.

With this equipment it will be possible to measure the quenching cross-sections for several flame constituents. Preliminary experiments in a cell of CO have been done, to obtain the effective fluorescence life time. The work to be taken up in the immediate future is the measurement of quenching factors and collision cross-sections for CO and atomic oxygen in flames.

4B. Coherent anti-Stokes Raman scattering (CARS)

In the laser diagnostic technique called coherent anti-Stokes Raman scattering (CARS) a laser beam carrying information on the population distribution in rotational and vibrational molecular states is generated in a measurement volume which is spatially confined to the overlap region between three focused laser beams. A typical experimental set-up is shown in Fig. 4B.1 and a CARS spectrum of high resolution is shown in Fig B2. The CARS signal generated carries information on the instantaneous (10 ns) concentration of species and temperature. Also non-equilibrium type

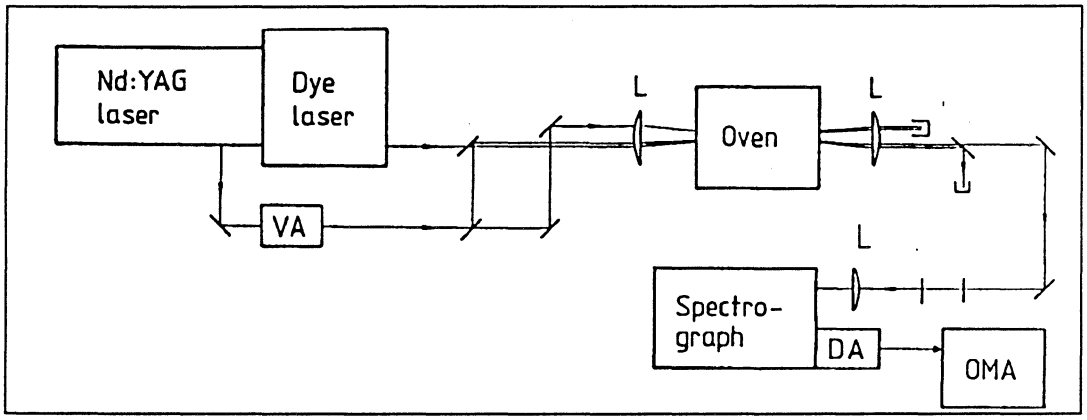

Fig. 4B.1.
Schematic layout of experimental CARS set-up showing the laser beams focussed and overlapped in the measurement volume and the spatially and spectrally isolated CARS signal entering the spectrograph and detection equipment

(e.g. non Boltzmann) temperature distributions can be determined. Some of the advantages of the technique are:

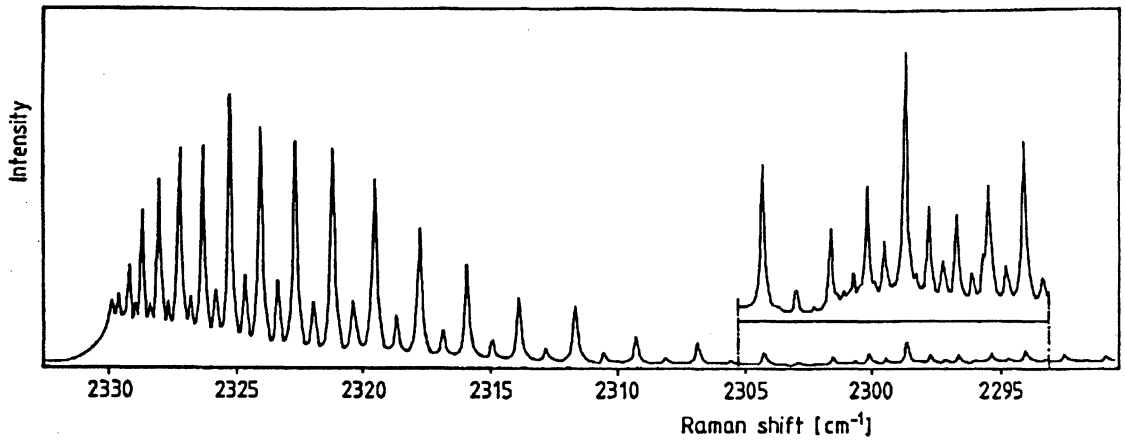

Fig. 4B.2.
High resolution vibrational CARS spetrum of the nitrogen Q-branch

- Directionality of signal which makes possible spatial filtering to supress luminous background.
- Instantaneous measurement. Probability distribution functions of temperatures in a turbulent environment can be recorded.
- Remote sensing technique. No (mechanical) perturbation of the measurement object.

The accuracy and precision of CARS - Several aspects concerning the accuracy and precision of CARS thermometry have been investigated. While detector and shot noise limit the precision at low signals, the single-shot standard deviation in broad-band CARS thermometry when high signal levels can be obtained is limited by stochastic variations of the laser intensity as a function of frequency. The influence of these variations on the signal-to-noise ratio and therefore also on the temperature precision have been modelled in collaboration with the Department of Mathematical Statistics [4B.1,4B.2]. The theoretical predictions were tested against experimental, standard deviations in single-shot, temperature measurements made on the basis of several different experimental approaches and resulted in a general agreement within about 20% for the configurations tried [4B.3,4B.4]. The best temperature precision was obtained using so called dual, broad-band techniques [4B.5] where two of the laser beams (i.e. two of the photons in the four photon interaction process) are generated by dye lasers operating in the broad-band configuration and for rotational CARS thermometry we are now using this type of technique exclusively. The accuracy of vibrational CARS thermometry has been investigated by studying systematic errors introduced due to inaccurate knowledge of experimental and molecular parameters [4B.6,4B.7]. Generally the combined inaccurary due to such systematic errors can be limited to about 1 %. Several additional measurements were performed in this work. The maximum laser intensity that could be used without affecting the temperatures determined were studied. While the vibrational population distribution is fairly susceptible, the rotational population distribution is more stable to high laser intensity. The non-linear gain characteristics of the diode array detectors used for signal detection were investigated and our computer code for determining temperatures from experimental data was described and tested [4B.6]. All these investigations supported our assumption that we could reliably report single-shot temperatures with an error less than 50 K.

The concentration of an element can be determined from the CARS spectral signature from the interference between a molecule-specific resonant signal and a uniform, non-resonance background [4B.8,4B.9]. The ratio of the signal strength of these contributions may depend on the fluctuations of the laser intensi because the two contributions have different response times. The intensity fluctuations of two of our YAG laser systems have therefore been investigated and characterized by a mathematical model for different operating conditions [4B.10].

Rotational CARS - Performing rotational CARS was initially considered to be experimentally difficult in comparison with vibrational CARS, but recent developments [4B.5] have significantly simplified and improved the rotational CARS technique. Several different approaches to rotational CARS were tested with regard to ease of operation, signal strength and, as mentioned earlier, single-shot temperature precision [4B.3]. As shown in Table B1 the signal strength obtainable differs significantly for different experimental approaches. Although the temperature sensitivity at flame temperatures is generally better for vibrational CARS, rotational CARS has a number of potentially attractive features [4B.11-4B.13]. In particular, rotational CARS could be attractive at high pressures, sooty environments and for multiple species detection. As mentioned above, rotational CARS is also less sensitive to high laser intensities. The possibility of using excited vibrational states for thermometry is also discussed in Ref. B11.

	Pulse energy (mJ)			Peak signal strength (counts)	
	ω_a	ω_b	ω_c	N_2, 1 atm T=295 K	Flame, 1 atm T=1800 K
RDBC(DCM)	33	33	57	$5\cdot10^6$	$3\cdot10^3$
RDBC(R 610)	51	51	57	$2\cdot10^7$	$3\cdot10^3$
RDBC(2 dyes)	33	45	18	$4\cdot10^5$	$5\cdot10^2$
CRC(R 610)	33	20	18	$1.5\cdot10^5$	$4\cdot10^2$
CRC(C 500)	82	9	80	$1\cdot10^6$	$6\cdot10^2$

Table 4B.1.
Pulse energies for input laser beams and resulting peak signal strength for different rotational CARS techniques

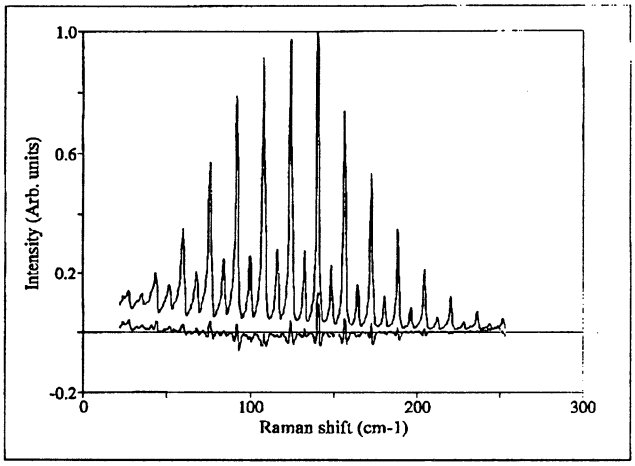

Fig. 4B.3.
Experimental rotational CARS spectrum of pure nitrogen at 599K and 15 bar (upper curve). Lower curve is the difference between the experimental spectrum and the theoretical fit. Evaluated temperature is 589 K

High pressure rotational CARS - In order to investigate the capability of rotational CARS to function as a tool to determine the time and space-resolved temperature and the concentration of major species in high temperature, high pressure applications, a systematic study of nitrogen thermometry under these conditions has been performed. The spectra were generated in pure nitrogen enclosed in a high pressure cell (maximum 18 bar), which was placed in a high temperature oven that can attain a temperature of 2300 K. The true temperature in the oven was measured with a thermocouple. The temperatures of the recorded spectra are evaluated by a least-square fit to a library of theoretical

spectra calculated for different temperatures. Both the fitting programme and the programme that calculates the theoretical spectra from molecular constants have been developed at the Combustion Centre from a code for vibrational CARS. The results for low temperature, 300- 900 K, and a pressure between 1 and 15 bar indicates the ability to predict the temperature in this region with an accuracy of 1-2 % for 100 accumulated spectra [4B.14]. An example of a high-pressure, rotational CARS specrumt and the best fit is shown in Fig. 4B.3.

Development of dye lasers for CARS - When employing the broad band laser techniques for generating CARS spectra one squanders most of the energy from the dye laser, as a vibrational CARS spectrum covers a width of only about 10 cm^{-1} and the rest of the broad band profile of approximately 100 cm^{-1} is not used. Therefore it would seem judicious to try to concentrate the energy from the dye laser into a width of roughly 5-10 cm^{-1}. Inserting a dispersive element into the cavity of a dye laser could be a means of achieving a spectral condensation, i.e. reducing the band width of the output signal while the total energy remains much the same. It has been shown [4B.15] that it is possible to achieve spectral condensation by inserting prisms in the cavity of a dye laser, see Fig. 4B.4. Employing one or more prisms would yield a dye laser band width of 10-15 cm^{-1} useful in CARS experiments.

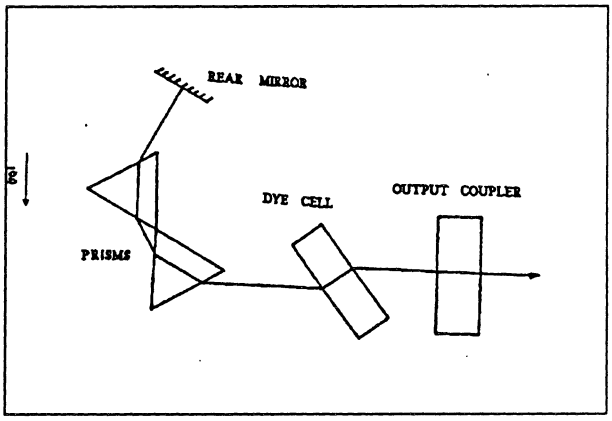

Fig. 4B.4.
The dye laser cavity

This dye laser concept has been further developed by introducing an amplifier placed after the oscillator, and using a vertical arrangement of prisms. A band width of 7 cm^{-1} has been achieved using Rhodamine 640 and one prism. Measurements have been made in colinear CARS using a dye laser with one prism and a mixture of Rhodamine 610 and Rhodamine 640. The increase in spectral intensity, i.e. the pulse energy divided by the band width, was measured to be a factor of 7. The strength of the CARS signal increased by a factor of 6, when employing the narrow-band dye laser, (26 cm^{-1}), compared to the one measured with the broad-band dye laser, (180 cm^{-1}).*CARS applications* - Of all the diagnostic laser methods under investigation, temperature measurements by vibrational CARS is the one closest to being routinely used for data production on real combustion systems.

During this period we have, in collaboration with the Department of Chemical Engineering, measured the temperature profile of N_2 gas in a forced laminar tubular flow heated to 1000 C. The aim was to validate the heat transfer equations usually used to calculate the temperature profile. As a result of these measurements it was possible to determine the Nusselt number in the Nusselt equation for laminar flow

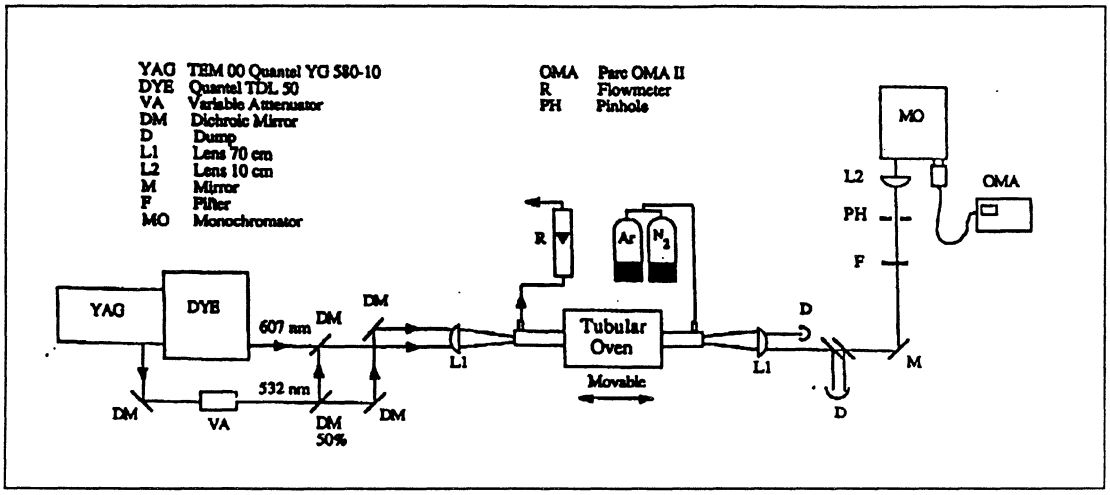

Fig. 4B.5.
Experimental set-up for temperature profile measurement in a tubular oven.

through tubes [4B.16]. These measurements were made with an ordinary laboratory set-up shown in Fig. 4B.5. An example of the results is shown in Fig. 4B.6.

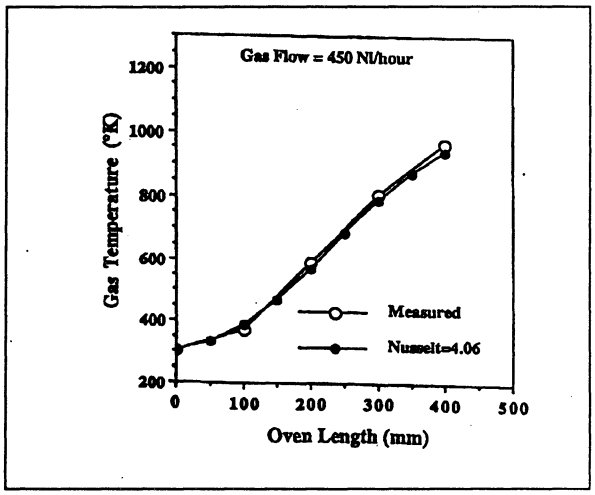

Fig. 4B.6
Temperature profile in tubular oven.

During the period increasing interest in temperature measurements on combustion systems has led us to develop a mobile CARS unit. The unit is remotely controlled (30 m) and data acquisition and data evaluation are done using a fast PC. The layout is shown in Fig. 4B.7. We have also developed and tested our own two-wavelength CARS (2-λ) method. The 2$-\lambda$ method produces a signal that is about 10 times stronger than that produced by the conventional, broad-band methods. This provides the possibility of decreasing the probe volume and using polarisation techniques to suppress non-resonant signals. Using this method the temperature can be very rapidly determined from the experimental data. The CARS unit measures the temperature over 5 ns ($5x10^{-9}$s)intervals at a rate of 10 Hz . As an example a probability density function (PDF) measured with the 2-λ method is shown in Fig. 4B.8. The first real hard test of this CARS unit will be the measurements, in October 1990, on a propane-fueled validation rig at Volvo Airspace in Trollhättan.

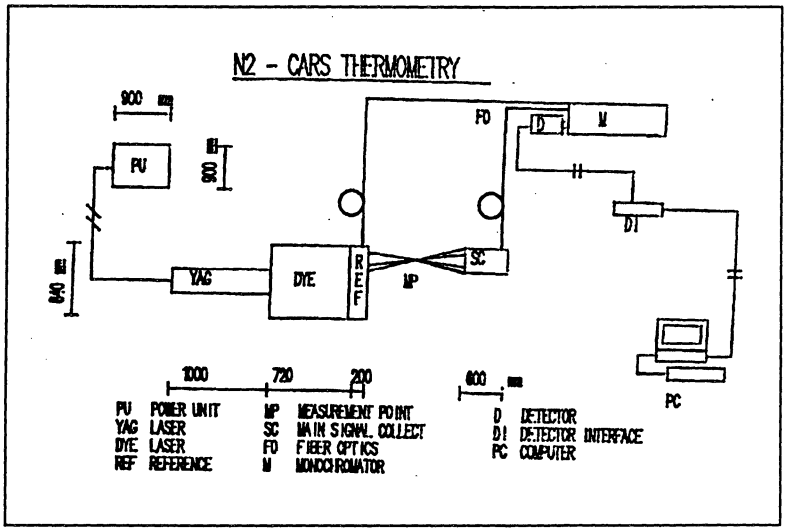

Fig. 4B.7.
Layout of mobile CARS unit

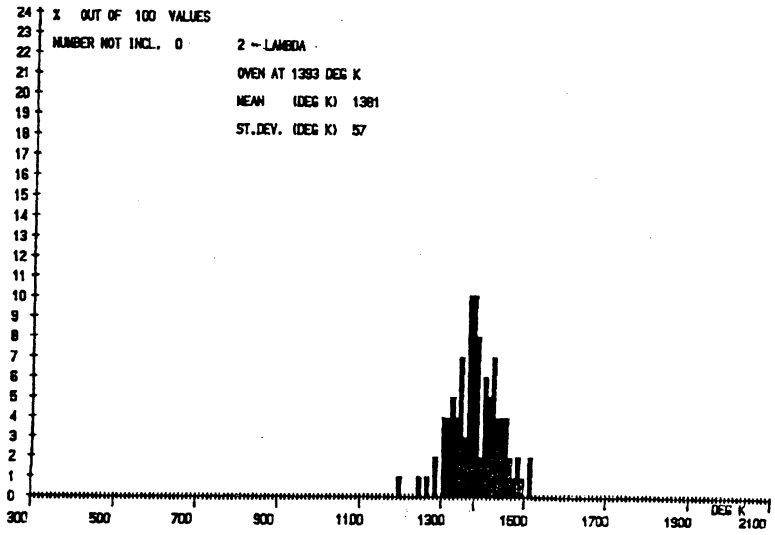

Fig. 4B.8.
Probability density function (PDF) obtained with the 2-λ method for the tubular oven

4C. Experiments related to soot formation

The starting point of the project concerning soot studies was the perceived need for determining soot properties in sooting flames. A technique was developed in which a pulsed Nd:YAG laser was used together with combined measurements of Rayleigh scattering and absorption. By measuring both absorption and scattering, information was obtained on the size of the soot particles, their concentration and their volume fraction in the pre-mixed methane/oxygen flames studied [4C.1]. By translating the burner vertically, different heights in the flame could be probed and thereby information on the time evolution of the soot parameters was obtained. In the study in Ref. C1, a home-built, porous-plug burner was used which leads more or less to results of local character, as difficulties may arise in comparing these results with those obtained by other groups. Therefore a commercially-available, water-cooled, porous-plug burner was procured from McKenna Products Inc, which has become a standard burner in the combustion research field. A study was then made to find fuel/oxidant mixtures suitable for flame diagnostics. This made demands on features such as flame stability, and required that the sooty region lifted above the burner. Mixtures of ethylene and oxygen/nitrogen fulfilled these requirements and a couple of standard flames with different equivalence ratios have been used for several

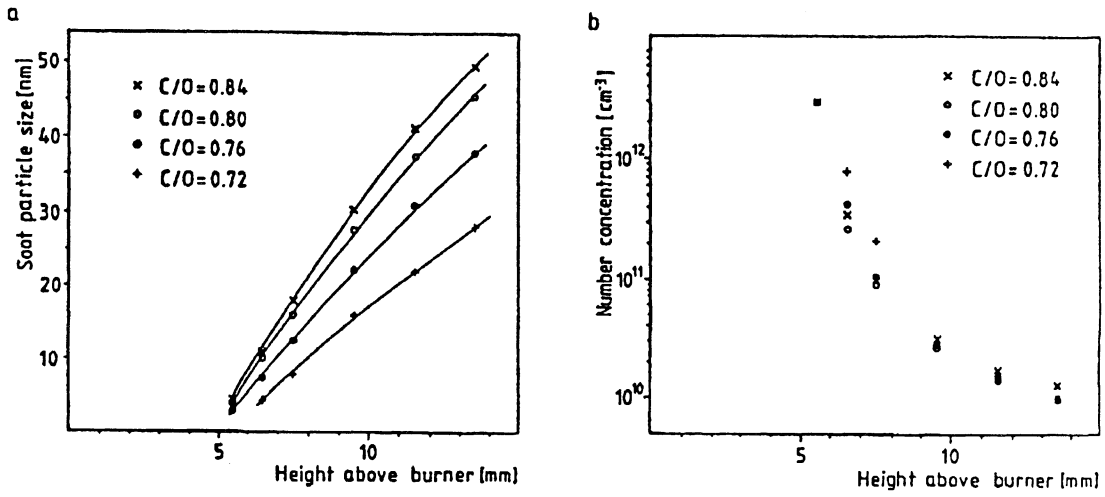

Fig. 4C.1.
Profiles of; a) soot particle size, b) soot particle concentration, evaluated from the scattering/extinction equations at different C/O-ratios

diagnostic measurements in recent years. Firstly, as described above, scattering/extinction measurements were made to characterise the soot properties in the flames [4C.2]. As shown in Fig. 4C.1 a and b, soot particle size and concentration are illustrated as a function of the height above the burner for four sooting flames with different C/O ratios. The nucleated soot particles grow very fast, whereas the numerical concentration is initially very high and decreases as a function of the height above the burner because of coagulation.

In air-fed combustion, high mole fractions of nitrogen - generally of the order of 0.6-0.7 - will be present. The nitrogen is basically inert and a diagnostic method based on nitrogen detection can thus be expected to give a high signal in any region of a premixed flame. To determine temperatures in the present flames, much work has been done with the technique of Coherent Anti-Stokes Raman Scattering (CARS), which can generally be used in two variants; Vibrational CARS and Rotational CARS. These techniques have been described in section B, and here only their applicability to sooty flame investigations will be addressed. When using vibrational CARS in sooting flames, a spectral interference was observed [4C.3-C7], and it is shown in Fig. 4C.2. The reason was that laser-produced C_2 radicals absorbed part of the generated spectrum. A way to circumvent this interference is to use two dye lasers instead of one, and then, by letting the Raman resonance couple to a narrowband dye laser, the CARS spectrum can be obtained in a region free of interference. However, this necessitates the added complexity of pumping a second dye laser. Another effect which can be seen in the spectrum in Fig. 4C.2 is the high background level at lower Raman shifts, which is due to the more pronounced non-resonant CARS background in highly sooting flames. This means that both the non-resonant background and the temperature must be fitted to obtain correct temperatures when performing vibrational CARS measurements in sooty flames.

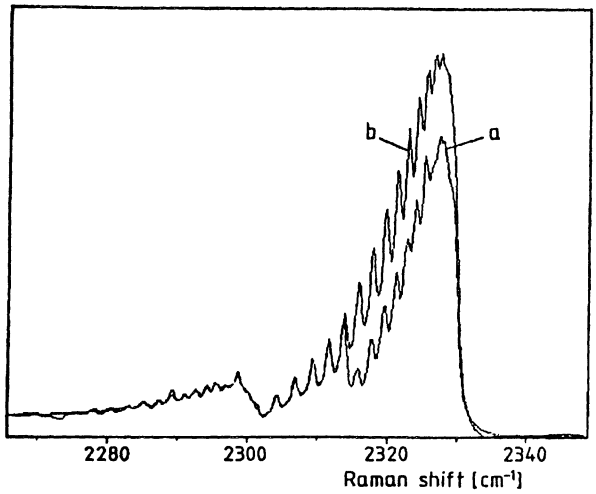

Fig. 4C.2.
Curve a: Vibrational N_2 CARS spectrum recorded in a premixed sooty ethylene/oxygen/nitrogen flame with C/O = 0.84, showing strong C_2 absorption interference for wavenumbers above 2313 cm^{-1}.
Curve b: Theoretically generated spectrum fitted to the experimental spectrum for Raman shifts ranging from 2283.0 cm^{-1} to 2312.2 cm^{-1}. Both temperature and non-resonant background were fitted.

Also the rotational CARS technique (in the dual-broadband approach) was applied to the sooty flames [4C.7-C9]. As can be seen in Fig C3, no marked spectral interference can be observed. The effect of an increased non-resonant background was not severe, as such variations did not greatly change the evaluated temperature. Perhaps the most prominent problem in the application of rotational CARS to sooty flames is the spectral vicinity of the CARS spectrum to the green laser beam at 532 nm. For example, in sooting flames a strong Rayleigh/Mie component will be scattered in the forward direction, which often results in an unwanted contribution to the signal in the detector. By adjusting the polarizations of the incident laser beams it is, however, possible to obtain the polarization of the CARS signal orthogonally to the

scattered component. This means that the scattered component can be suppressed, but at the expense of the CARS signal.

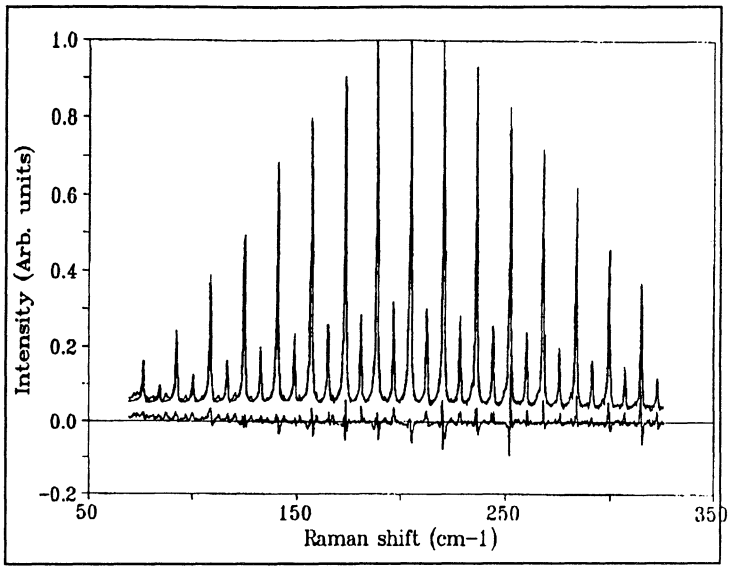

Fig. 4C.3.
Experimental and theoretical CARS spectra (above) and their difference spectrum (below). The experimental spectrum was recorded in the same flame and probe point as the spectrum in Fig. C2, and the evaluated temperature was 1625 K.

As described above, the C_2 radical can cause spectral interference effects in diagnostic situations. To suppress undesired C_2 emission signals, it is thus important to gain a deeper understanding of such interference. A study was performed in which a pulsed Nd:YAG laser beam, at wavelengths of 266, 355 and 532 nm, was focussed at different heights in the "standard" ethylene/oxygen/nitrogen flames [4C.10]. The fluorescence signals detected by the spectrograph and the optical multichannel analyzer in the visible and the C_2 Swan bands were very prominent features in the spectra obtained. It has generally been thought that laser-produced C_2 originates from laser ablation of soot particles, but the present results show C_2 bands also in soot-free regions of the flames. Various findings supported the assumption that aromatics produced the C_2 interference, even if contributions from soot in the sooty regions could not be excluded. At the wavelength of 266 nm, however, several molecules contributed to the C_2 signal and only a minor contribution came from the soot.

The question of "Which are the precursors of soot?" is very important to the soot community today. In some of the theories aromatics play an important role. In a forthcoming project, detection of benzene and the phenyl radical in "standard" ethylene flames will be investigated using laser-induced fluorescence. Also the broadband fluorescence from polyaromatic hydrocarbons (PAHs) will be investigated in greater depth with guidance from previous preliminary experiments. In conclusion, even if weak processes such as spontaneous Raman scattering are difficult to apply in the diagnostics of sooting flames, several techniques - as described above - are very promising [4C.11].

4D. Optical tomography

Tomography is an established method for the reconstruction of quantitative 2-D or 3-D, spatially-resolved measurements from multi- angular, integrated measurements (projections). Optical tomography is a versatile diagnostic technique for the study of combustion and fluid flows. However, much of the previous optical tomography work has examined stable flames and flows using sequentially recorded projections. Since many interesting flows such as explosions and turbulence, are highly fluctuating techniques for simultaneous recordings of the projections are desirable. We have developed two such techniques: an arrangement for the simultaneous recording of emission projections for the determining the distribution in flames of species in excited states, and a tunable differential interferometer for temperature and density determination by interferometric tomography.

We have demonstrated that emission tomography can yield spatially-resolved distributions of the radicals in excited states in flames [4D.1,D3]. Measurements with high temporal resolution of, for example, CH provide important information about the motion of the flame front. Such information is useful for monitoring the development of explosions or turbulent combustion. Fig. 4D.1 shows the experimental arrangement for the simultaneous recording of 3 emission projections. Reconstructions are performed with a modified MART (Multiplicative Algebratic Reconstruction Technique) algorithm which has proven to yield good quality reconstructions from as few as 2 or 3 projections. Fig. 4D.2 shows the distribution of CH in the excited state in a slot Bunsen flame as reconstructed from 3 projections. Using a Rayleigh scattering technique the distribution can be calibrated to absolute number density.

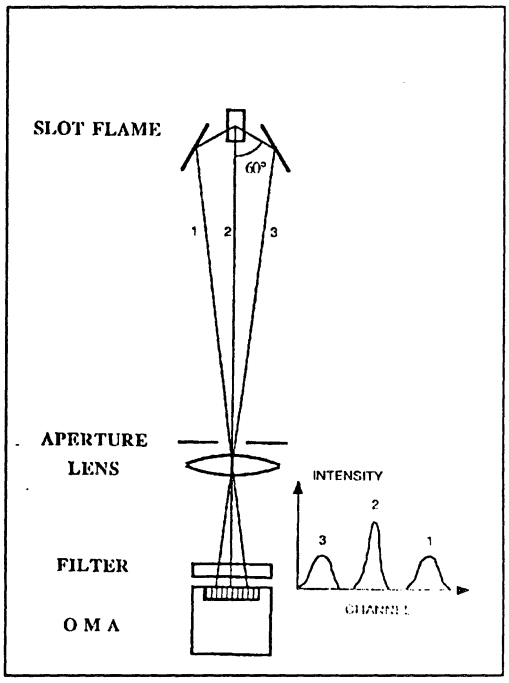

Fig. 4D.1.
Experimental arrangement for simultaneous recording of 3 emission projections with an optical multichannel analyzer

Tomographic reconstruction from integrated measurements of the phase (refractive index) can yield spatially-resolved values of temperature or density. Previously demonstrated techniques using a Mach-Zehnder interferometer and scanned beam deflection suffer from sensitivity to drift and slow data acquisition, respectively. Differential interferometers are much less sensitive than conventional interferometers to mechanical and thermal drift, since both interfering beams are geometrically superimposed. We have constructed a tunable, stable, differential interferometer which allows measurements on a wide range of fluid flows and flames [4D.2,D3]. A diagram of the interferometer is shown in Fig. 4D.3 The birefringent calcite crystal separates the vertically and horizontally polarized light by a distance Δx which can be varied by tilting the crystal. This allows

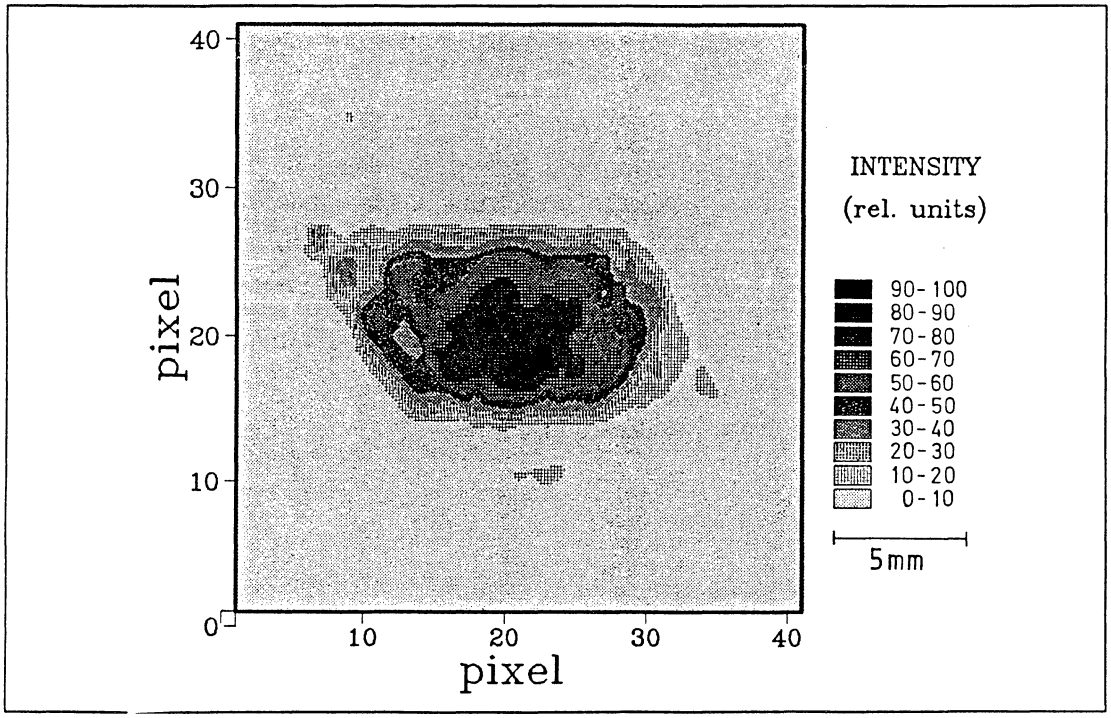

Fig. 4D.2.
Tomographic reconstruction of CH emission of a slot bunsen flame 25 mm above burner

the sensitivity of the interferometer to be matched to the gradients of the flow. Fig. 4D.4 shows a tomographic reconstruction of a rectangular methane jet in air. A multiple arm arrangement with this interferometer would allow the instantaneous recording of the projections without problems due to fringe ambiguity and drift.

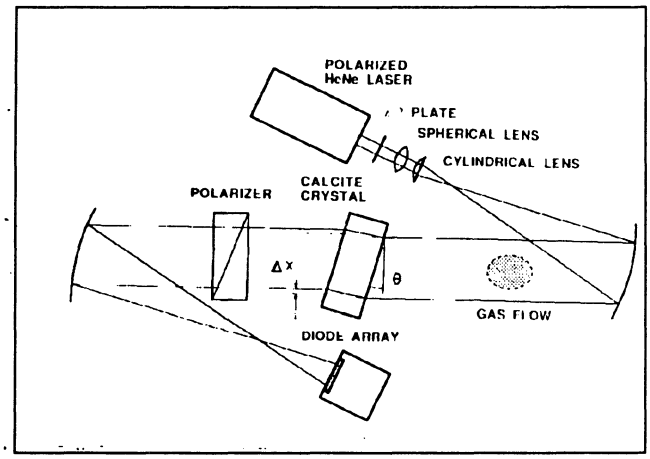

Fig. 4D.3.
Experimental arrangement for the tunable differential interferometer

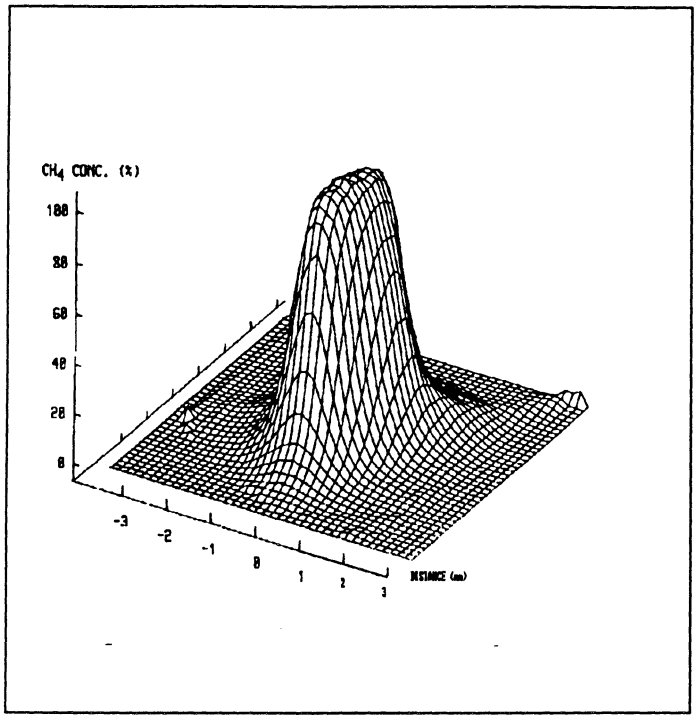

Fig. 4D.4.
Tomographic reconstruction of the concentration of methane in a subsonic asymmetric jet into air; the pixel size is 160x160 μm

4E. Chemical kinetics

Experimental investigation of low temperature hydrocarbon oxidation

Combustion chemical reactions taking place in the temperature region 200-500 C have been shown to have great importance for the occurrence of auto-ignition - a process that results in some persistent stability problems, such as engine knock and gas turbine lean combustion disturbances. For the construction of low emission combustors an increased understanding of this process is therefore of vital importance and the use of the resulting predictive model should be of great importance in the development of combustion chambers.

For this reason this project and the project concerning chemical modelling at the Combustion Centre in Lund are both principally oriented towards low temperature combustion. The modelling has now resulted in an extensive and detailed description of the chemistry [4E.1]. The model, however, now needs experimental data from a well-stirred reactor in order to be further developed to give correct predictions over a large enough range of oxidation conditions to be of interest in industrial applications.

During this two-year period a well-stirred reactor system has therefore been constructed, built and set up in a laboratory dedicated to this purpose. The system has recently been partially tested with satisfactory results. Initially, during the next stage of this project, (beginning 901001) normal- and iso- butane will be used as fuels and

experimental results, most importantly data on the concentration of stable oxidation products obtained on using gas chromatography and laser techniques, will then be used in the continuing modelling work. Later on we will pay some attention to the lighter hydrocarbons, but there is also some interest in heavier fuels like neopentane, heptanes and iso- octane.

The well-stirred reactor (WSR) - During a nine months' visit at Dr. Pilling's laboratory in Oxford 1987/88 useful experience of their first kind of WSR was gained. This was of some importance for the subsequent construction of the LTH reactor system - which, as a consequence, resulted in a stainless steel reactor equipped with a surrounding container mainly for safety reasons . One of the main differences between our reactor and the English second kind of WSR (also in stainless steel) is that ours has a modular construction with perfectly cylindric symmetry in the reaction zone, with optical access in a module connected at the reactor outlet close to the mixing region. The reason for choosing a reactor with optimal internal symmetry is that the risks for imperfect mixing are thereby minimized, which is of the greatest importance from the modelling point of view, since the model assumes perfect mixing of the reactants and the products. Slight disturbances may be expected in the British reactor, in which optical access is in the reaction region by means of optical "arms" welded to the reactor body. Certain precautions have been taken there, but it remains to be seen how good the results are. An obvious advantage of their design is that they can optically probe the gas mixing and any fast change of reaction rate without an extra delay. However, with the precise knowledge of flow rate and internal volume it should be possible to take that delay into account for the LTH reactor.

Consequently, the two well-stirred reactors are to some extent complementary, and that is a reason for cooperation between our groups. Another reason is that results from one group may need to be confirmed and/or complemented by the other to obtain more certain and/or complete information of low temperature hydrocarbon oxidation.

Both the reactors are of the jet-stirred kind with the gaseous reactants entering through a small (ca 1 mm) hole drilled in two to four of the otherwise closed metal tubes having a diameter of ca 3 mm. Jets are then established at each of the inlets, the number, position and orientation of which have been given by Bush (*S F Bush, Trans Instn Chem Engrs 47 (1969)*) to give a perfectly homogeneous mixture of gases.

Since our model will later need to be tested at higher temperatures for studies of auto-ignition prediction, we have far-reaching plans for a new reactor suited for such investigations. This reactor will inevitably be of the tubular kind and therefore it will deviate from the above-mentioned requirements for perfect mixing. With our WSR we shall be able to observe influences of improper homogenuity on experimental results by removing two of the optimal four inlets. In that way we will have a slightly tubular reactor. Larger intermediate modules may also be mounted between the two end surface flanges to produce a more pronounced tubular construction.

Another way to use the modular reactor design is to get some information on surface reactions by simply mounting an intermediate module of a different size while keeping the reactor perfectly well-mixed. This is done by mounting a half-size

cylinder open at the middle and removing two of the inlets. In that way the ratio of reactor volume to internal surface area will decrease, and consequently the surface reactions should then contribute to a greater extent under such circumstances. We will also have the possibility of observing any influence on the experimental results by the material of which the reactor surface is made by putting in glass liners which now have been made to fit both reactor sizes.

Modelling of auto-ignition

Current theories of knock in spark ignition engines seem to point to a role of the low temperature oxidation (600-800 K) of the fuel in the end gas of the cylinder. The characteristics of auto-ignition change in a systematic manner, where short and branched hydrocarbons show less tendency to ignite compared to straight and long hydrocarbons. The RON (Research Octane Number) exhibits a similar dependence on fuel structure. Morley (*C Morley, "A fundamentally based correlation between alkane structure and octane number", Combust Sci and Technol 55 (1987)*) has shown that a qualitative prediction of the RON number for a large number of different alkanes is possible on the basis that low temperature oxidation plays a role in the promotion of knock.

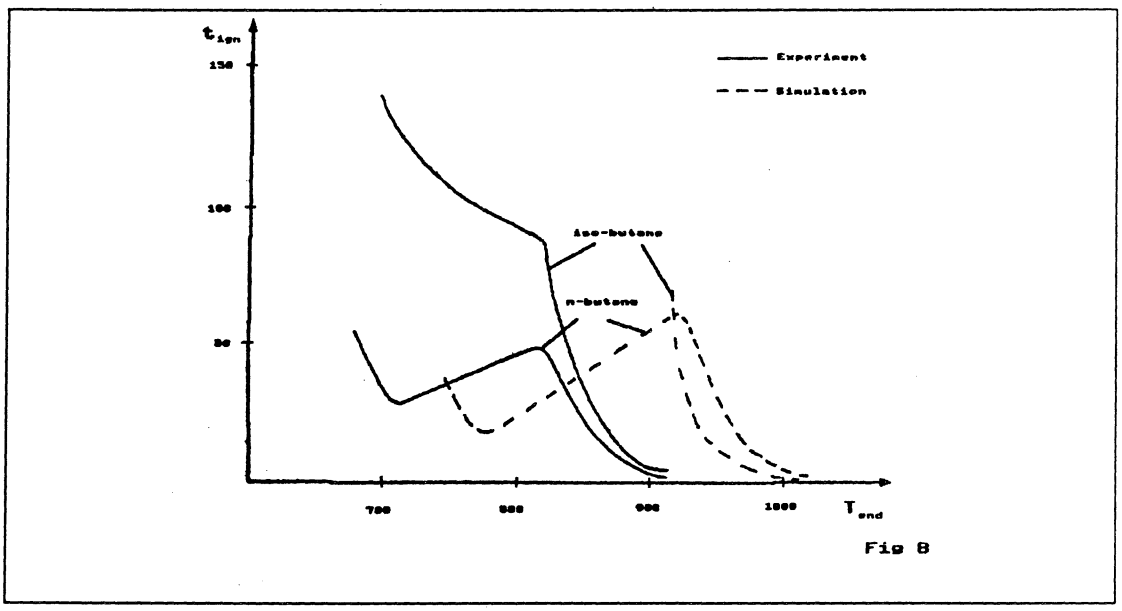

Fig. 4E.1.
Ignition delay time as a function of end-of-compression temperature for normal- and iso-butane

Results of butane modelling - The theoretical work has so far been directed towards the investigation of the low temperature oxidation in air of hydrocarbons in the NTC (Negative Temperature Coefficient) region at high pressures. Models for the oxidation of the two isomers of butane, iso- and normal-butane have been assembled. The models are an extention of a model of acetaldehyde combustion [4E.4] and their results have been compared with experimental results and are shown to work satisfactorily. The results from the modelling of butane oxidation have been compared with experimental RCM (Rapid compression Machine) data (*P Gray, D Bradle,*

J F Griffiths and W Nimmo, "Effects of turbulence and enhanced heat transfer on the spontaneous ignition of lean hydrocarbon-air mixtures", Dept of Phys Chem and Dept of Mech Eng, University of Leeds, private communication), where the ignition delay time as a funcion of end of compression temperature was determined. Some information of concentrations of fuel and intermediate species from a research engine experiment (*R M Green, "Experimental studies of end-gas autoignition", Presented at IEA 6th Task Leaders Meeting, Asilomar, September 10-13, 1985*), have also been used. The results from the modelling are satisfactory and reproduce the ignition delay times fairly well for both butane isomers.

Model reduction. If kinetic models are to be incorporated in multi-dimensional simulations, a reduction of the kinetic models will be necessary because of the fairly long computational time needed for a detailed model.

A reduction scheme has been developed and tested for the n-butane model, reducing the initial 256 reactions and 74 species to 51 reactions and 18 species with a reduction in execution time by a factor of 9. The reduction has been made in four separate steps, and the rate constants in the reduced model have been calculated from the full model, and no fitting procedure has been involved. We will try to extend the reduction of the model further to a size comparable to the model by Cox with 15 reactions (*R A Cox and J A Cole, "Chemical aspects of the autoignition of hydrocarbon-air mixtures", Combustion and Flame, 1985*).

4F. Sparks and spark ignition

The increasing restrictions on the levels of emission of various gases and particulate matter from a combustion process has directed attention to various possibilities of reducing the amount of harmful exhaust products. One of them is to use a lean mixture of fuel and air, but this will require a different ignition system from that used today in Otto- engines. Moreover, the electrical properties of the ignition system directly influence the combustion, so there are several reasons for studying the ignition process in detail. The aim of the work on sparks and spark ignition at the Combustion Centre is to characterize the state of the gas early in the sparking process and to follow the development with time of the spark to the combustion phase, also to determine the quality of the combustion, and to relate this to the electrical properties of the ignition system, and further to study the influence of the geometrical arrangement of the electrodes. The work is being done both experimentally and theoretically, with a fruitful interplay between them. The ignition process is a complex phenomenon, in which several mechanisms with different time-scales cooperate; surface processes on the electrodes, the formation of the plasma in the gas, shock-waves, the fluid flow of the expansion of the hot gas, radiative processes, and chemical reactions in the mixture.

Three types of ignition systems are used in the experimental work; conventional inductive, conventional capacitive and ultra-fast capacitive. The latter has been built at the Combustion Centre, and the two others are commercially available. The electrical characteristics of these systems can be found in [4F.1]. The main feature of the ultra-fast system is that it deposits its energy in the gas much faster than the other two; ns-scale and ms-scale, respectively. To compare the performance of these different systems they were fired in a constant-volume cylindrical chamber, which

can be filled with different gases and pressures up to 4 atm. In the work presented here the chamber was filled with nitrogen or a combustible mixture of air and methane or propane. The electrode material and the geometry of the spark gap, as well as the amount of energy released by the spark, can be varied. The spark current is measured by a coaxial resistor and the spark voltage is measured electro-optically using a capacitively coupled Pockels' cell. The properties of the spark itself have been measured mainly by optical methods; one- and two-wavelength laser interferometry, as well as ionization probes have been used to detect the flame-front. The performance of these methods has been compared with a fiber-optical detection method [4F.1]. With this experimental set-up the spark and spark-induced phenomena have been studied over five time decades (0.02-2000 microseconds).

In the first time-region, 20-500 ns, pulsed, two-wavelength laser interferometry has been used to investigate the development with time of the spark produced by the ultra-fast ignition system in nitrogen . The spark is cylindrically symmetric and confined to the region between the electrodes in this time domain. By Abel inverting the interferograms, the radial distribution of the density of electrons and atoms is given, and from these the temperature and pressure can be calculated on the assumption that the spark is in a state of local thermodynamic equilibrium. However, the central part of the spark at early times, where sub-vacuum densities of atoms were obtained from the Abel inversion, could not be analyzed. This was most likely due to the assumption that atomic refractivity is independent of temperature. A theoretical calculation of the refractivity of hydrogen atoms as a function of temperature, pressure and wavelength has been made, [4F.2]. It was found that the atomic refractivity does indeed depend on the temperature, and also on the wavelength, neither of which was accounted for in the Abel inversion. This is shown in Fig. 4F.1, where it can be seen that for very high temperatures the atomic refractivity behaves as the electronic refractivity. The

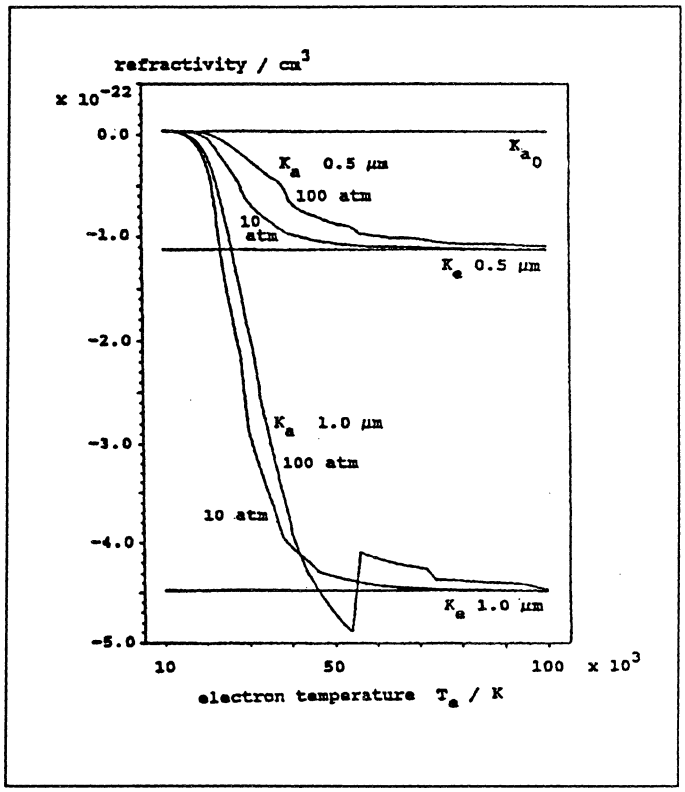

Fig. 4F.1.

The calculated refractivity of the components of a hydrogen plasma. K_a and K_e is the refractivity of atoms and electrons, respectively, and K_{a0} is the low-temperature value of the atomic refractivity used in the Abel inversion. The pressure and the wavelength are shown behind the K's. (From [F2].)

interest in the central part of the spark in the early stages is motivated by the fact that it is here that the major energy transfer from the electrical system to the gas takes place. To be able to calculate the energy deposited in the gas, the physical state of the plasma must be known. The early state also furnishes the initial conditions for the numerical modeling work [4F.3] of the continuing development of the spark in the first time region. The experimentally determined values of the number density of atoms and ions, the temperature, the pressure and the density agrees fairly well with the corresponding calculated values from this model [4F.3,F4], see Fig F2. The length of the laser pulses utilized in the recording of the interferogram is approximately 10 ns, so the experimental values are averaged over this time interval. This smearing, most pronounced for shorter times, of any sharp changes of the physical variables of interest makes it difficult to distinguish which of the different computational schemes proposed in [4F.3] gives the best agreement with the experiments. To do this, the physical state of the spark must be determined for longer times.

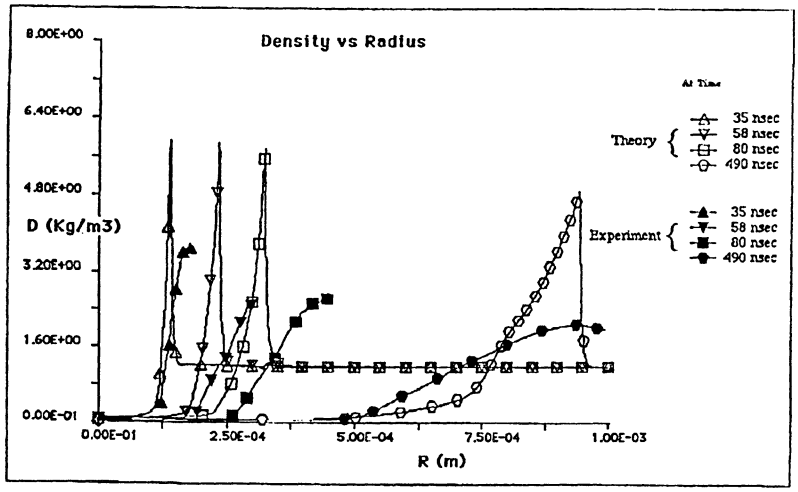

Fig. 4F.2.
Comparison between the calculated and measured values of the density in a spark in nitrogen. (From [F4].)

In the next time domain, 0.5-50 microseconds, the spark expands and goes from a cylindrical symmetry through a spherical symmetry towards a toroidal symmetry, and the shock-wave moves away from the plasma. Pulsed laser interferometry and Abel inversion gives the space- and time-resolved density distribution of the shock-wave. For longer times the effect of turbulent mixing can be seen in the interferograms [4F.4]. The intensity of this turbulent mixing is high enough to explain the increase of the flame speed, i.e. the rate of combustion, observed when using the ultra-fast ignition system compared to the flame speed when a conventional system is used [4F.1]. The strength of this turbulence increases as the power release time of the ignition system decreases. The radial expansion of the shock-wave and the spark

plasma have been measured in this region in a methane-air mixture. The expansion speed in this region is approximately the speed of sound.

In the last time region, up to 2 ms, a flame kernel is produced which expands outwards as a combustion wave. In Fig. 4F.3a the flame speed in the ultra-fast ignition system is compared with that in a conventional capacitive system. It can be seen that the flame speed is 2-3 times faster in the ultra fast system. However, this will also depend on the electrodes, their geometric arrangement and the material they are made of (Fig. 4F.3b). The effect of the electrodes and the amount of total electrical energy released from the ignition system and the pressure in the chamber on the flame speed are investigated in [4F.5], where also the statistical spread of the breakdown voltage is determined.

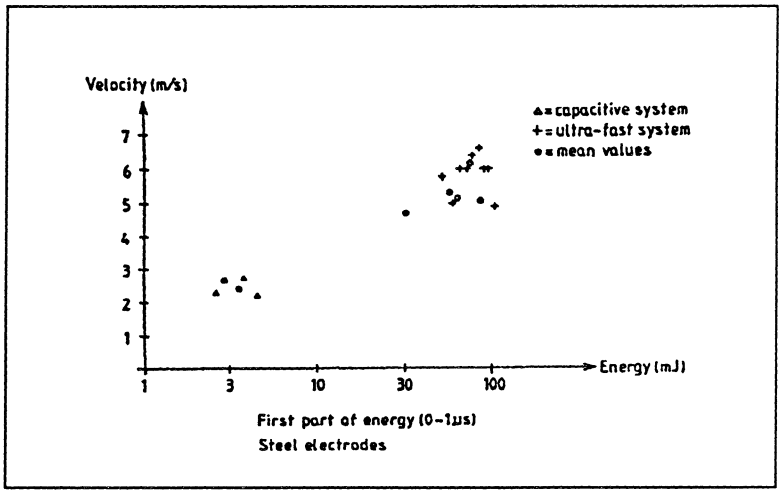

Fig. F3a.

To determine the coupling between the spark and the electrical circuit producing it, a mathematical model of a spark circuit has been developed [4F.6]. In order to derive an equation for the spark circuit the capacitance and inductance of the spark must be defined. They are introduced via the energy integral of the Maxwell equations. A relation between current and voltage for the spark gap is also necessary, which in principle requires the solution of the Maxwell equations, as well as the transport equations for the spark plasma. The energy integral gives the total power generation of the spark in terms of the defined capacitance and inductance. The total power generation has been

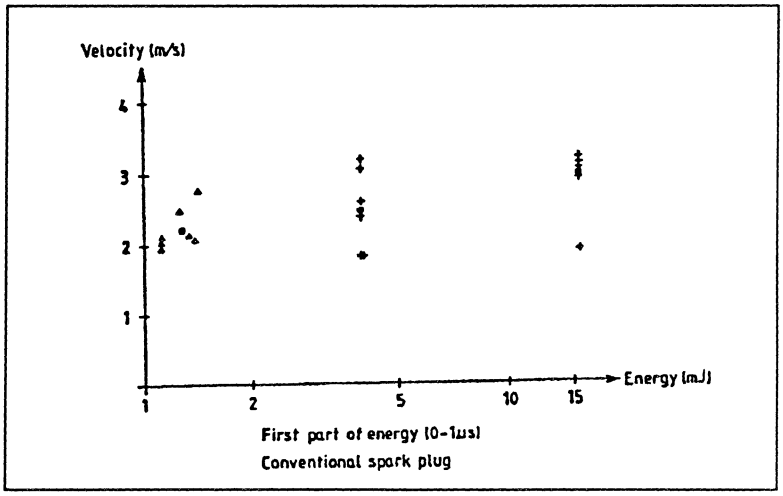

Fig. 4F.3b.

a. The flame speed as a function of energy in the spark for coaxial steel electrodes.

b. The flame speed as a function of energy in the spark for conventional spark plug. (Both from [F1].)

determined experimentally. It is shown that the capacitive and inductive contributions to the power are of importance in fast sparks. This is not the case for slow spark circuits. The coupling between the field equations, the Boltzmann equation and the circuit equations can be found from conservation equations. The set of equations have been solved numerically. For the fast spark studied in this work it has been shown that the non-linear resistance of the spark may be given analytically as a function of current. The capacitance and inductance, on the other hand, vary slowly with time. In Fig. 4F.4 an example of a fit of theoretical calculations to experimental results is shown. The work shows that even minor changes in the electrical parameters of the ignition system can cause widely different behaviour of the spark.

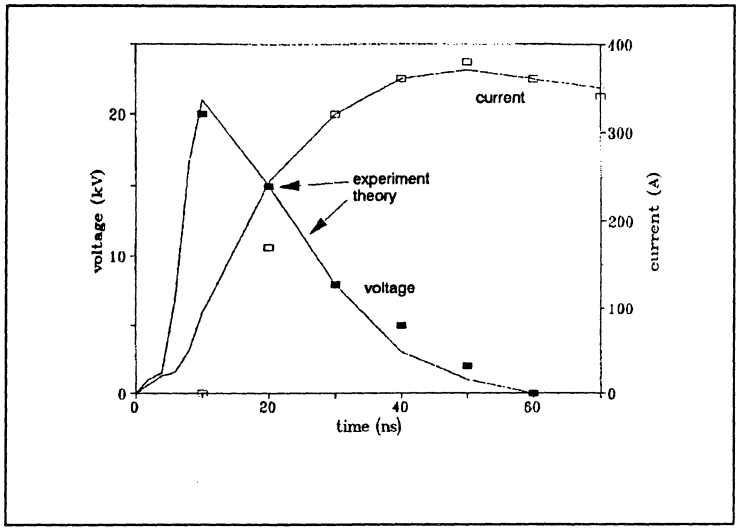

Fig. 4F.4.
Comparison between the experimental and calculated values of the current and voltage for a spark in nitrogen. (From [F6.)

The experimental and theoretical work performed on sparks and spark ignition at the Combustion Centre is a collaboration between Professor Thure Högberg, Dr Göran Holmstedt, Dr Ebbe Lundgren, Mohammed Akram, Juha Aunola, and Lars Martinsson. Four undergraduate students have done their Master of Science diploma work in this field; Rikard Carlsson, Bengt Johansson, Mats Lindelöw, and Hans Sturesson.

4G. Further technique developments

In addition to the combustion research activities described above a project concerning the development of new techniques is being supported by STU. These activities are being pursued in close collaboration with the atomic spectroscopy, remote sensing and medical spectroscopy programmes at the division.

During the last two-year period, three projects have been pursued: multi-colour radical emission imaging, frequency modulation spectroscopy and degenerate four-wave mixing.

Multi-colour radical emission imaging - In emission spectra from flames, bands due to several, mutually interacting species occur. In addition, a strong, unstructured background emission due to soot incandescence is frequently present. These features are shown in Fig. 4G.1. for the case of an acetylene/oxygen flame. Point measurements in the spectral domain are very useful in revealing these features. However, multi-point or imaging measurements in the spatial domain using

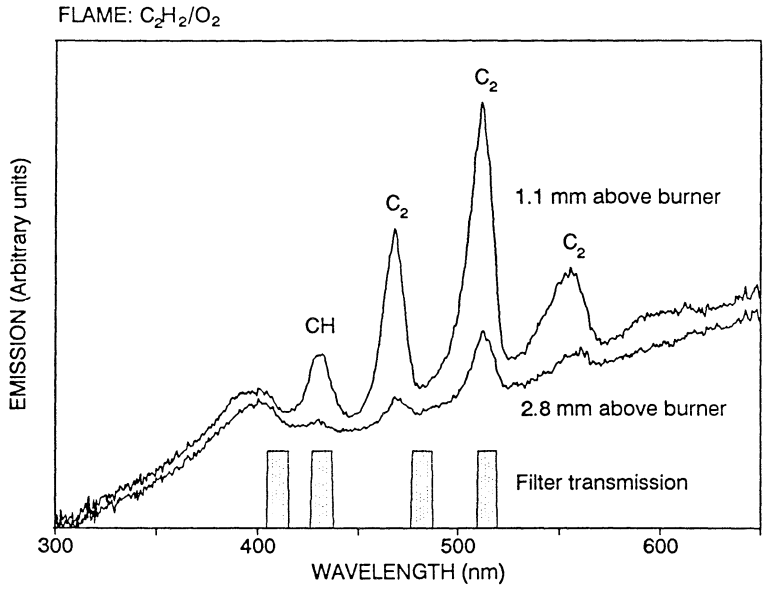

Fig. 4G.1. Recordings of the flame emission spectra of a sooty acetylene/oxygen flame at two different heights above the burner.

a CCD detector are frequently desirable, but these would normally be limited to single-colour detection through a chosen band-pass filter. We have now developed a technique for multi-colour, simultaneous imaging of several species using a special optical system [4G.1]. Individually spectrally filtered images are placed side by side on a common image intensifier, the output of which is viewed by a CCD camera, as shown in Fig. 4G.2. This allows simultaneous imaging of up to four different flame radicals, or radical emission imaging unaffected by soot incandescence with exposure times as short as a few μs. Simultaneous imaging of a flame in the CH and C_2 emission bands and at

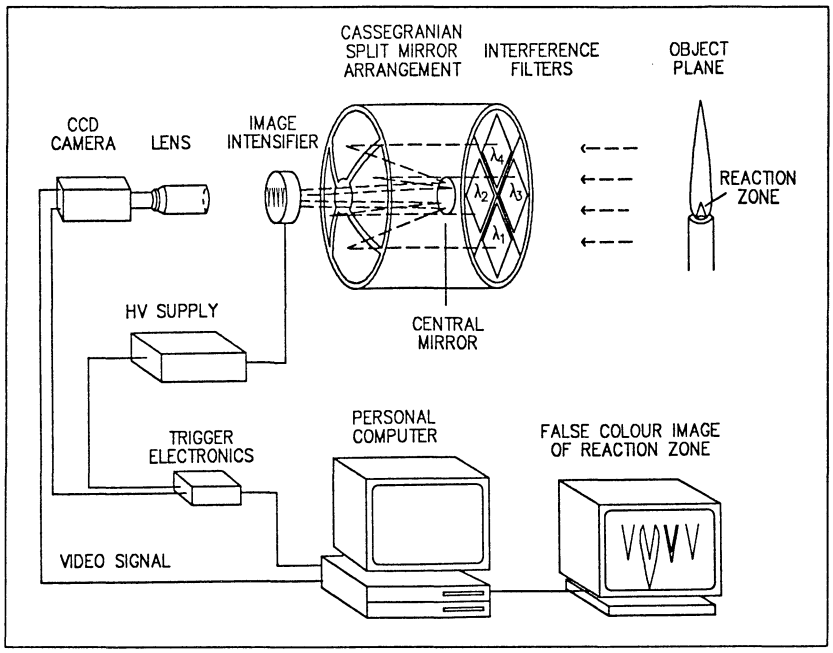

Fig. 4G.2. Set-up for multi-colour imaging of flame radical emission.

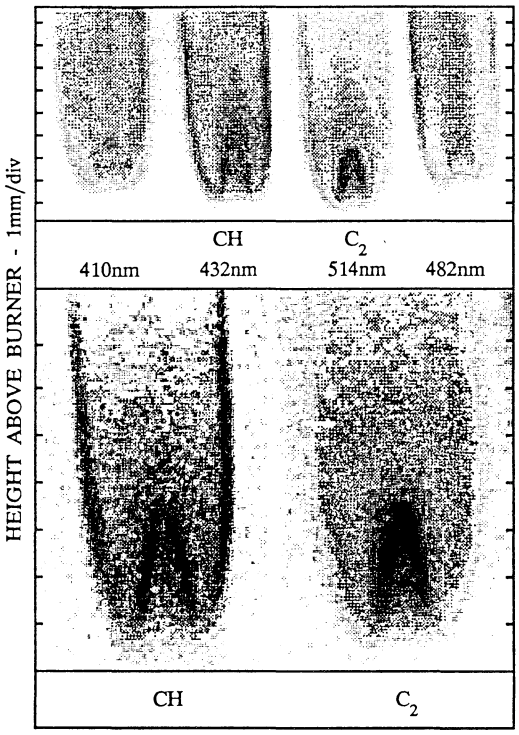

Fig. 4G.3. Simultaneous recordings from CH and C2 emission bands and at neighbouring background-intensity wavelenghts used to produce background-free radical emission images.

close-lying background-level wavelengths is shown in Fig. 4G.3. After suitable subtraction, the background-free radical emissions can be imaged. The techniques can readily be extended to simultaneous multi-species active imaging using laser-induced fluorescence.

Frequency modulation (FM) spectroscopy - Very sensitive absorption measurements can be performed using FM spectroscopy. Sidebands are generated on the optical carrier frequency with an electro-optic modulator driven by microwaves. Since the sidebands are equally strong and

of opposite phase a microwave modulation in the transmitted beam is normally cancelled. If one of the sidebands is attenuated by an absorption line, assymmetry occurs and a modulation can be detected. Extensive studies using CW and pulsed dye lasers are reported in [4G.2]. Recently, we have implemented frequency modulation spectroscopy using tunable diode lasers, which are particularly suitable for this type of experiment [4G.3]. By simultaneously modulating at two frequencies (two-tone version) detection can be achieved at a conveniently low beat frequency. A diode laser spectrometer based on this principle is shown in Fig. 4G.4. A recording for molecular oxygen with a detectivity of 0.0001 per cent absorption is shown in Fig. 4G.5. Tomographic mapping of flame radicals using frequency modulation absorption spectroscopy is planned.

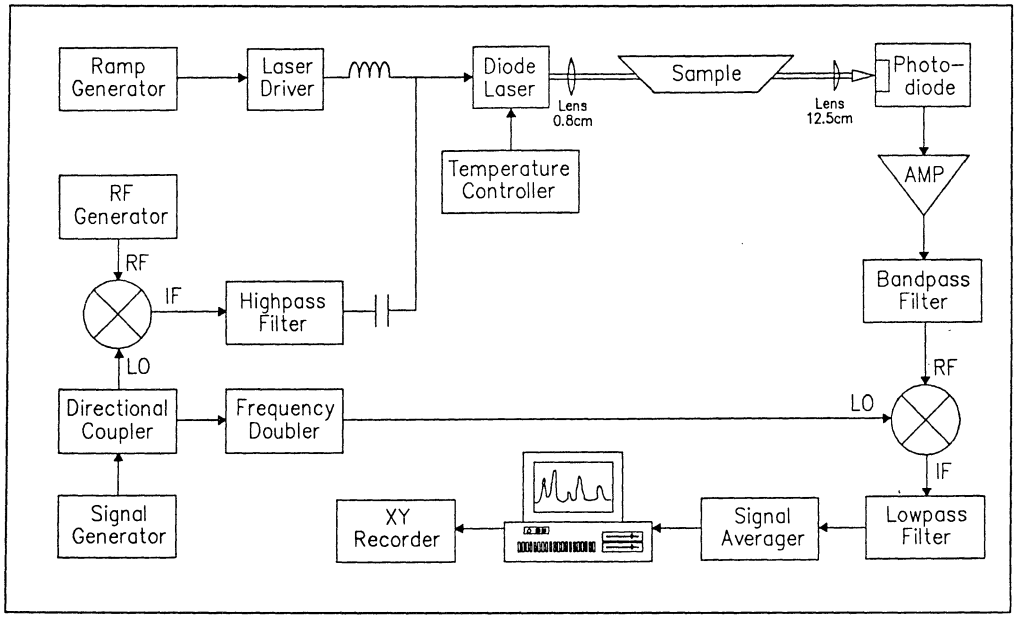

Fig. 4G.4. Set-up for two-tone diode laser frequency modulation spectroscopy.

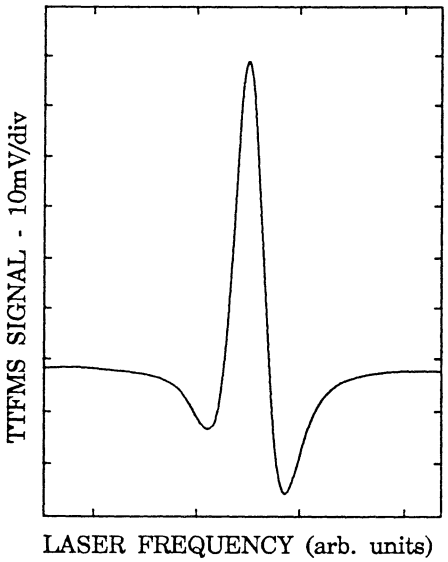

Fig. 4G.5. FM spectroscopy recording of an oxygen line. The quality of the recording corresponds to an absorption detectivity of 0.0001 per cent.

Degenerate four-wave mixing (DFWM) - The DFWM method has the potential to combine the advantages of laser-induced fluorescence (sensitivity) and CARS (coherent signal). Extensive experiments using both CW and pulsed dye lasers have been performed on sodium atoms in cells and in flames to study the possibilities and limitations [4G.4]. A special feature of the degenerate four-wave mixing signal is that it is phase-conjugated, i.e. it constitutes a true replica of the probe beam used for the sample interrogation. Thus, distortions due to flame turbulence can be eliminated, as illustrated in Fig. 4G.6, for the case of

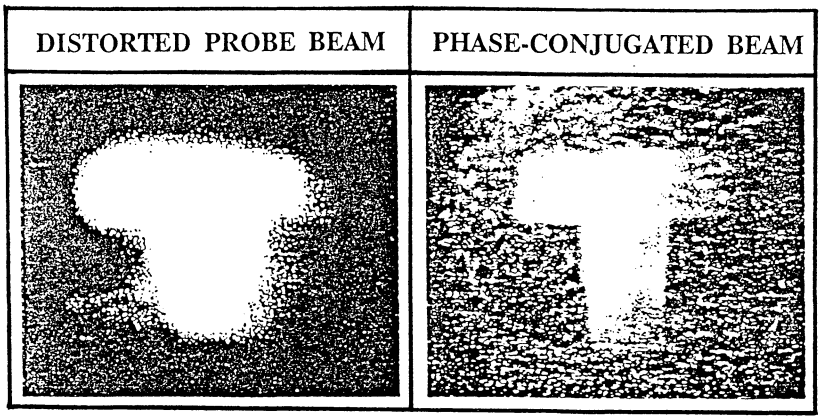

Fig. 4G.6. Illustration of image blurring by a flame and restoration using a phase-conjugation mirror set-up in a sodium-seeded flame.

a sodium-seeded flame. The left image of a T-shaped object is blurred when the beam carrying the information is passed through a second flame. Using the sodium phase-conjugating mirror a sharp image can still be obtained, as shown in the right part of the figure. This

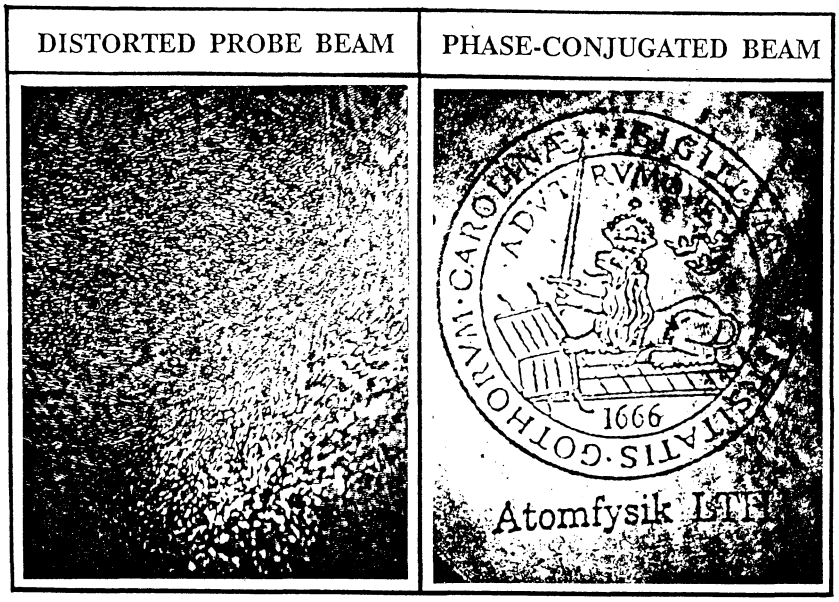

Fig. 4G.7. Illustration of image blurring by a frosted glass beam distorter and image restoration by phase-conjugation in a $BaTiO_3$ crystal.

aspect of DFWM is even more clearly demonstrated in Fig. 4G.7, showing distorted and restored images in an experiment utilizing a $BaTiO_3$ crystal and argon laser light passing through a sheet of frosted glass [4G.5].

Results from this project were recently presented in an invited paper [4G.6].

References

4A.1. U Westblom and M Aldén, "Simultaneous multiple species detection in a flame using laser-induced fluorescence", Appl. Opt. 28, 2592 (1989).

4A.2. J E M Goldsmith, M Aldén and U Westblom, "Photochemical Effects in Multiple-Species Fluorescence Imaging in Hydrogen-Nitrous Oxide Flames", Accepted for publ. in Appl. Opt.

4A.3. U Westblom and M Aldén, "Laser-Induced Fluorescence Detection of NH_3 in Flames with the Use of Two-Photon Excitation", Appl. Spectr. 44 (1990).

4A.4. U Westblom, S Agrup, M Aldén and P Cederbalk, "Detection of Nitrogen Atoms using Two-Photon Laser-Induced Fluorescence and Investigations of Photo-Chemical Effects", Subm. to Appl. Opt.

4A.5. S Agrup, U Westblom, M Aldén and P Cederbalk, "Detection of Nitrogen Atoms using Two-Photon Laser-Induced Fluorescence and Stimulated Emission: Applications to Combustion Studies", Conference on Lasers and Electro optics, 1990, Los Angeles, USA.

4A.6. U. Westblom, S. Agrup, M. Aldén and P. Cederbalk, "Flame Detection of Nitrogen Atoms using Two-PhotonLaser-Induced Fluorescence and Stimulated Emission", 23nd Int. Conference on Combustion, Orleans, 1990.

4A.7. M. Aldén, P.-E. Bengtsson and U. Westblom, "Flame Detection of Carbon atoms and C_2 molecules using Laser- Induced Fluorescence", In prep.

4A.8. E. Fridell, U. Westblom, M. Aldén and A. Rosén, "Spatially resolved laser-induced fluorescence imaging of OH produced in the oxidation of hydrogen on platinum", Accepted for publ. in Journ. of Cat.

4A.9. U. Westblom and M. Aldén, "Spatially resolved flow velocity measurements using laser-induced fluorescence from a pulsed laser", Opt. lett., 14, 9 (1989).

4A.10 M Aldén, U Westblom and J E M Goldsmith, "Two-Photon-Excited Stimulated Emission from Atomic Oxygen in Flames and Cold Gases", Opt. Lett. 14, 305, (1989).

4A.11 M Aldén, P-E Bengtsson and U Westblom, "Detection of Carbon Atoms in Flames using Stimulated Emission Induced by Two-Photon Laser Excitation". Opt Comm 71, 263 (1989).

4A.12 U Westblom, S Agrup, M Aldén, H Hertz and J E M Goldsmith, "Properties of Laser-Induced Stimulted Emission for Diagnostic Purposes", Appl Phys B 50, 487 (1990).

4A.13 S Agrup, U Westblom and M Aldén "Detection of Atomic Nitrogen using Two-Photon Laser-Induced Stimulated Emission: Application to Flames", Chem Phys Lett, 170, 406 (1990).

4A.14 S Agrup, U Westblom, M Aldén H Hertz and J.E.M. Goldsmith, "Applications of Two-Photon Induced Stimulated Emission for Diagnostic Purposes", National Meeting on Atomic and Molecular

Physics, Stockholm- Helsingfors, June 6-8, 1989
4A.15 U Westblom, S Agrup, M Aldén, P-E Bengtsson, H Hertz and J.E.M. Goldsmith, "Two Photon Laser Induced Stimulated Emission", IEA XI Task Leaders Meeting, Örenäs Castle Hotel, June 25-30, 1989
4A.16 P-E Bengtsson, M Aldén and U Westblom, "Application of Two Photon Laser Induced Stimulated Emission for Detection of Carbon Atoms in Flames", 2nd European Conference on Quantum Electronics, EQEC '89, Dresden DDR, August 28 - September 1, 1989.
4A.17 U Westblom and M Aldén, "Imaging Techniques using Laser-Induced Fluorescence in Combustion Diagnostics", Paper presented at Förpex -89, Lund 1989.
4A.18 U Westblom and M Aldén, "Multiple species detection in a flame using Laser-induced Fluorescence", IEA 1988, X:th Task Leaders meating, Amalfi
4A.19 U Westblom and M Aldén, "Spatially resolved flow velocity measurements using Laser-induced Fluorescence from a pulsed laser" IEA 1988, X:th Task Leaders meeting, Amalfi
4A.20 M Aldén, "Coherent anti-Stokes Raman Scattering and Laser-Induced fluorescence combustion flow diagnostics". Invited Paper at CLEO 89, Baltimore 1989
4A.21 M Aldén, "New Techniques: Stimulated emission at a diagnostic tool", Invited talk at the Gordon Conference 1989
4A.22 M Aldén and W Wendt, "Detection of Nitrogen molecules through multiphoton laser excitation and N_2^+ fluorence", Opt Comm 69 , 31 (1988)
4A.23 H M Hertz, M Aldén and S Svanberg, "Correction of imaging errors in flames" Appl Phys B B 45 , 33 (1988)
4A.24 U Westblom and M Aldén, "Multiple species detection in flames using Laser-induced Fluorescence", Svenska Fysikersamfundet, Linköping, Sweden, 1989.
4A.25 U Westblom, S Agrup, M Aldén and P-E Bengtsson, "Application of two-photon induced stimulated emission for detection of flame species", Svenska Fysikersamfundet, Linköping, Sweden, 1989.
4B.1. S Kröll and D Sandell, "The influence of laser mode statistics on noise in nonlinear optical processes - application to single-shot broadband CARS thermometry", J Opt Soc Am B 5, 1910-1926 (1988)
4B.2. S Kröll, M Aldén, P-E Bengtsson, H Edner, D Nilsson and D Sandell, "The influence of laser mode amplitude and laser mode phase fluctuations on spectral noise in coherent anti-Stokes Raman scattering, poster, Quantum Electronic and Laser Science Conference (QELS '89), Baltimore, USA, April-89.
4B.3. M Aldén, P-E Bengtsson, H Edner, S Kröll and D Nilsson, "Rotational CARS: a comparison of different techniques with emphasis on accuracy in temperature determination", Appl Opt 28, 3206-3219 (1989)
4B.4. M Aldén, P-E Bengtsson, H Edner and S Kröll, "Accuracies and signal strengths of rotational CARS - comparison between different experimental methods", poster, XXII International Symposium on Combustion, Seattle, USA, August-88.
4B.5. M Aldén, P-E Bengtsson and H Edner, "Rotational CARS generation through a multiple four-color interaction", Appl. Opt. 25 , 4493-4500 (1986).
4B.6. S Kröll, M Aldén, P-E Bengtsson and C Löfström, "An evaluation of precision and systematic errors in vibrational CARS thermometry", Appl Phys B 49 , 445-453 (1989)

4B.7. S Kröll, M Aldén, P-E Bengtsson and C Löfström, "Fundamental and practical aspects on temperature determination using coherent anti- Stokes Raman scattering", Svenska Fysiker-samfundets sektionsmöte för Atom- och Molekylfysik, Linköping, Sweden, November 1989

4B.8. S Kröll, M Aldén, P-E Bengtsson and C Löfström, "On the statistics of multimode YAG lasers and the ratio between resonant and nonresonant CARS signal contributions", Paper presented at 9:th European CARS workshop, Dijon, France, March-90.

4B.9. S Kröll, M Aldén, P-E Bengtsson and C Löfström, "Do pulsed YAG lasers obey coherent rather than chaotic statistics? Implications for CARS diagnostics", poster presented at the Conference on Lasers and Electro-Optics (CLEO-90), Anaheim, USA, May-90.

4B.10. S Kröll, M Aldén, P-E Bengtsson, C Löfström and R J Hall, "The statistics of multimode YAG laser radiation with implications for quantitative CARS spectroscopy in combustion diagnostics", submitted to J. Opt. Soc. Am. B.

4B.11. S Kröll, P-E Bengtsson, M Aldén and D Nilsson, "Is rotational CARS an alternative to vibrational CARS for thermometry?", Appl. Phys. B 51 , 577-582 (1990).

4B.12. M Aldén, P-E Bengtsson, H Edner, S Kröll and D Nilsson, "Rotational coherent anti-Stokes Raman scattering for temperature deter-mination - applicability and accuracy", poster, XI international conference on Raman spectroscopy, London, England, September-88.

4B.13. M Aldén, P-E Bengtsson, S Kröll and D Nilsson, "Applications of rotational CARS for combustion studies", Gordon Research Conferences, Plymouth State College, USA, July, 1989.

4B.14. L Martinsson, M Aldén, P-E Bengtsson and S Kröll, "Calibration of a Computer Code for Rotational CARS at High Temperature and High Pressure", Poster presented at the 9th European CARS Workshop, Dijon, March 19-20, 1990.

4B.15. H Neij and A Nilsson, "Investigation of different dye laser concepts for combustion diagnostics", Lund Reports on Atomic Physics, LRAP-104, Lund, June 1989.

4B.16. H Miller, C Löfström, I Bjerle and M Aldén, "The Measurement of Forced Convection Heat Transfer for Laminar Tube Flow", Int Com in Heat and Masstransfer, (Acc for publication)

4B.17. M Aldén, "Industrial application of CARS", Invited talk at the XX Int Conf on Raman Spectroscopy, London, Sept -88

4B.18. M Aldén and W Wendt, "Application of CARS Spectroscopy to the detection of SO_2", Appl Spectr 42 , 1421 (1988).

4B.19. C Löfström, M Aldén and S Kröll, "Mobilt CARS system för temperaturmätning i förbränningssystem", Posterbidrag till Förpex 1989, Lund

4B.20. A Nilsson, M Aldén, H Neij and P-E Bengtsson, "Application of a prism dye laser in CARS spectroscopy", To be published.

4C.1. P-E Bengtsson and M Aldén, "Application of a Pulsed Laser for Soot Measurements in Premixed Flames", Applied Physics, B 48, 155-164,1989

4C.2. P-E Bengtsson and M Aldén, "Soot Particle Measurements in Premixed Ethylene Flames using a Pulsed Laser Method", J. Aerosol Sci., 959-962, 1988

4C.3. P-E Bengtsson, M Aldén, S Kröll and D Nilsson, "Vibrational CARS Thermometry in Sooty Flames: Quantitative Evaluation of C_2

Absorption Interference", Combust. Flame, in press
4C.4. P-E Bengtsson, D Nilsson, M Aldén and S Kröll, "Vibrational CARS Thermometry in Sooty Flames", Paper presented at the 8th European CARS Workshop, Oxford, England, March 20-21, 1989
4C.5. P-E Bengtsson, M Aldén, S Kröll and D Nilsson, "Temperature Measurements in Sooty Flames using Vibrational CARS", Paper presented at the 11th IEA Task Leaders Meeting, Örenäs Castle Hotel, June 25-30, 1989
4C.6. P-E Bengtsson, M Aldén, S Kröll and D Nilsson, "Coherent Anti-Stokes Raman Scattering for Temperature Determination in Sooty Flames", Paper presented at the 2nd European Conference on Quantum Electronics, EQEC'89, Dresden, Östtyskland, August 28-September 1, 1989
4C.7. P-E Bengtsson, M Aldén, S Kröll and L Martinsson, "A comparison of Vibrational CARS and Rotational CARS for Thermometry in Sooty Flames", Paper presented at the 23rd International Conference on Combustion, Orleans, France, July 22-27, 1990
4C.8. P-E Bengtsson, D Nilsson, M Aldén and S Kröll, "Rotational CARS Thermometry in Sooty Flames and at 40 atm, 293 K", Paper presented at the 8th European CARS Workshop, Oxford, England, March 20-21, 1989
4C.9. P-E Bengtsson, L Martinsson, M Aldén and S Kröll, "Rotational CARS Thermometry in Sooty Flames", Comb. Sci. and Tech., to be submitted
4C.10. P-E Bengtsson and M Aldén, "Optical Investigation of Laser-Produced C_2 in Premixed Sooty Ethylene Flames", Combust. Flame, 80 , 322 -328(1990).
4C.11. P-E Bengtsson, M Aldén, S Kröll och D Nilsson, "Laserdiagnostik i sotig förbränningsmiljö", Paper presented at FÖRPEX'89, Förbränningsteknisk Projektexposé, Lund, November 14-15, 1989
4D.1. H M Hertz and G W Faris, "Emission tomography of flame radicals", Opt Lett 13 , 351-353, (1988)
4D.2. G W Faris and H M Hertz, "Tunable differential interferometer for optical gradient tomography", Appl Opt 28 , 4662-4667 (1989)
4D.3. H M Hertz and G W Faris, "Techniques for instantaneous optical tomography in fluid flows and flames", Proc Conf on Lasers and Electro-Optics, ThC2 (1988)
4E.1. G Olson and R A Cox, "High pressure autoignition of butane - chemical modelling study", In preparation.
4E.2. P Cederbalk, "Experimental Combustion Chemical Research at the Combustion Centre at LNTH", presented at Combustion Chemistry Research in the CEC and Sweden at the Royal Institute of Technology, Stockholm, March 9-10, 1989.
4E.3. P Cederbalk, "Oxidationsexperiment vid Låg Temperatur med Relation till Självantändningsproblematiken" presented at FÖRPEX (Förbrännings- teknisk Projektexposé), Lund Institute of Technology, November 14-15 1989.
4E.4. J Cavanagh, R A Cox and G Olson, "Computer modelling of cool flames and ignition of acetaldehyde", To be published.
4F.1. M Lindelöw and H Sturesson, "An experimental study of flame kernel development at different spark energies using new detection systems", Lund Reports on Atomic Physics, LRAP-103, Lund 1989.
4F.2. L Martinsson, "Calculation of the refractivity of the components of a spark in hydrogen for the evaluation of two-wavelength interferograms", Proc. 11th Task Leaders Meeting,

IEA, June 26-29 1989, Glumslöv, Sweden.
4F.3. M Akram and E Lundgren, "Numerical modelling of spark-discharges in air", Proc. 11th Task Leaders Meeting, IEA, June 26-29 1989, Glumslöv, Sweden.
4F.4. G Holmstedt, J Aunola, T Högberg, and L Martinsson, "Time and space resolved study of break down, ignition and flame kernel development of inductive and capacitive ignition systems", Proc. Workshop and Exposition on Fluid Mechanics, Combustion and Emissions in Reciprocating Engines, Hotel La Palma, Capri, Italy, April 1-4, 1990.
4F.5. R Carlsson and B Johansson, "A study of inductive and capacitive ignition and kernel development", Lund Reports on Atomic Physics, LRAP-89, Lund 1988.
4F.6. T Högberg and G Holmstedt, "The short-duration spark characteristics relevant to ignition in engines and spark coupling to the electric circuit", Proc. Workshop and Exposition on Fluidmechanics, Combustion and Emissions in Reciprocating Engines, Hotel "La Palma" Capri, Italy, April 1-4 1990.
4F.7. G Holmstedt, T Högberg, E Lundgren, M Akram, J Aunola and L Martinsson, "Gnistantändnigsstudier vid FTC", Proc. Förbränningsteknisk projektexpose, nr. 3, November 14-15 1989, Lund (in Swedish).
4G.1. S. Andersson-Engels, P. Kauranen and S. Svanberg, Spatial mapping of flame radical emission using a spectroscopic multi-colour imaging system, Submitted to Appl. Phys. B
4G.2. P. Kauranen, Frequency modulation spectroscopy, Lund Reports on Atomic Physics LRAP-102 (1989)
4G.3. O. Lindblad, Frequency modulation diode laser spectroscopy for sensitive trace species detection, Lund Reports on Atomic Physics, to appear
4G.4. P. Bengtsson, Degenerate four-wave mixing as an analytical tool, Lund Reports of Atomic Physics LRAP-99 (1989)
4G.5. S. G. Pettersson and Wang Dadi, Unpublished results (1990)
4G.6. S. Svanberg, Laser spectroscopy applied to energy, environmental and medical research, in N. Omenetto (ed.), Resonance Ionization Spectroscopy (Plenum, New York, to appear)

5. ENVIRONMENTAL REMOTE SENSING

Hans Edner, Bo Galle*, Jonas Johansson, Pär Ragnarson, Sune Svanberg, Eva Wallinder

* Swedish Environmental Research Institute (IVL)

In the field of environmental remote sensing general interest lies in the development of spectroscopic techniques, both laser and non-laser, to measure mostly atmospheric pollutants, but some of the techniques are also applied for terrestrial and aquatic studies. The differential absorption lidar (DIAL) technique has been employed in several measurements of atomic mercury in the atmosphere, of both industrial and geophysical origin. These measurements have been performed with a mobile lidar system, while a fixed DIAL system has been developed for vertical ozone profile measurements in the planetary boundary layer and the free troposphere. A non-laser method used for long-path absorption measurements in the atmosphere is the differential optical absorption spectroscopy (DOAS) method. Here special emphasis has been placed on the construction of an automatic multi-path system. Tests of a single-ended system employing retroreflectors have also been made. Detailed spectroscopic studies have been performed on ozone, ammonia and aromatic hydrocarbons, including field measurements in different environments. Finally, laser-induced fluorescence has been investigated as a tool in vegetation and water quality studies.

The remote sensing work at the department is primarily supported by the Swedish Environmental Protection Board (SNV) and the Swedish Board for Space Activities (DFR). Some review articles have been published [5.1-3] and several contributions have been made at various national and international conferences [5.4-10].

Since October 1990 activities in environmental sensing have also been channelled through the Centre for Environmental Measurement Technology (CENTEC). This is a collaboration within Lund Institute of Technology between the Departments of Atomic Physics, Nuclear Physics, Work Environment Technology, Mathematical Statistics, Organic Chemistry 2 and Technical Analytical Chemistry. The aim of the centre is to enhance and coordinate research and teaching in environmental sensing technology. It should initiate the development of new measurement techniques and combinations of those already existing to tackle complex environmental problems.

5A. Differential absorption lidar

The mobile DIAL system has been upgraded with a new more powerful laser source (Continuum YG 682-20 Nd:YAG laser and TDL 60 dye laser). Frequency doubling/mixing both to the UV and IR regions with crystal tracking systems is included, thus giving a total tuning range of 190-4500 nm. A dual wavelength option, consisting of a rotating parallel glass plate and two tuning mirrors inside the dye laser cavity, allows rapid switching between two preset wavelengths. The system also has been updated with two new AT computers for system steering/data acquisition and data evaluation. A major revision of the software aimed at more user-friendly programs is presently being performed. During the last two years the mobile DIAL system has been used in several measurements on mainly two atmospheric species; atomic mercury

and ozone. It has also been used together with a fluorosensor system for vegetation and water analysis, as will be discussed later.

Mercury is the only atmospheric gaseous pollutant occurring as free atoms. Mercury is released from e.g. chlorine-alkali plants, refuse incineration plants and crematoria. Mineralizations, geothermal reservoirs and volcanoes are also known to be associated with elevated atomic mercury concentrations. Mercury can be monitored by the DIAL technique using the mercury resonance line at 253.65 nm, which can be generated with sufficient power by frequency doubling of a dye laser using a BBO crystal. We have earlier demonstrated DIAL measurements of mercury emissions from a chlorine-alkali plant as well as measurements of low background values [5A.1]. Previous measurements of atomic mercury in geothermal fields in Iceland will be published shortly [5A.2], and some reviews of mercury DIAL are given in Refs. [5A.3-5].

The increasing frequency of cremation means that the crematoria today constitute a major source of mercury emissions in Sweden. In fact, more mercury today comes from crematoria than from refuse incineration plants, due to more efficient separation of mercury-containing material. The emission of mercury from crematoria is expected to increase in the future, due to higher frequency of cremations and higher contents of dental amalgam. There is therefore a need for a reduction of these emissions, and new filtering systems are presently being investigated. Coupled to these studies there is a demand for accurate monitoring techniques. We have investigated the potential of optical techniques in this context [5A.6]. The mobile DIAL system has been used to monitor the emission from the unfiltered crematorium in Lund. Further measurements have been made at the Råcksta crematorium in Stockholm [5A.7], during a test period when selenium was added during the cremation process, which should reduce the mercury emission. Fig. 5A.1 shows an example of the mercury content in the outgoing plume versus time during a cremation. The laser beam was directed closely over the chimney from about 200 m. The DIAL technique was here combined with measurements made by extracting a small flow

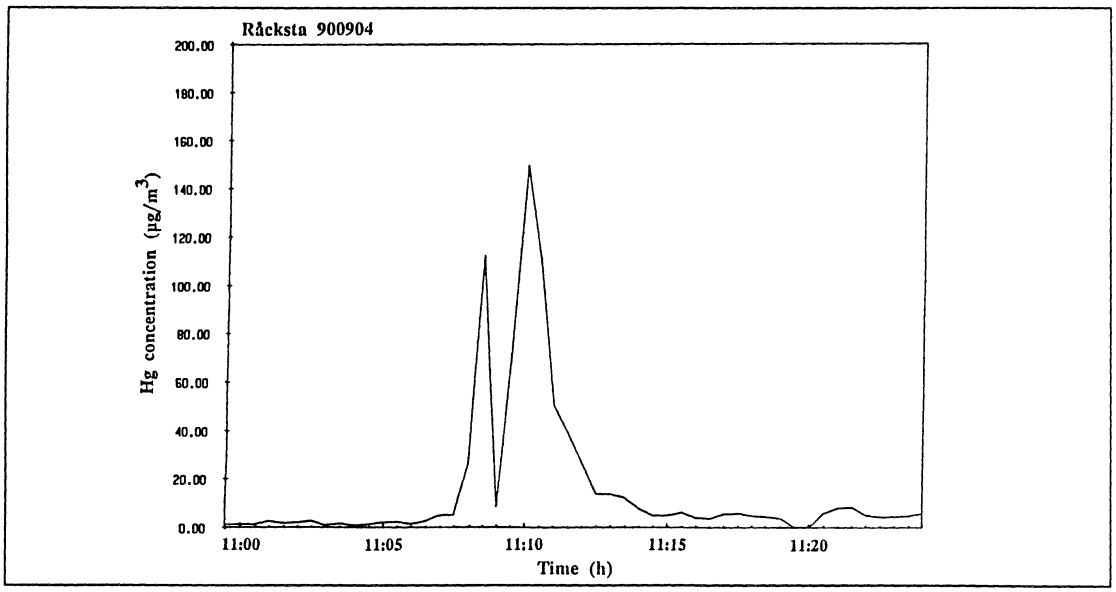

Fig. 5A.1. DIAL measurement of the Hg emission from a crematorium.

from the smoke channel through a small quartz cell, where a Zeeman-modulated mercury lamp was used to monitor the mercury concentration (Quicky Hg-monitor from Semtech AB).

Extensive field experiments were performed with the mobile DIAL system during September-October 1990 in the Tuscany region in Italy. Measurements of atmospheric mercury were made at a chemical plant in Rosignano Solvay, in the mercury mining area around Abbadia S. Salvatore (Mt. Amiata) and at geothermal fields in Piancastagnaio, Castelnuovo, Larderello and Lagoni Rossi [5A.8]. Very high concentrations were found near geothermal plants, as can be seen in Fig. 5A.2, which shows the on- and off-resonance lidar returns. This is in strong contrast to the results found in Iceland, where geothermal energy extraction was found to create very small amounts of atomic mercury. A computer-generated vertical charting of a spreading plume is shown in Fig. 5A.3. It should be noted that concentrations over 1 $\mu g/m^3$ are obtained. Fig. 5A.4 shows the distribution of mercury near a cooling tower at the geothermal plant in Castelnuovo. The figure is a composite of vertical and horizontal scans as indicated by the dots. The mercury concentrations are clearly separated from the visible water vapour plume. Very high concentrations were also found at the abandoned mercury mine at Abbadia S. Salvatore. This was particularly true in the area of the distillation plant. The degassing of deposited roasted cinnabar (HgS) also contributes substantially to the local atmospheric concentration. Lidar studies of the vertical profiles of the gas above the deposits were made. In an unexplored area of natural geothermal manifestations (Lagoni Rossi) considerably lower concentrations were found, although clearly measurable. All the measurements in the Tuscany region were made in cooperation with the CNR-Istituto di Biofisica (R. Ferrara et al.) in Pisa, which supplied the results of point measurements with a gold amalgamation technique combined with flameless atomic absorption. Extensive intercomparison between the different techniques was made. Several papers discussing various aspects of the field campaign are presently being prepared.

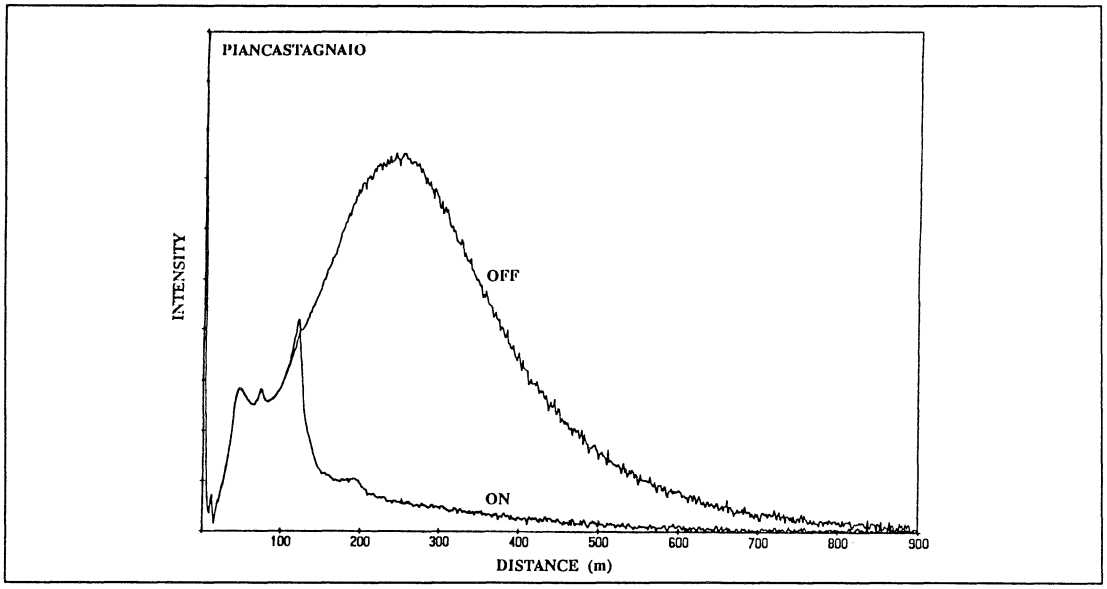

Fig. 5A.2. Lidar signals on and off the Hg resonance line (253.65 nm) near an Italian geothermal plant.

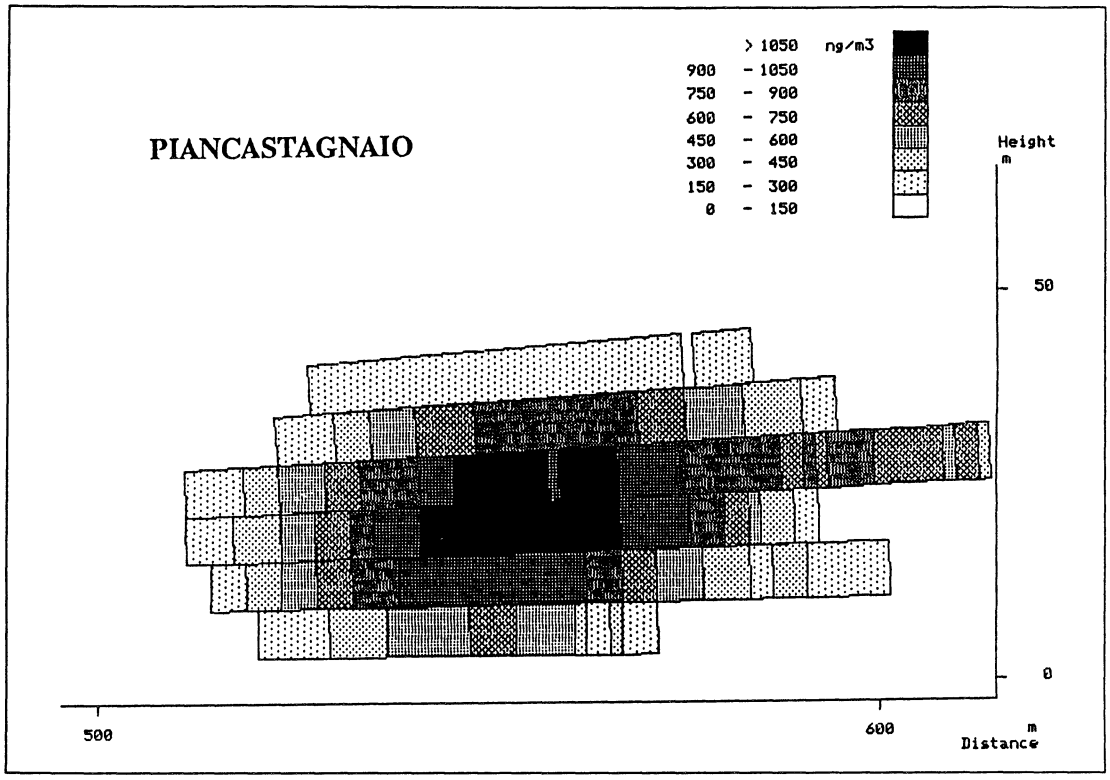

Fig. 5A.3. Vertical charting of a spreading Hg plume.

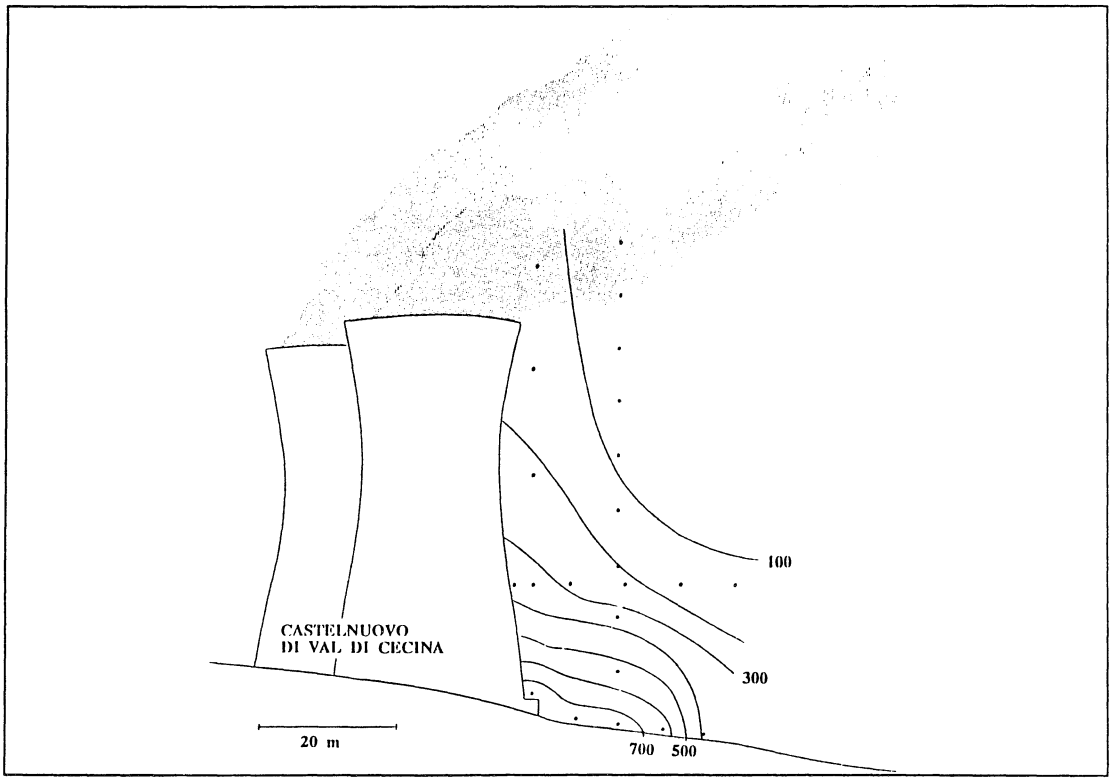

Fig. 5A.4. Distribution of atomic Hg in the vicinity of cooling towers at a geothermal plant (Hg concentrations in ng/m^3).

Since 1988 the group has been participating in the European cooperation project TESLAS (Tropospheric Environmental Studies by Laser Sounding), which is a subproject of the Eureka project EUROTRAC. EUROTRAC is an environmental project studying the impact of human activities on the troposphere over Europe. It is an interdisciplinary project involving field measurements, laboratory studies and comprehensive model simulations of the physical and chemical processes involved in atmospheric chemistry. The goal of the subproject TESLAS is to reach, in an initial phase, a consensus on the performances of a state-of-the-art lidar for ozone measurements in the planetary boundary layer and the free troposphere, to develop optimized systems and to validate the data during intercomparison campaigns. The key challenges of TESLAS are:

Ozone measurements using UV lidar in the presence of aerosols.
Measurements on aerosols using visible and IR lidars.
Measurements on ozone using IR lidar in the 9 to 11 μm region.

Technical challenges of the project:
- Detection spectral filtering
- Pulse-pair repetition frequency optimization
- Reduction of signal dynamics
- Data reduction and corrections
- Laser source selection

Within this project a fixed lidar system has been developed, which is especially dedicated for tropospheric ozone measurements [5A.9-12]. The system is based on a KrF excimer laser with an unstable resonator (Lambda Physik LPX 210iF), which gives a wavelength of 248 nm. The output energy is about 420 mJ, of which 240 mJ are within 0.4 mrad divergence. The light is Raman shifted in one or two specially constructed 1.5 metre long Raman cells, which can support a pressure of up to 100 bar. Using hydrogen as the Raman shifting medium, the appropriate wavelengths for ozone measurements are 277 nm and 313 nm. By using deuterium in a second cell additional wavelengths at 268 nm and 292 nm can be generated. Some measurements on the Raman shifting efficiency have been performed in order to find the optimum pressure of the Raman shifting medium [5A.13]. If hydrogen is used together with the excimer laser, the maximum efficiency for the first Stokes component is almost 30 %, and for the second 15 %, as can be seen in Fig. 5A.5. The maximum for the first and second Stokes component does not occur at the same pressure. If a quadrupled Nd:YAG laser is used instead (266 nm), the efficiency is 50 % for the first Stokes component at 299 nm. Some preliminary tests on deuterium have also been made. The efficiency was found to be slightly less than that for hydrogen, as was expected. It has been reported that the efficiency increases if an inert gas is added to the Raman-shifting medium. Tests have been performed, with helium as the inert gas, to verify this, but only small effects have been seen.

Fig. 5A.6 shows an overview of the ozone lidar system. The Raman-shifted laser beam is sent out off-axis or coaxially with a receiving telescope. In order to obtain a vertical beam path from the ground-floor laboratory turning mirrors are used. The mirrors are mounted on a carriage which is pushed out through a hole in the wall. The horizontal telescope (31-cm diameter, off-axis) receives the backscattered light and transmits it to the detection unit. The

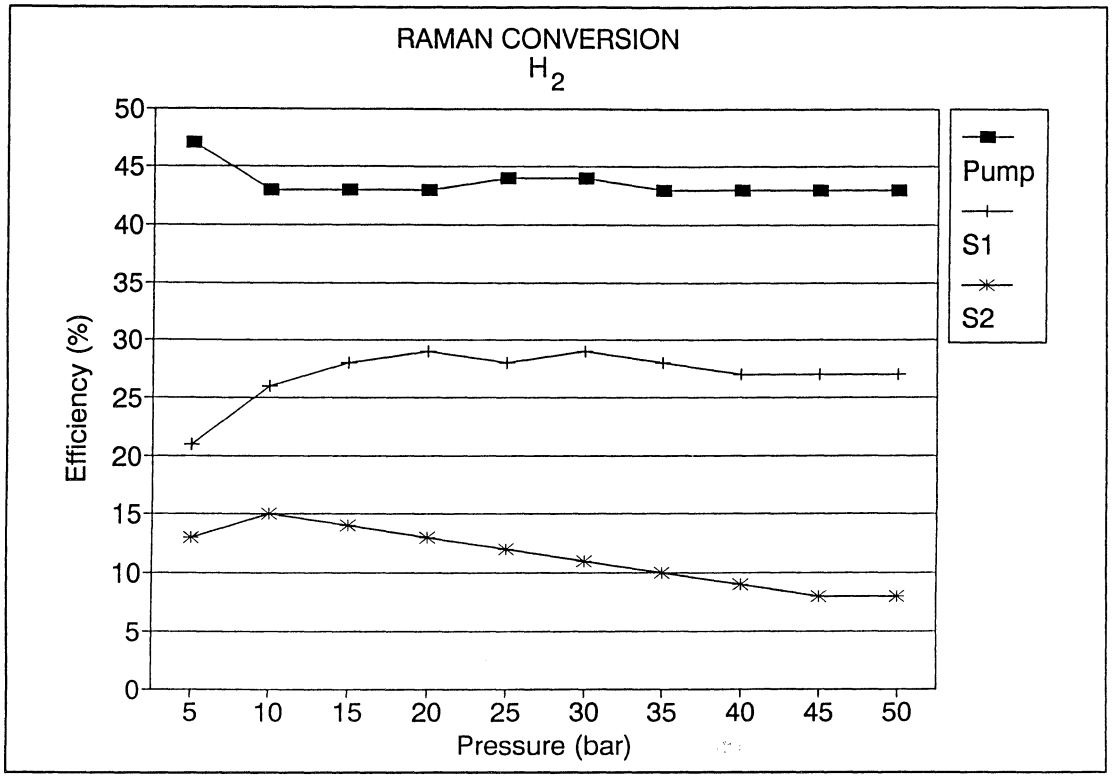

Fig. 5A.5. Raman shifting efficiency as a function of hydrogen pressure.

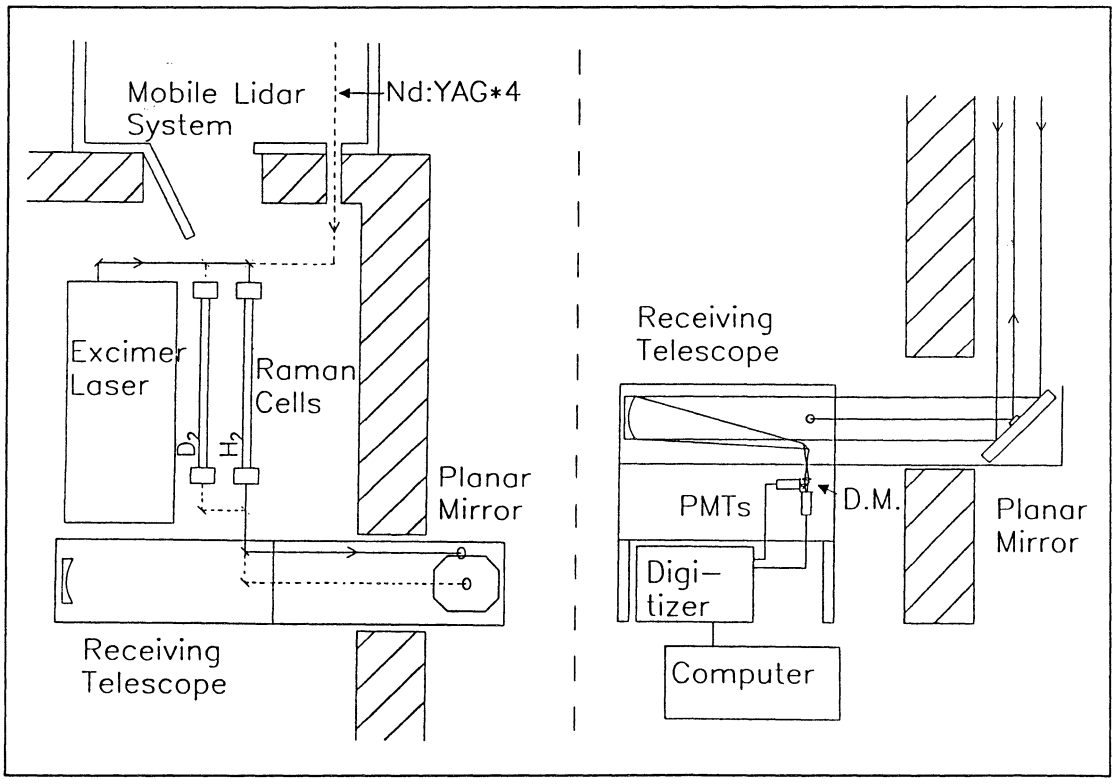

Fig. 5A.6. Overview of the ozone lidar system.

detection unit is equipped to accommodate a spectrometer, enabling several wavelengths to be monitored simultaneously. So far only two wavelengths have been used with a dichroic beam-splitter as a separator. Some preliminary measurements of the ozone concentration above Lund have been performed. The two wavelengths used were 277 nm and 313 nm, achieved by Raman shifting the light in a Raman cell filled with 10 bar of hydrogen. This is where the second Stokes component (i.e. 313 nm) is most efficiently shifted, according to previous measurements. The first Stokes component is almost twice as strong as the second at this pressure. Fig. 5A.7 shows an example of an ozone profile from 700 m up to 2600 m height measured for 2 minutes. The concentrations are calculated with a vertical resolution of about 100 m and are corrected for differential Rayleigh extinction but not for possible aerosol contributions. The ozone concentration near the ground obtained with the DOAS system, discussed later, is also indicated in the figure.

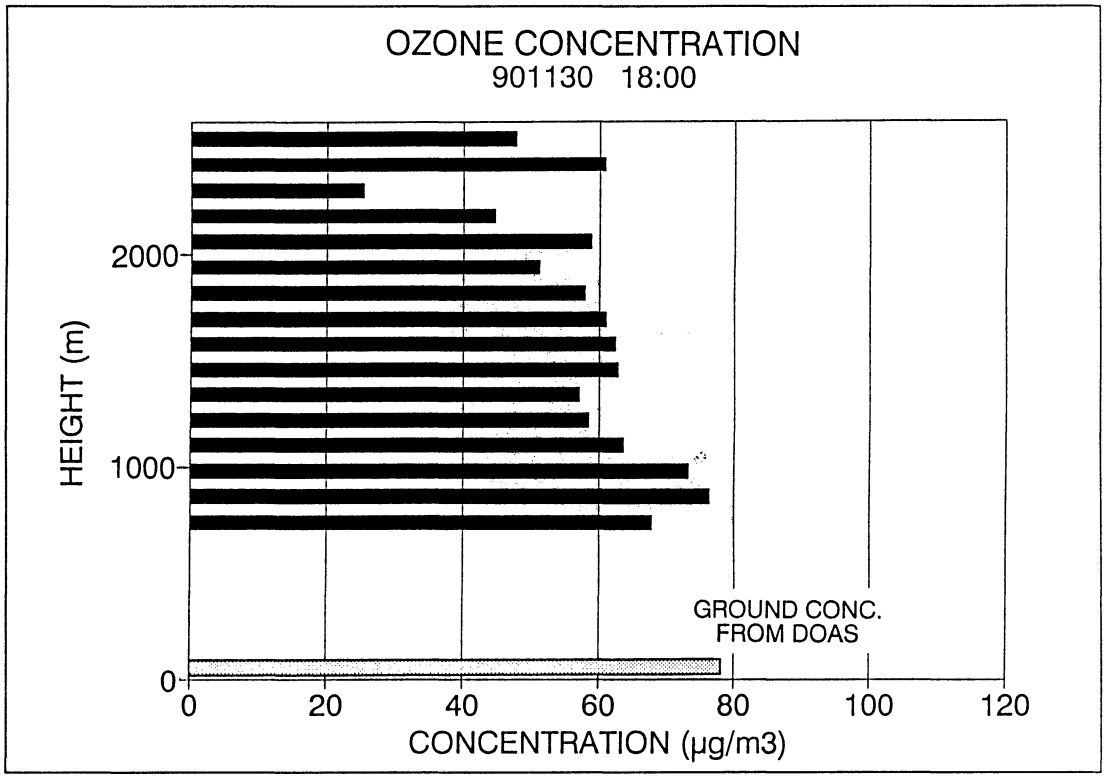

Fig. 5A.7. Vertical profile of ozone concentrations over Lund.

Ozone measurements have also been performed using the tunable dye laser in the mobile lidar system. In this way it was possible to optimize the wavelength pair so as to minimize the interference from SO_2. The wavelength pair used was 278.7 nm and 286.25 nm which is almost the maximum separation possible with the dye used. The beam was directed horizontally, which made it possible to compare the results with data taken with the DOAS system at the same time. The agreement between the two methods was not completely satisfactory and more thorough intercomparisons are being planned.

5B. Differential optical absorption spectroscopy

The DOAS system at the department is now a fully computer-controlled system for automatic atmospheric air pollution monitoring [5B.1,2]. A receiving optical telescope can sequentially tune in on light-beams from distant high-pressure xenon lamp light sources to cover a large area. Using an astronomical code, celestial sources can also be sought and tracked. A beam-finding servo system and automatic gain control allow unattended long-term monitoring. Meteorological data from a weather station are stored together with the concentrations of the desired species. A high-resolution monochromator can be adapted to the system for detailed atmospheric spectroscopy. Fig. 5B.1 shows an overview of the present system, while Figs. 5B.2 and 5B.3 show some examples of multi-path and multi-species measurements. The development of the DOAS system and detailed spectroscopic studies of some species have been performed within the TOPAS (Tropospheric Optical Absorption Spectroscopy) project, also a subproject of EUROTRAC [5B.3].

Together with the Swedish Environmental Research Institute (IVL) a new set-up for the DOAS technique using retroreflectors has been investigated [5B.4-6]. A retroreflector is a mirror arrangement constructed to return a light-beam exactly parallel to the incoming light. This quality is sustained over a wide angle interval for the incoming light (typically ± 15°). Comparative tests between this retroreflector set-up and a traditional double-ended set-up have been made. The results show that with the proper choice of components a light efficiency comparable to, or even exceeding, the efficiency obtained in a traditional double-ended set-up with the same transmitting and receiving area can be obtained. The retroreflector

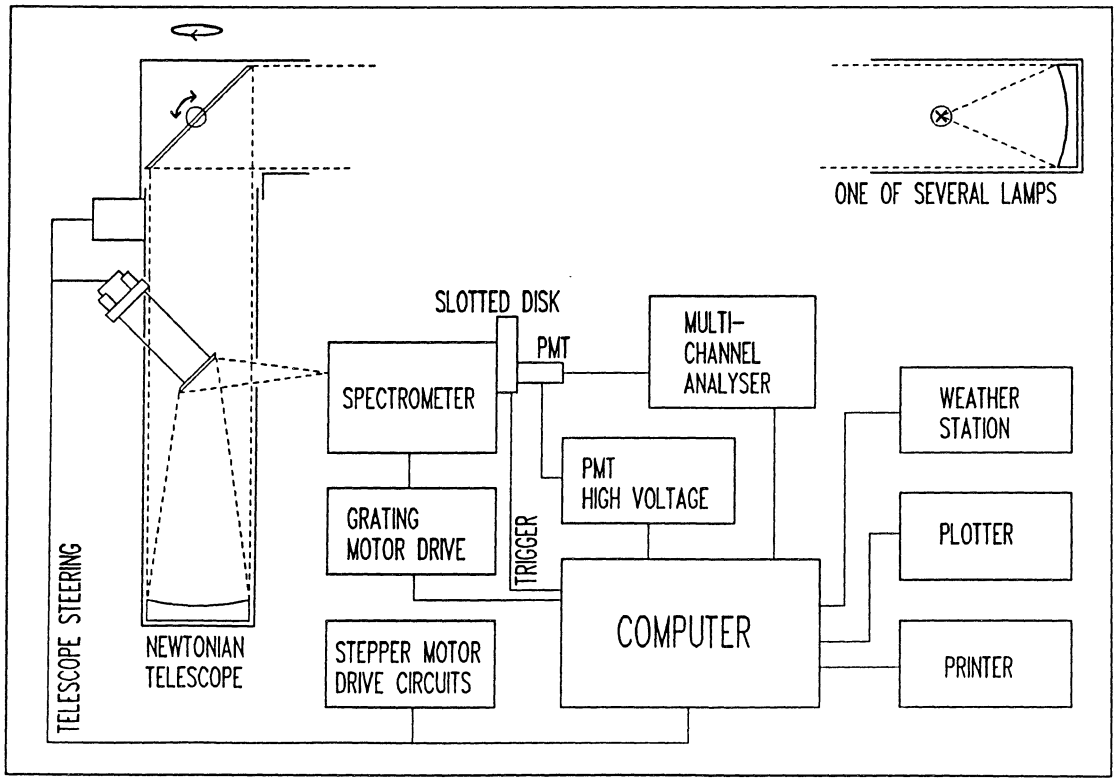

Fig. 5B.1. Interactive multi-path DOAS system.

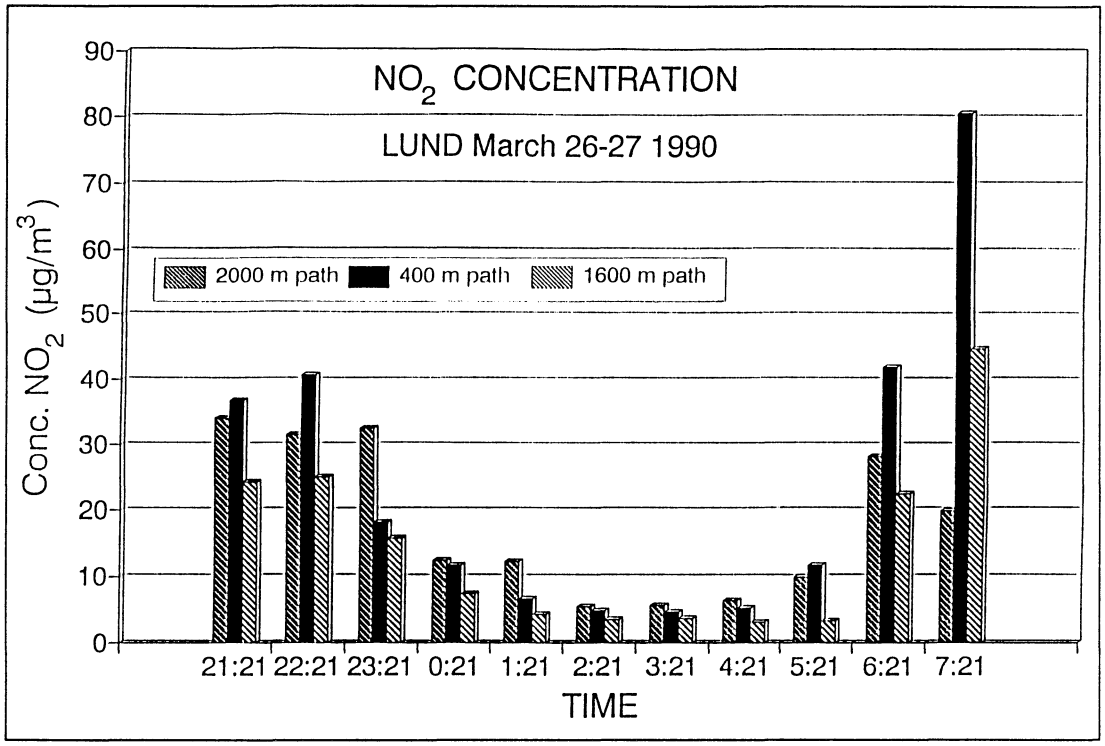

Fig. 5B.2. Nitrogen dioxide measurements over 3 atmospheric paths in Lund.

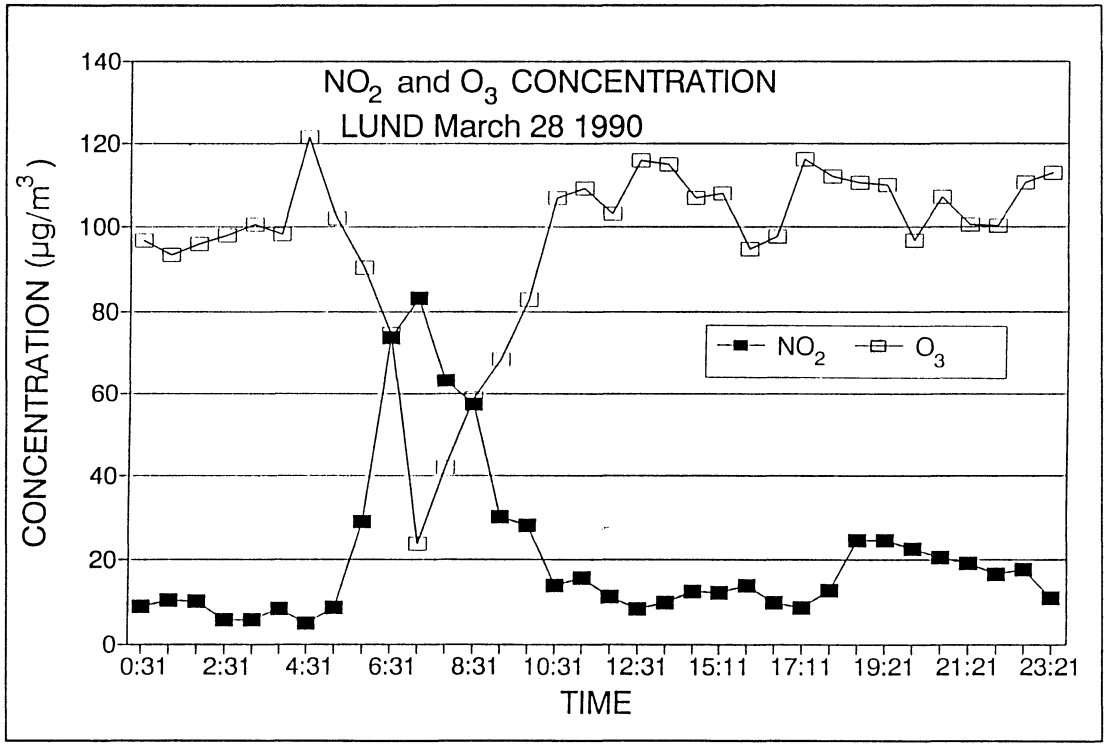

Fig. 5B.3. Simultaneous DOAS measurement of the diurnal variation of nitrogen dioxide and ozone in Lund. The anticorrelation between these two species can be seen.

set-up has been tested successfully in various hardware configurations and applications for about a year. Apart from its obvious advantages of being 'single-ended' and easy to align, some other advantages may be pointed out. The two most important ones are concerned with accessibility to the lamp. In some of the spectral regions where DOAS measurements are carried out the spectral structure of the lamp interferes with the air absorption spectra. This problem can be reduced with software techniques or by normalizing to a previously recorded lamp spectrum. As the lamp spectrum is specific for each lamp and is also affected by aging, the ideal procedure would be to record a lamp spectrum of the lamp used for each measurement, and to use this for normalization. The retroreflector set-up described here should make this possible. The second advantage is concerned with the problem of reducing sky-light interference. Under some meteorological conditions, e.g. hazy sunny days, sky light may be scattered into the field of view of the receiving telescope and interfere with the lamp spectra. With a retroreflector system the lamp may be blocked out at certain intervals, allowing the interfering sky-light to be recorded and then subtracted, from the DOAS spectrum. In modern DOAS systems a diode array is used to record the spectrum. In these systems it is necessary to be able to compensate for the difference in sensitivity between different diodes as well as subtraction of 'dark counts'. Both of these needs are fulfilled with the above mentioned procedures.

The precision of the DOAS technique is vitally dependent on an accurate determination of the differential absorption cross section for the studied species. It is also important to determine the optimum wavelength range to be utilized, particularly with regard to maximum differential cross section, minimum atmospheric attenuation and minimum interference from other species. The wavelength region around 328 nm (Huggins bands) with rather weak ozone bands has been the most used wavelength range for ozone measurements with DOAS. We have investigated the possibility of utilizing the wavelength range below 300 nm. The differential absorption features of ozone from 250 to 305 nm have been studied using a White multi-pass cell [5B.7,8]. The 280-285 nm wavelength range has proved to be a very good alternative to the Huggins bands. The maximum differential absorption cross section in this interval is $10.7 \cdot 10^{-20}$ cm^2/molecule (0.2 nm spectral resolution). This gives a theoretical detection limit of 0.7 $\mu g/m^3$ (1 km light path, least detectable optical density = 10^{-4}), which is a factor of 15 better than at 328 nm. A comparison has been made with the absorption spectra of sulphur dioxide, nitrogen dioxide and oxygen over the current wavelength range. This study shows that normally the only source of interference is sulphur dioxide, which, however, can be handled in the correlation process. Fig. 5B.4 shows an atmospheric spectrum recorded in Lund together with a composite of the correlation spectra of ozone and sulphur dioxide, which gives the best fit.

The distribution and fluxes of gaseous ammonia concentrations in the atmosphere are critical parameters in the study of the chemistry of acid rain, as well as the photochemistry of the atmosphere. Consequently, accurate monitoring methods for ammonia are needed within EUROTRAC, especially in the subproject BIATEX. Ammonia absorbs quite far down in the UV region 170-220 nm, with the strongest lines around 195 nm. This makes DOAS monitoring of ammonia difficult, since the normal atmospheric attenuation is very high at these short wavelengths. The Schumann-Runge bands of oxygen make the atmosphere

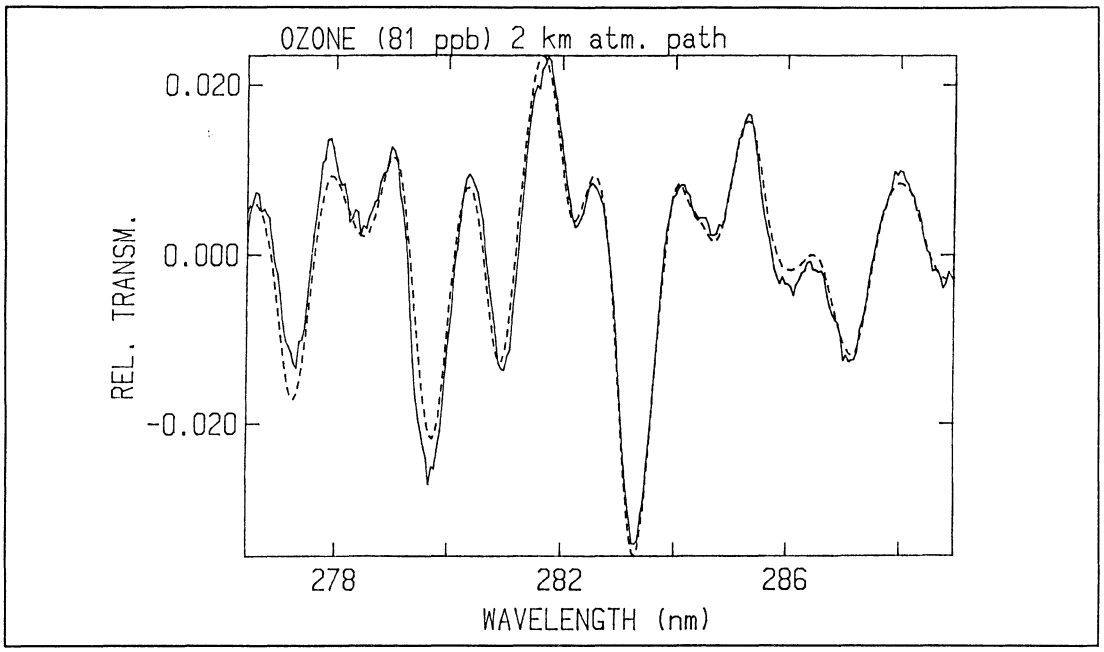

Fig. 5B.4. Atmospheric spectrum recorded in Lund (solid line) and correlated with an ozone and sulphur dioxide calibration spectrum (dashed line). The spectrum corresponds to 161 μg/m^3 ozone and 2.5 μg/m^3 sulphur dioxide.

nearly opaque below 200 nm over moderate distances, but also in the region 200-220 nm there is attenuation, due mainly to a dissociation continuum of oxygen. Therefore, the optimum pathlength for ammonia measurements will be shorter than for many other species. We have investigated the possibility of using DOAS techniques to measure ambient and elevated concentrations of ammonia [5B.9]. The absorption spectrum has been studied and compared with interferring spectra of oxygen, sulphur dioxide, nitric oxide and nitrogen dioxide with different spectral resolution. A field test in a rural area has also been performed. A 265 m atmospheric path was used and ammonia could be monitored in the spectral region 207-218 nm, with a detection limit of 1 ppbv. Figure 5B.5 shows an atmospheric spectrum, evaluated to 9.5 ppbv, together with the correlation spectrum used.

Aromatic hydrocarbons, used mainly as solvents in many industrial processes are hazardous to the lungs and brain when inhaled due to their general toxicity, and also believed to be carcenogenic. In urban areas much of the lighter hydrocarbons originate from traffic. Due to the considerable difference in size and shape between different hydrocarbons their absorption varies in different parts of the electro-magnetic spectrum. Benzene and its derivatives have absorption bands around 250 nm which originate from the excitation of the unlocalized π-bindings in the benzene ring and the fine structure of the spectrum results from vibrational transitions. The differential absorption spectra around 260 nm of 12 different benzene derivatives have been investigated and preliminary studies of their mutual interference as well as the interference from oxygen, ozone and sulphur dioxide have been performed [5B.10]. Fig. 5B.6 illustrates the inherent problem in aromatic hydrocarbon monitoring in situations

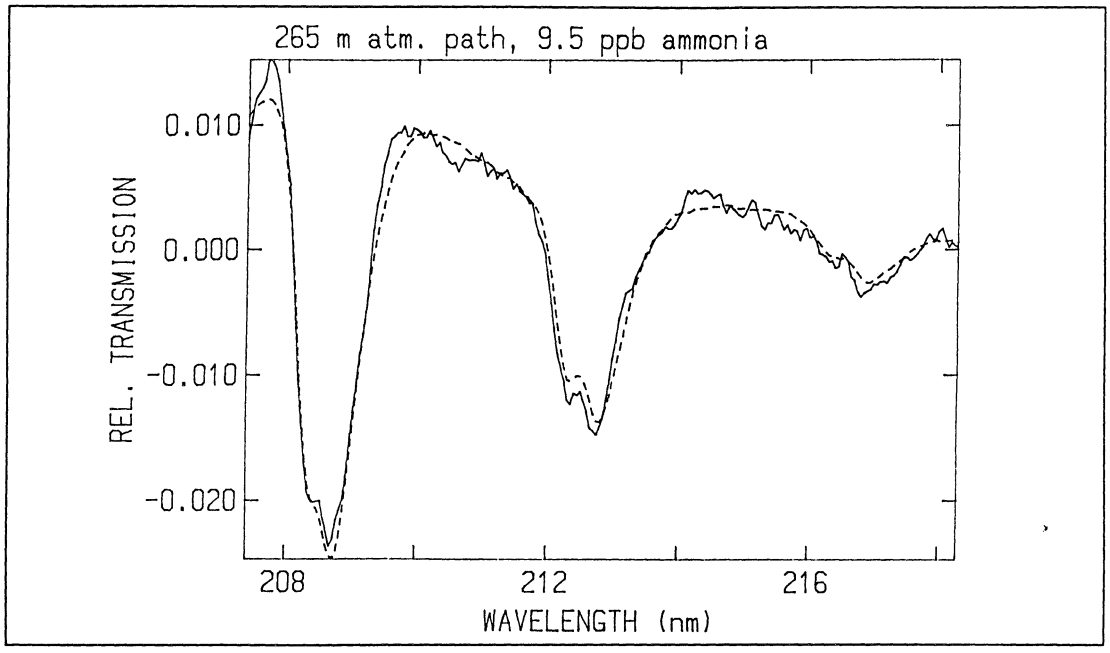

Fig. 5B.5. Atmospheric absorption spectrum of ammonia (9.5 ppbv) measured over a 265 m path, shown together with a fitted calibration spectrum.

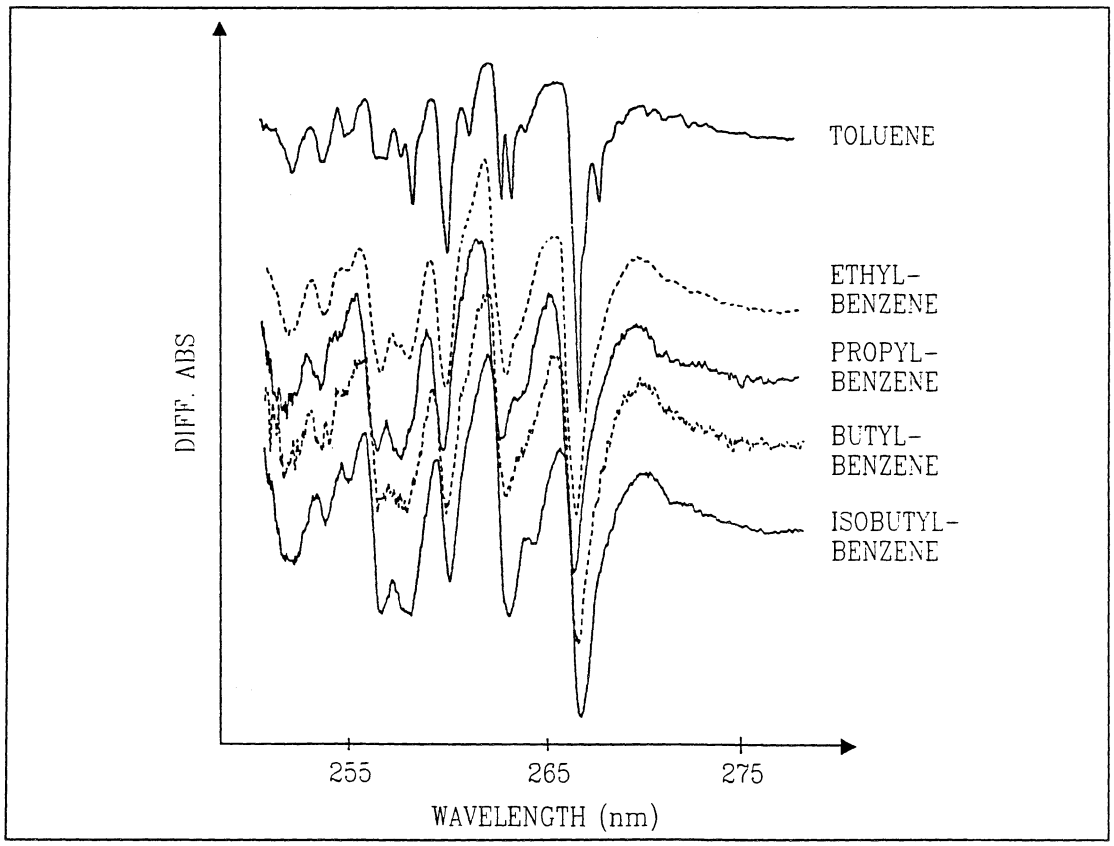

Fig. 5B.6. Differential absorption spectra of different benzene derivatives.

where there is a mixture of several hydrocarbons. As can be seen, many of these species have similar absorption features. The choice of wavelength region and the hydrocarbons that are correlated are therefore very critical factors in many applications. In order to study these problems a field measurement has been performed at the Volvo plant in Göteborg. Further planned investigations include the use of improved algorithms in the correlation process.

5C. Laser-induced Fluorescence

Laser-induced fluorescence (LIF) is being investigated as a tool in water quality studies and for the detection of stress and early damage to vegetation due to exposure to pollutants. During the last year the group has joined two European projects, called LASFLEUR and EUROMAR, aimed at measurements on vegetation and sea-water, respectively.

The main challenge of LASFLEUR is to be able to detect ozone damage to vegetation at an early stage, by remote sensing of laser-induced chlorophyll fluorescence. The goal is the development and testing of a European airborne multispectral chlorophyll fluorescence lidar for vegetation monitoring over large areas, based either on spectral ratio and/or on time-resolved measurements. In Lund, as a first step, a ground-based remote sensing LIF system was constructed by combining the mobile lidar system with the medical fluorosensor. The frequency-tripled Nd:YAG laser at 355 nm was used as the excitation source. An optical fibre at the focus of the transmitting/receiving telescope transferred the fluorescence light to the detection system. The spectrometer and optical multichannel analyser of the medical fluorosensor was used to analyse the signal. Some preliminary tests of this combined system were made in Lund during the early autumn. Maple leaves were examined for example. During the last week of the Italian field campaign, more dedicated measurements were made in the beech forests of Pian di Novello in cooperation with the Italian group at the Instituto Ricerche sulle Onde Elettromagnetiche (IROE) in Florence, lead by Professor Luca Pantani. Measurements were performed on beech tree leaves in particular, but also on other types of vegetation which could be found in the surroundings; raspberry leaves, silver fir, sallow leaves, etc. Fig. 5C.1 shows a typical spectrum of green beech tree leaves, found in the shadow. Two chlorophyll peaks can be seen, one at 685 nm and one at 735 nm. The fluorescence around 450 nm is from the wax layer of the leaves and the small peak in the yellow could be beta caroten, which had started to build up though the leaves appeared green. During the field campaign intercomparisons were made with the Italian group who used a different excitation wavelength. Measurements of the respiratory process in individual leaves were performed simultaneously.

The remote sensing work within EUROMAR is directed towards the development of advanced methods for a better evaluation of the biological, chemical and physical situation of coastal seas from airborne and shipborne platforms. The development includes lidar sensors for profiling measurements in the upper water layers of coastal areas, also based on fluorescence and Raman scattering. Interesting targets are the profiling of turbidity and monitoring of algae, Gelbstoff and artificial tracers. As a part of this project, the last few days in Italy were dedicated to measurements of the water of the Arno river. Three different sites were examined: upstream of

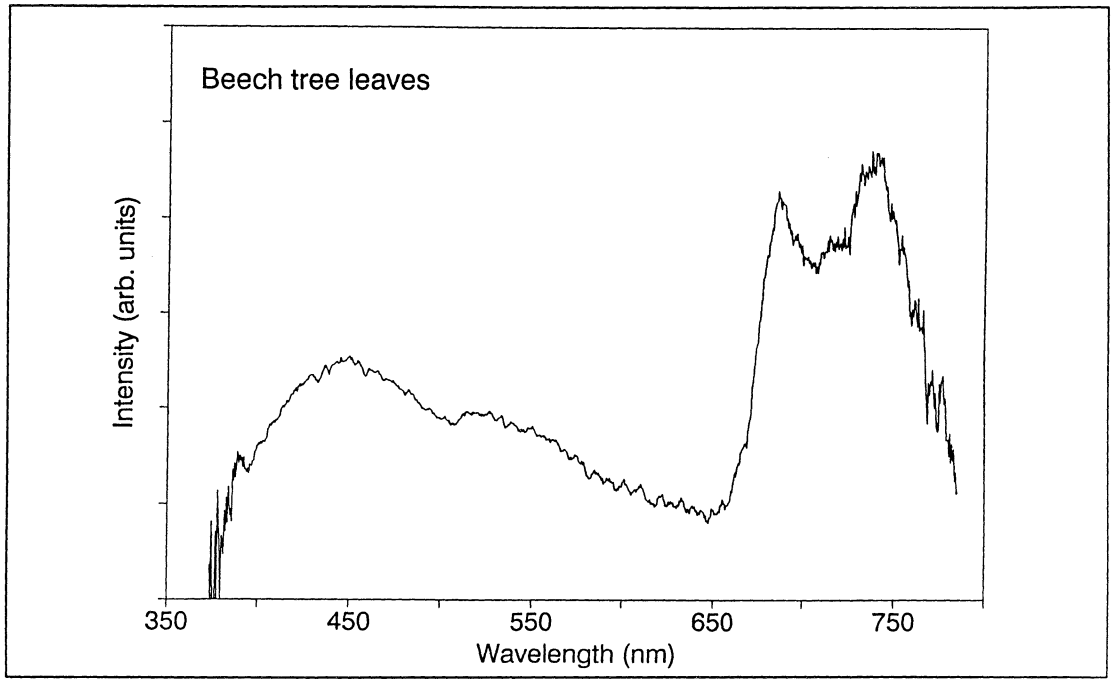

Fig. 5C.1. LIF spectrum of beech leaves.

Florence, downstream of Florence and at Marina di Pisa, at the mouth of the river. Different distances from the shore were examined at all three sites. Fig. 5C.2 shows a spectrum from the site downstream of Florence. It can be seen, for example, that the water contains some chlorophyll, due to algae in the water. The water Raman peak can also be seen.

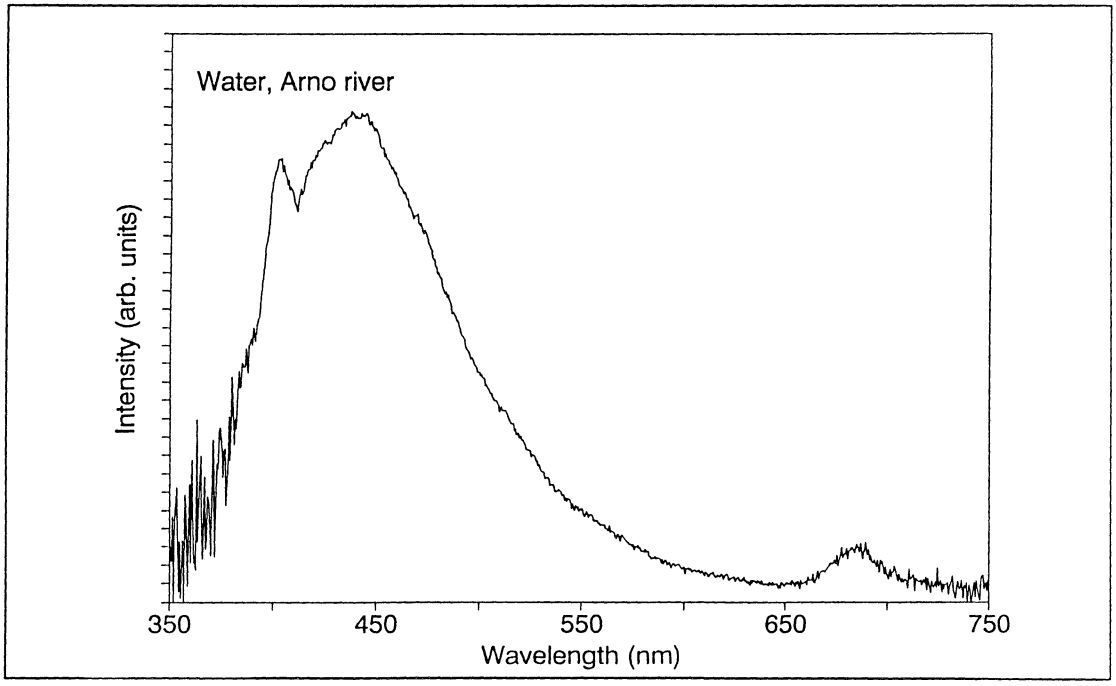

Fig. 5C.2. LIF spectrum of water in the Arno river.

References

5.1. H. Edner and S. Svanberg, Laser kartlägger luftföroreningar och nyttigt ozon, NFR:s årsbok 1988/89: Forska på tvären (1989).

5.2. S. Svanberg, Environmental monitoring using optical techniques, in Applied Laser Spectroscopy, Eds. M. Inguscio and W. Demtröder, Plenum Press, New York, to appear.

5.3. S. Svanberg, Remote sensing with active optical techniques, Remote Sensing / Swedish Space Corporation No. 19 (1990).

5.4. S. Svanberg, Atmospheric pollution monitoring using laser lidars, International School of Quantum Electronics: Course on Optoelectronics for Environmental Science, Erice, Italy, Sept. 3-12, 1989 (Plenum Press, New York, to appear).

5.5. S. Svanberg, Laser fluorescence spectroscopy in environmental monitoring, International School of Quantum Electronics: Course on Optoelectronics for Environmental Science, Erice, Italy, Sept. 3-12, 1989 (Plenum Press, New York, to appear).

5.6. H. Edner, Laserradarteknik för mätning av luftföroreningar, Elmia Energi & Miljö 90, Jönköping, 23-27 april 1990.

5.7. S. Svanberg, Laser spectroscopy applied to energy, environmental and medical research, Kemistdagar i analytisk kemi, Lund, 17-21 juni 1990.

5.8. S. Svanberg, Laser spectroscopy applied to energy, environmental and medical research, 5th International Symposium on Resonance Ionization Spectroscopy and its Applications (RIS-90), Varese, Italy, Sept. 16-21, 1990.

5.9. H. Edner, Optical remote sensing of atmospheric pollutants, International Electro-Optic Exposition '90, Taipei, Taiwan, Oct. 18-21, 1990.

5.10. H. Edner, Environmental monitoring using lidar techniques, International Electro-Optic Exposition '90, Taipei, Taiwan, Oct. 18-21, 1990.

5A.1. H. Edner, G.W. Faris, A. Sunesson and S. Svanberg, Atmospheric atomic mercury monitoring using differential absorption lidar techniques, Appl. Opt. **28**, 921 (1989).

5A.2. H. Edner, G.W. Faris, A. Sunesson, S. Svanberg, J.Ö. Bjarnason, H. Kristmannsdóttir and K.H. Sigurdsson, Lidar search for atmospheric atomic mercury in Icelandic geothermal fields, J. Geophys. Research, accepted.

5A.3. H. Edner, G.W. Faris, P. Ragnarson, A. Sunesson and S. Svanberg, Lidar measurements of atmospheric mercury, International Congress on Optical Science and Engineering: Environment and Pollution Measurement Sensors and Systems, The Hague, The Netherlands, March 14-15, 1990, SPIE Proceedings **1269**, 73 (1990).

5A.4. H. Edner, P. Ragnarson and S. Svanberg, Lidar and DOAS measurements of atmospheric mercury, International Conference on Mercury as an Environmental Pollutant, Gävle, Sweden, June 11-13, 1990.

5A.5. H. Edner and S. Svanberg, Lidar measurements of atmospheric mercury, Water, Air, & Soil Pollution, accepted.

5A.6. H. Edner, Optiska metoder för mätning av kvicksilverinnehållet i rökgaser från krematorier, Lund Reports on Atomic Physics, LRAP-110 (1989).

5A.7. H. Edner, P. Olsson and E. Wallinder, Mätning av kvicksilver med optisk teknik vid Råcksta krematorium, Lund Reports on Atomic Physics, LRAP-118 (1990).

5A.8. H. Edner, P. Ragnarson, S. Svanberg, E. Wallinder, R. Ferrara, B.E. Maserti and R. Bargagli, Differential absorption lidar mapping of atomic mercury of geophysical origin, submitted for CLEO '91.

5A.9. S. Svanberg, Vertical ozone sounding with lasers (TESLAS), IVA-symposium 6 dec. 1988: Vad händer i luften över Europa?, IVA-rapport 366, Ingenjörsvetenskapsakademien, Stockholm (1989).

5A.10. H. Edner, P. Ragnarson, S. Svanberg and E. Wallinder, Vertical ozone probing with lidar, Nordic Symposium on Atmospheric Chemistry, Stockholm-Helsinki, Dec. 6-8, 1989.

5A.11. H. Edner, P. Ragnarson, S. Svanberg and E. Wallinder, Vertical lidar probing of ozone and related trace species - A contribution to the EUROTRAC subproject TESLAS, EUROTRAC Annual Report 1989, Part 7 (1990).

5A.12. H. Edner, P. Ragnarson, S. Svanberg and E. Wallinder, Vertical lidar probing of ozone and related trace species - A contribution to the EUROTRAC subproject TESLAS, to be published in the EUROTRAC Annual Report 1990.

5A.13. M.J.T. Milton, A. Sunesson, J. Pelon, G. Ancellet, J. Bösenberg, W. Carnuth, H. Edner and L. Stefanutti, Raman-shifted laser sources for DIAL measurements of ozone in the free troposphere, 15th International Laser Radar Conference, Tomsk, USSR, July 23-27, 1990.

5B.1. S. Spännare, An interactive steering system for DOAS measurements, Diploma paper, Lund Reports on Atomic Physics, LRAP-117 (1990).

5B.2. H. Edner, P. Ragnarson, S. Spännare and S. Svanberg, A differential optical absorption spectroscopy (DOAS) system for urban atmospheric pollution monitoring, to appear.

5B.3. R. Amer, H. Axelsson, H. Edner, B. Galle, P. Ragnarson and M. Rudin, Development of DOAS for atmospheric trace species monitoring - A contribution to the EUROTRAC subproject TOPAS, EUROTRAC Annual Report, Part 7 (1990).

5B.4. H. Axelsson, B. Galle, K. Gustavsson, P. Ragnarson and M. Rudin, A transmitting/receiving telescope for DOAS measurements using retroreflector technique, Optical Remote Sensing of the Atmosphere Topical Meeting, Incline Village, Nevada, Feb. 12-15, 1990.

5B.5. H. Axelsson, B. Galle, K. Gustavsson, P. Ragnarson and M. Rudin, A transmitting/receiving telescope for DOAS measurements using retroreflector technique, EUROTRAC Symposium '90, Garmisch-Partenkirchen, Germany, April 2-5, 1990.

5B.6. H. Axelsson, B. Galle, K. Gustavsson, P. Ragnarson and M. Rudin, A transmitting/receiving telescope for DOAS measurements using retroreflector techniques, submitted to Applied Optics.

5B.7. H. Axelsson, H. Edner, B. Galle, P. Ragnarson and M. Rudin, Differential absorption cross section of ozone in the 250-350 nm wavelength range, EUROTRAC Symposium '90, Garmisch-Partenkirchen, Germany, April 2-5, 1990.

5B.8. H. Axelsson, H. Edner, B. Galle, P. Ragnarson and M. Rudin, Differential optical absorption spectroscopy (DOAS) measurements of ozone in the 280-290 nm wavelength region, Appl. Spectr., Dec. 1990.

5B.9. H. Edner, R. Amer, P. Ragnarson, M. Rudin and S. Svanberg, Atmospheric NH_3 monitoring by long-path UV absorption spectroscopy, International Congress on Optical Science and Engineering: Environment and Pollution Measurement Sensors and Systems, The Hague, The Netherlands, March 14-15, 1990, SPIE Proceedings **1269**, 14 (1990).

5B.10. H. Axelsson, H. Edner, A. Eilard, A. Emanuelsson, B. Galle, H. Kloo and P. Ragnarsson, Mätning av aromatiska kolväten med DOAS - En studie av tillförlitlighets och interferensproblem, IVL Rapport L90/311 (1990).

6. LASER APPLICATIONS TO MEDICINE AND BIOLOGY

Stefan Andersson-Engels, Roger Berg, Petra Hansson, Hans Hertz, Niklas Hildebrand, Jonas Johansson, Sune Montán, Sune Svanberg,

Since the start of medical laser applications at the division of Atomic Physics in 1982 work has been carried out in close collaboration with the Lund University Hospital. The work has covered many diverse areas of medicine in connection with 19 different clinics. Applications to biology have been initiated mainly related to fluorescence recordings and basic optical research on damage to vegetation. The instrumentation used in all these experiments has been developed by the physicists at the division of Atomic Physics to meet the specific demands of the unique experimental situations for the various applications. In this work, the feedback from the medical departments and clinics has been very valuable.

Our recent work has been presented in a large number of invited talks and review articles [6.1-6.9]. Two PhD theses and two diploma works have been presented within the project during the two last years [6.10-6.13]. The medical applications of lasers can basically be divided into diagnostics and treatment. Treatment covers everything from the ablation of tissue using high-power lasers to photochemical reactions obtained with a weak laser, sometimes together with a drug introduced into the body. Diagnostics covers the recording of fluorescence after laser excitation at a suitable wavelength and measurements of optical parameters, such as scattering and absorption using transillumination of tissue. When designing a diagnostic laser system for use in a clinical situation, several important factors have to be seriously considered.

Firstly, a suitable excitation wavelength has to be chosen, depending on which chromophores in the tissue are of interest for the diagnosis. A detailed knowledge of the fluorescence properties of the different chromophores present in the tissue is necessary for an acceptable result. For free atoms the absorption peaks are narrow and easy to distinguish. However, for molecules in tissue, the absorption peaks are broadened by rotational vibrational movements and also by interactions between the molecules. Thus, we require an excitation wavelength which gives optimum excitation of the chromophore of interest while not exciting the other constituents of the tissue.

Secondly, the origin of the structures in the fluorescence spectra of the chromophores must be identified whether the full spectrum is going to be presented or the intensity at a few chosen wavelengths will be used to obtain a demarcation criterion. In Fig. 6.1, the fluorescence spectra of five different purified substances which are likely to be found in human tissue are presented. Collagen and elastin are strong fluorophores in the larger human arteries. Nicotinamide adenine

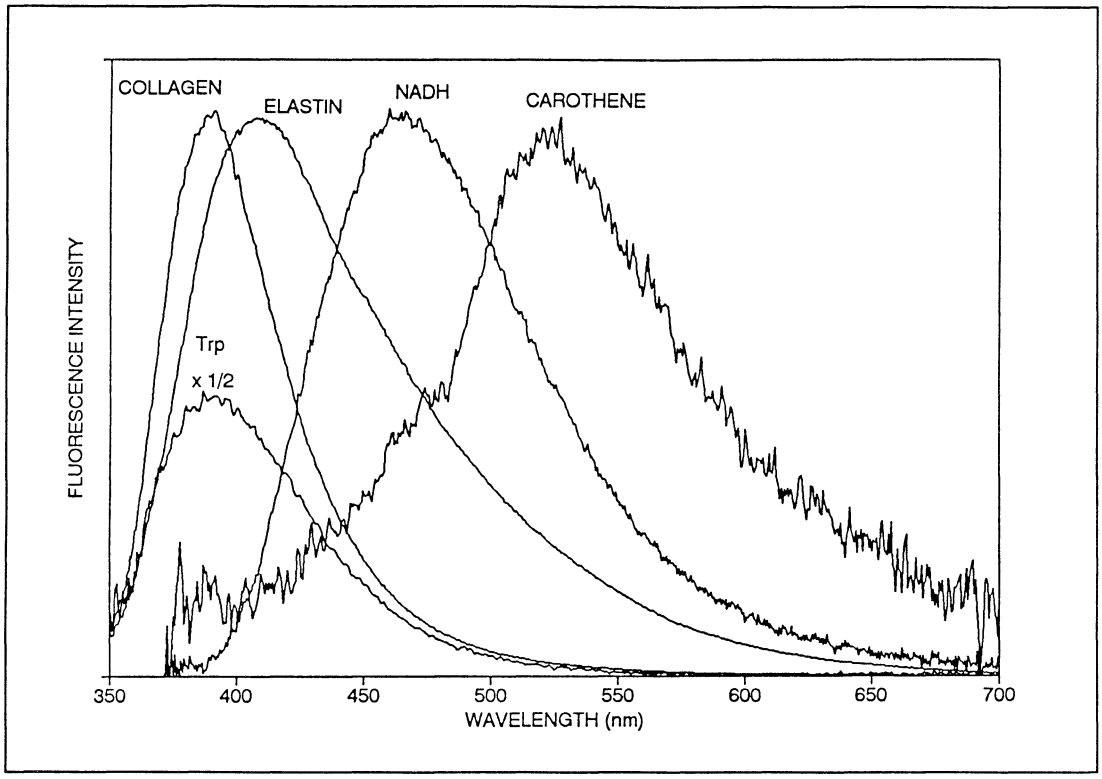

Fig. 6.1. Fluorescence spectra from: L-tryptophan, collagen I, elastin, β-NADH and β-carothene. The excitation wavelength was 337 nm.

dinucleotide (NADH) and tryptophan are the main fluorophores in muscle tissue excited with UV light. Another characteristic of the fluorescence is the lifetime of the excited state which is different for different chromophores. By using a short-pulse laser, this feature can also be used for tissue diagnostics. The decay time of the polarization of the fluorescence also shows some potential for diagnostics.

In some cases the optical properties of the endogenous chromophores are not sufficient to characterize different tissue types. In order to enhance the optical demarcation of malignant tumours it is possible to inject a tumour seeking drug. A clinically used drug is hematoporphyrin derivative (HpD) with its characteristic double-peaked fluorescence structure in the red region. The intrinsic fluorescence from the tissue, the autofluorescence, on the other hand, has been shown to decrease in malignant tumours compared with normal tissue. In the demarcation of malignant tumours it is advantageous to use both the HpD-related fluorescence and the autofluorescence, to enhance the tumour demarcation. The drug-specific fluorescence and the autofluorescence can be used to form a ratio which has the advantage of being dimensionless. Such a ratio will be independent of the distance to the object, the shape of the object and to laser intensity variations, parameters which might be difficult to control. In many cases the autofluorescence contains information that can be used to increase the demarcation ratio between tumour and the surrounding tissue. This has been observed for many different tumour types using a nitrogen laser as an excitation source.

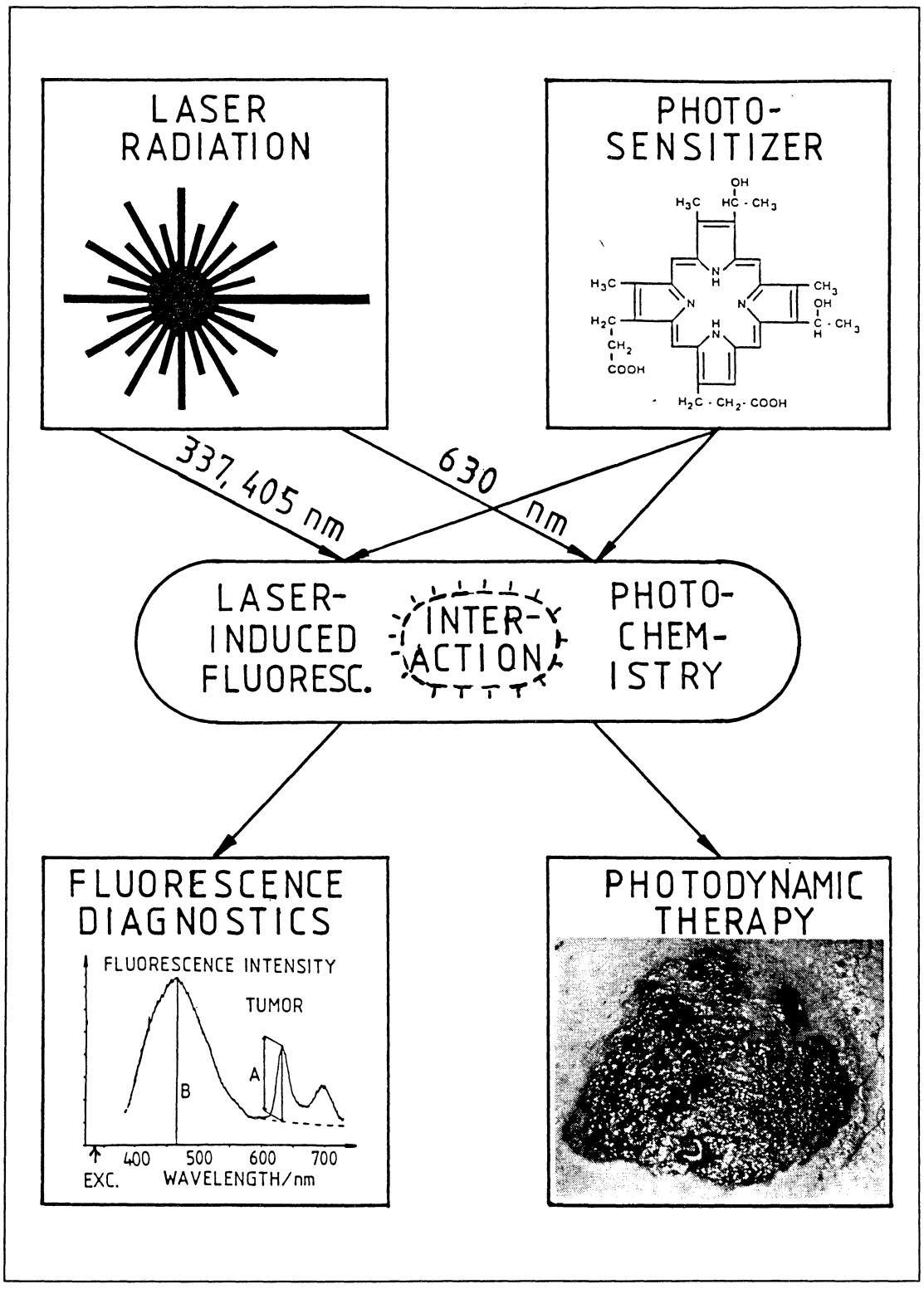

Fig. 6.2. Schematic illustration of the diagnostic and therapeutic use of photosensitizers in combination with laser radiation. To the lower left is a fluorescence spectrum from tissue injected with HpD for 337 nm excitation. To the lower right is a photograph showing necrosis of a basalioma 48 h post photodynamic therapy.

HpD can also be used for local treatment of malignant tumours. In this process, called photodynamic therapy (PDT), the excited state energy is transferred to the oxygen molecules in the tissue. The tissue oxygen molecules are excited to a singlet state, which is known to be very cytotoxic. Thus the HpD-containing tumour is transformed into necrotic tissue in the PDT process. The double use of HpD is illustrated in Fig. 6.2. Apart from sensitizing malignant tumours intravenously, the injected HpD will also give rise to an unwanted skin sensitization for a period of about four to six weeks. It would be desirable to find a photosensitizer without this side-effect.

There are many attractive treatment modalities utilizing high-power lasers. Most such lasers (e.g. YAG lasers) are used for surgical work producing smooth cuts with immediate coagulation. Using excimer lasers it is possible to ablate layers of tissue as thin as a few microns. A very promising application of excimer laser ablation is the remodeling of narrowed or obstructed blood vessels. Since 1987 we have been investigating the possibility of using the intrinsic fluorescence from atherosclerotically diseased arteries to steer an excimer ablation laser. Since the fluorescence from an atherosclerotic plaque differs from that of a normal vessel wall, it is possible to use the signal from the fluorescence measurement device to enable an ablation laser. The emission from the plasma resulting from the ablation can also be used for plaque detection.

Among non-medical applications, the investigation of chlorophyll fluorescence from trees in a field measurement in Florence, Italy can be mentioned (see section 5). In this case our mobile fluoroscensor was attached to the mobile LIDAR system to obtain far field spectra of damaged trees at distances of more than 100 metres.

6A. Fluorescence recordings of experimental animal tumours

The search for new, more efficient photosensitizers for photodynamic therapy (PDT) and fluorescence diagnostics of tumours has been intensified. In 1960 Lipson *et al.* presented a derivative of hematoporphyrin (HpD) with much better qualities than its predecessors. Since then, a large variety of drugs have been developed. The most common, besides hematoporphyrin, are phthalocyanine, derivatives from chlorophyll such as chlorine, and other porphyrins, e.g. benzoporphyrin. The properties of an optimal fluorescence tumour marker are not the same as those of an optimal photosensitizer. This problem was addressed by our group in a comparative study of different drugs where the tumour demarcation potential was investigated using laser-induced fluorescence [6A.1]. It was found, that so far the best drug for fluorescence detection was a purified form of hematoporphyrin called Photofrin. At a later stage benzoporphyrin derivative monoacid, a newly developed photosensitizer, was included in the study [6A.2]. The fluorescence spectra of adenocarcinoma tumours in injected rats are presented in Fig. 6.A.1 for some of these photosensitizers.

In 1984, we found that not only the fluorescence of the photosensitizer contributed to the tumour demarcation but also the autofluorescence from endogenous chromophores, provided a UV light source was used. One of the best examples of this is observed for certain brain tumours where a demarcation ratio of 80 was obtained using both

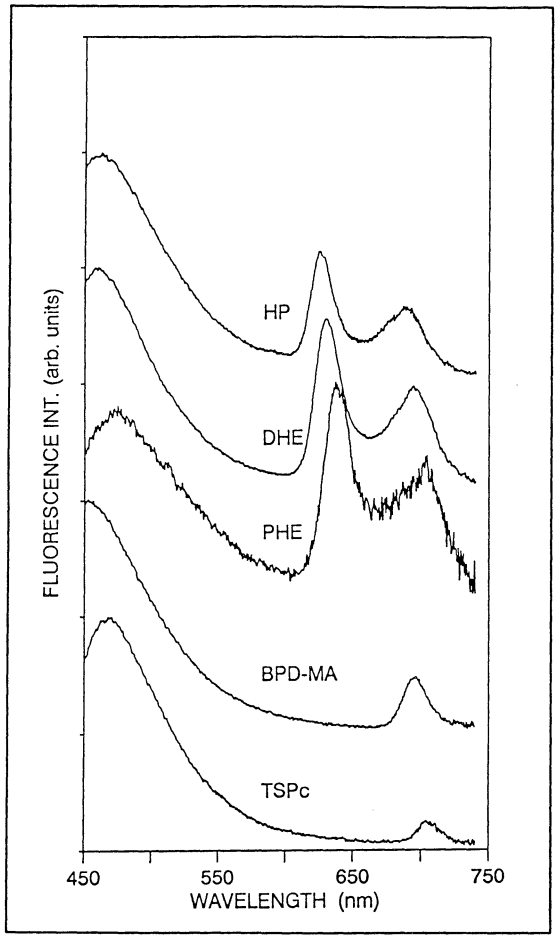

Fig. 6A.1. Fluorescence spectra from tumours of rats injected with: hematoporphyrin, dihematoporphyrin, poly hematoporphyrin, benzo porphyrin derivative mono acid and tetra sulfonated phthalocyanine. The excitation wavelength was 337 nm.

the autofluorescence and the hematoporphyrin fluorescence [6A.3]. We found that the best demarcation criterion can be written in the form (A-D)/B, [6.10] where A is the porphyrin-related fluorescence intensity at 630 nm, D is the fluorescence background intensity at the same wavelength and B is the maximum of the autofluorescence intensity obtained at about 470 nm. This is a spectroscopic "trick" to condense as much of the spectroscopic information as possible into one value, a value that is a measure of tumour presence.

In order to investigate the fluorescence contribution from a malignant tumour, a mechanical separation of the tumour was performed. The fluorescence from the fraction with the vital tumour cells and from the fibrotic stromal part of the tumour was measured. The porphyrin-related signal showed about the same intensity for the two fractions, while the autofluorescence signal varied considerably [6A.4]. The fluorescence from the cell fraction showed a very low intensity, while the stromal part exhibited higher values. The autofluorescence from the stroma of the tumour showed a maximum at about 390 nm, which may be interpreted as a contribution from collagen. The total autofluorescence from malignant tissue is probably mainly due to the fibrotic "skeleton" of the tumour, while the fluorescence from the tumour cells themselves makes a negligible contribution.

So far, only point monitoring of diseased tissue has been presented here. However, these methods become even more useful when they are

extended to imaging of an area of the tissue. In 1987 we presented a method for the imaging of tumours using the spectroscopic criteria found to be suitable in the point measurements. The first system for spectrally enhanced 2-D imaging was assembled in 1989, consisting of a Cassegranian telescope with the front mirror split into four parts and an image-intensified 2-D CCD detector [6A.5]. In this way, four images of the same area, but in different colours, could be recorded for each laser shot. These images were reduced to one image by pixel-by-pixel calculation of the four images in a PC-computer using the (A-D)/B criterion. Images were produced with high values for tumour and low values for surrounding tissue. False colour representation was used to further enhance the contrast.

Finally the techniques presented here can, to good advantage, be extended to the time domain. It was shown that hematoporphyrin has a fluorescence decay time of about 15 ns, whereas tissue autofluorescence has a decay time of about than 1 ns [6C.5]. This can be used to further enhance the tumour demarcation by using short-pulse lasers (e.g. nitrogen laser) in connection with fast gating detection [6C.4]. The imaging system presented above has a gating time as short as 5 ns, which is short enough to take advantage of the temporal characteristics of fluorescence.

6B. Clinical laser applications to tumours

The equipment used for the measurement of laser-induced fluorescence has been assembled into a more compact version and placed on a trolley [6B.1]. This mobile system has a 180 μJ nitrogen laser coupled to a dye laser, acting as an excitation source, with the possibility of using the nitrogen laser alone. The excitation as well as the fluorescence light is guided through a 600 micron quartz fibre, 3 m long, connected to an external fibre specially designed for each application. The fluorescence is captured with a spectrometer, recorded in an image-intensified diode array and displayed on an OMA mainframe or stored on floppy disks. The flexibility of this system has been demonstrated in neurosurgery, bronchoscopy, during resection of bladder tumours, and many other applications [6B.2]. Very high potential for fluorescence diagnostics was found for oral tumours, where the autofluorescence from endogenous porphyrins is sufficient for an accurate diagnosis of the type of tumour investigated. Astrocytoma tumours in human brains also seem to differ in fluorescence from surrounding tissue without any injection of a tumour marker. In the case of lung tumours, however, the fluorescence spectra from tumour and surrounding tissue are quite similar.

Another point monitoring system constructed at the Division of Atomic Physics is based on a mercury lamp and sequential recording of fluorescence at a few selected wavelengths using two different excitation wavelengths. The lamp in connection with a photomultiplier tube makes it a cheap alternative with good performance [6.12]. For different applications, a suitable set of three interference filters is inserted into a rotating filter wheel on the detection side. The system is controlled from a PC which calculates the demarcation criterion (A-D)/B. Our investigations have shown that once the fluorescence characteristics are known for a specific application, such a system is sufficient for a reliable diagnosis.

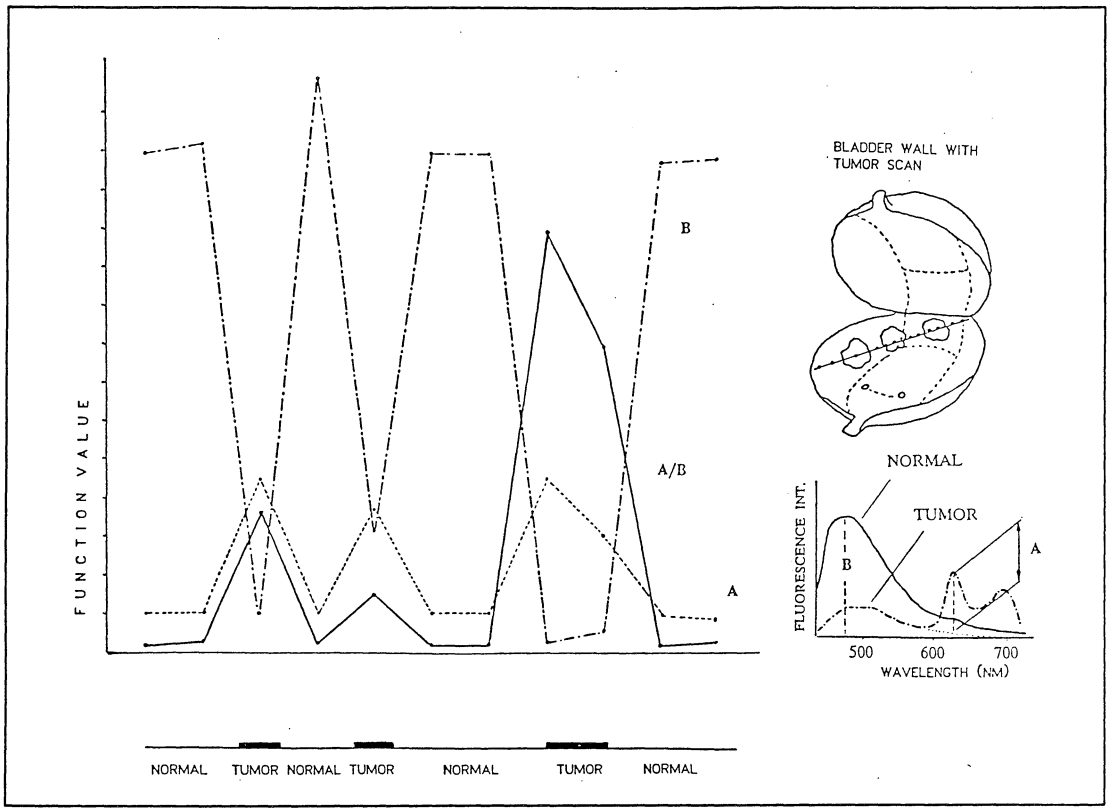

Fig. 6B.1. Fluorescence data obtained in a scan across three malignant superficial bladder tumours. The patient had been injected with 0.35 mg/kg b.w. DHE 48 h prior to the investigation. The location of the tumours as well as a typical fluorescence spectrum of the tumour and normal mucosa are shown to the right.

The two point monitoring systems mentioned above were both used in *in vivo* fluorescence measurements of malignant bladder tumours, including very thin superficial lesions, such as cancer *in situ (CIS)* and dysplasia (pre cancerous lesions). [6A.4] The investigation was performed in a collaboration between our group and the Department of Urology at the University Hospital in Leuven, Belgium. The patients we investigated were undergoing cystoscopic investigation for various reasons. Some of them had superficial tumours, either the first tumour occurrence or recurrences, verified during earlier investigations about a week earlier. These were treated with a Nd:YAG laser during the same procedure. Others were undergoing a regular checkup cystoscopy after Nd:YAG laser or photodynamic treatment 3 months earlier. A third group was undergoing a second cystoscopy due to recently discovered suspicious areas in the bladder wall some weeks earlier. The patients had been given a low dose of hematoporphyrin derivative, 0.35-0.5 mg/kg b.w. DHE intravenously 48 hours prior to the investigation. The drug doses used were below the threshold for skin photosensitization. With the fibre-optically equipped fluoroscensor and low dose of DHE, the demarcation ratio between malignant tumour and normal non-invaded bladder mucosa varied between 4 and 15, provided the drug-related fluorescence as well as the autofluorescence was included in the demarcation criterion. Discovery of cancer *in situ* and dysplasia was possible. A scan across a tumour

region is shown in Fig. 6B.1. All areas investigated were sampled for histopathological examination. In connection with the YAG laser treatment, the tumour bed was investigated. In some cases the underlying tissue showed signs of remaining malignant invasion after a first period of YAG treatment, and a complementary second YAG treatment was performed. After the repeated laser treatment the tumour bed showed no remaining malignant tumour. Thus the system incorporated guidance for the treatment procedure, enhancing the radicality.

6C. Fluorescence recordings of human atherosclerotic plaque

Our project concerned with the localization of atherosclerotic plaque in human arteries has been in progress since 1987. In the early work, we found that by using a nitrogen laser (337 nm) for fluorescence excitation, a substantial discrimination between plaque and normal arteries was obtained [6C.1]. Before 1987, only lasers in the visible region had been used as excitation sources. Extensive statistical studies were performed aimed at finding the optimal demarcation criterion for plaque. The equipment we used in these trials for recording of fluorescence spectra was mainly the fibre assisted OMA system. One important problem that was addressed was the interference in the fluorescence spectrum caused by the presence of blood. The blood does not exhibit any fluorescence under UV excitation, however, the light absorption by haemoglobin has sharp spectral structures and is very strong in some regions. Thus, a demarcation criterion which is not carefully chosen, may give different results when differing amounts of blood are present, a fateful characteristic when working in blood vessels. We have found two methods of eliminating this problem. First, one can use a demarcation ratio at two fluorescence wavelengths which show equally high blood absorption, and a high ratio for plaque and a low ratio for normal vessel. Two such wavelength pairs are 380 nm/437 nm and 520 nm/489 nm, the second one giving a high value only for lipidic plaque [6C.2]. The second method of obtaining blood-independent readings is to utilize the fluorescence decay time as a demarcation criterion [6C.3]. The fluorescence photons originating from the tissue are absorbed to the same amount regardless of the time the fluorescing molecule has been excited, as long as measurements are made only at one wavelength. The blood independence of a fluorescence decay recording is therefore trivial. This was shown in a study where a photomultiplier was used together with a boxcar integrator to form a ratio of the signal integrated from 0 to 5 ns. to the signal from 5 to 15 ns [6C.4]. As blood was poured over a plaque sample, the fluorescence-collecting optical fibre was withdrawn with the aid of a micrometer screw. In this way the demarcation ratio was stable for the different amounts of blood. The limit was instead set by the noise of the signals as the blood absorption increased.

It is of great importance for a reliable diagnosis that the fluorescence spectra of various plaque types and non-diseased vessels are well understood. To increase our knowledge on the causes of spectroscopic differences between spectra from plaque and normal vessels, we carried out an investigation where some purified substances as well as different regions of plaque were studied [6C.2]. The fluorescence was studied with regard to both the spectral shape and the decay time, while varying the excitation wavelength. Part of this study was performed at the MAX laboratory as it was here possible to vary the excitation wavelength easily. Examples of fluorescence

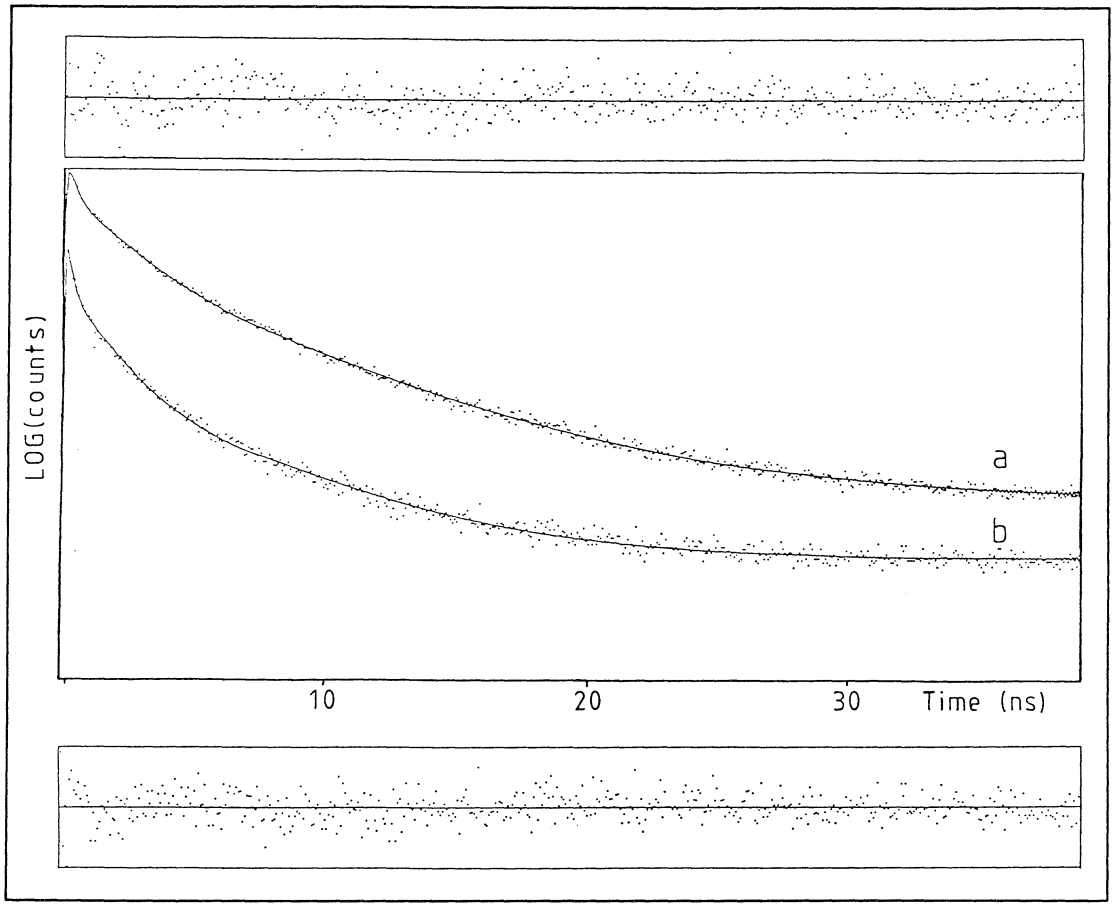

Fig. 6C.1. Fluorescence decay curves for 337 nm excitation: (a) thick plaque, (b) normal vessel wall; both curves 380 nm emission. The weighted residuals are included for thick plaque (above) and normal vessel (below).

decay curves are shown in Fig. 6.C.1 for an atherosclerotic plaque and a normal vessel wall. Using evaluation programs for a micro-VAX or a PC, the decay curves were evaluated based on the assumption that they consisted of up to three decay components [6C.5]. It can be seen in Fig. 6.C.1 that the decay time for plaque is longer than that for normal vessel wall. Using the results from the spectral recordings, the main difference between plaque and normal vessel was found to be an accumulation of collagen fibres and β-carothene in plaque tissue. The spectral shape of these was shown in Fig. 6.1.

6D. Tissue transillumination

A new application for lasers in medicine is tissue transillumination. The aim is to be able to detect cancer tumours by means of laser irradiation. One application could be to substitute X-rays with laser light when performing mammography. The technique is based on the characteristic absorption of light in the tumours due to the surrounding neovascularization. To be able to transilluminate the tissue, light with low absorption, i.e. red or near-infra-red light, must be used. The main problem is that in this wavelength region the dominating attenuation effect is not absorption but scattering. The

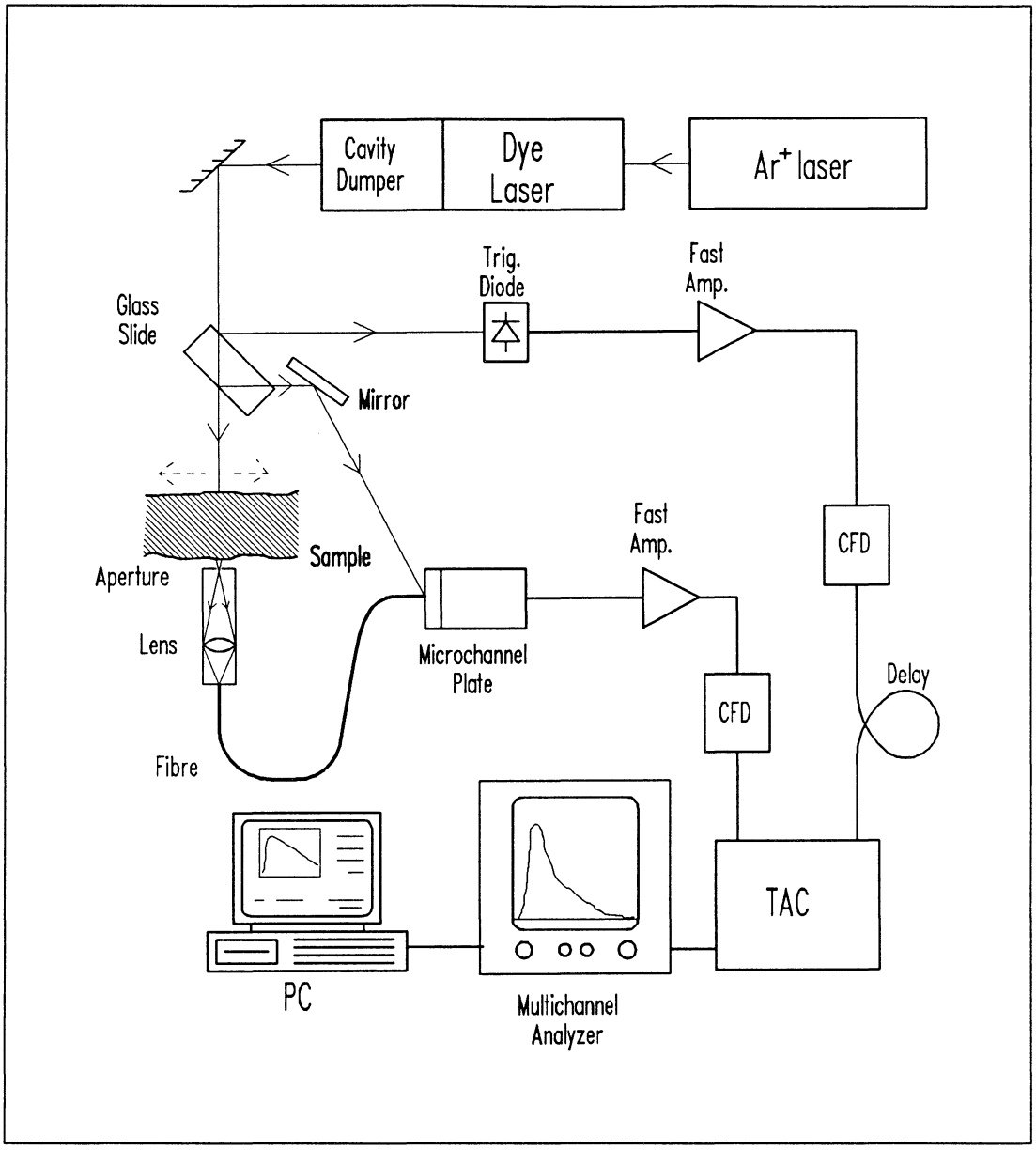

Fig. 6D.1. Experimental set-up for tissue transillumination.

scattering coefficient is of the order of 10 mm^{-1}, while the absorption coefficient is of the order of 0.1 mm^{-1}. The large scattering coefficient induces pronounced multiple scattering in the tissue, which leads to a decrease in contrast when tissue transillumination is performed. We have used a time-gating technique to reduce the effect of light scattering, thus enhancing the contrast [6D.1-3].

The time-gating technique is based on the concept that light which leaves the transilluminated tissue earlier has travelled a shorter and straighter path in the tissue than light exiting later. The "early" light is less scattered and thus contains more information on the spatial localization of the absorption. The experimental set-up is shown in Fig. 6D.1. The light source is a mode-locked Ar-ion laser

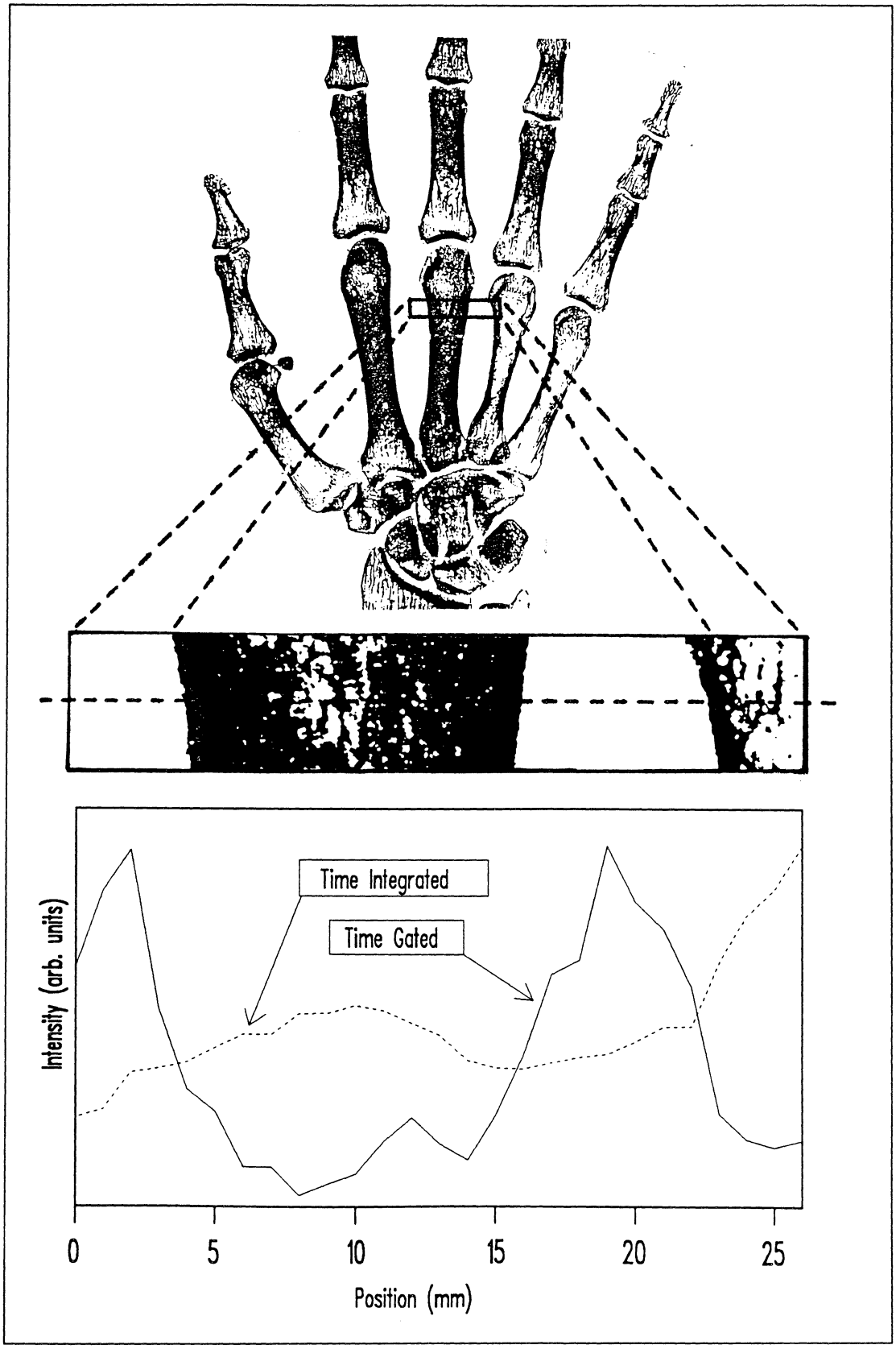

Fig. 6D.2. Scan across a human hand in vivo. *The solid curve is the light detected the first 80 ps and the dashed curve is the total amount of light detected.*

pumping a dye laser. The pulses are 6 ps wide. The laser pulses irradiate the tissue and the light is detected on the opposite side. To achieve time-resolved detection, delayed coincidence techniques are used. The output signal from the time-to-amplitude converter is fed to a multichannel analyser in which a histogram of the arrival time of the photons is formed, i.e. a temporal dispersion curve. To be able to compare different dispersion curves a small fraction of the incident light is led to the detector directly without passing the sample and this light thus creates a peak which acts as a time reference.

Figure 6D.2. shows a scan through a human hand *in vivo*. The scan was performed approximately 10 mm below the knuckle of the middle finger. Owing to considerable multiple scattering a significant fraction of the light exits more than 3 ns after the first transmitted light. The solid curve in the figure is the light detected during the first 80 ps of every dispersion curve. The dashed curve corresponds to the total amount of light detected at each point. As can be seen there in the figure there is a significant demarcation of the bones.

Since the scattering coefficient is of the order of 10 mm^{-1} the mean free path lengths for the photons is of the order of 100 μm and thus the probability of detecting light that has travelled across a tissue sample a few centimetres thick without being scattered at all is almost zero. The light detected with the time-gated technique is a weighted average absorption over a volume of the tissue. The difference is that with the time-gated technique this volume is much smaller and more localized.

Various models can be used to be able to simulate the photon propagation in tissue, e.g Monte Carlo simulations. In this model the path of a single photon in the tissue is tracked. The tissue is characterized by the scattering coefficient (μs), the absorption coefficient (μa) and the mean cosine of the scattering angle (g), which is a way of expressing the anisotropic scattering of the photons. By tracking a large number of photons it is possible to simulate the behaviour of the light in tissue.

Another model is based on the diffusion equation:

$$(1/c)\,\frac{\partial \Phi(\mathbf{r},t)}{\partial t} - D\nabla^2\Phi(\mathbf{r},t) + \mu a\Phi(\mathbf{r},t) = S(\mathbf{r},t)$$

where $\Phi(\mathbf{r},t)$ is the diffuse photon fluence rate, c is the speed of light in the tissue, D is the diffusion coefficient ($D=(3(\mu a+(1-g)\mu s))^{-1}$) and $S(\mathbf{r},t)$ is the photon source. The equation can be solved numerically using a computer and thus the light propagation can be calculated for different kinds of tissue. To verify the computer models and also simulate different kinds of tissue, phantoms with given optical properties can be made by mixing liquids with known scattering coefficients (Intralipid) and absorption coefficients (ink).

6E. Soft X-ray microscopy

The work described in this section was performed by Hans Hertz while he was with Dept. of Applied Physics, Stanford University. Work on high-resolution microscopy techniques is continued in Lund.

The development of novel methods for microscopy has had an immense impact on biological and medical sciences. So far biological studies have primarily been performed using the optical or the electron microscope. The latter yields very high resolution (nm) but requires extensive preparation of samples and operation in vacuum. For the observation of biological samples *in vivo*, optical microscopy is still the dominant tool, although attempts have been made to use, e.g., acoustic microscopy and atomic force microscopy. The major disadvantage of optical microscopy is that the resolution is limited by diffraction to approximately half of the wavelength of light. The aim of this project is to construct a microscope suitable for studies of biological objects *in vivo* with a higher resolution than is currently available.

Soft X-ray microscopy is currently emerging as a potential alternative for high resolution *in vivo* studies. By using soft X-rays in the 2.3-4.4 nm wavelength range the fundamental diffraction limit is reduced by two orders of magnitude. Furthermore, biological material exhibits a natural contrast in this wavelength range, due to differential absorption of proteins (i.e., carbon) and water (i.e., oxygen). Soft X-rays also penetrate tens of μm in water. Thus studies of unstained, unfixed and unsectioned cells in an aqueous environment are feasible.

To date, most soft X-ray microscopy experiments have been performed using synchrotron radiation as the soft X-ray source in combination with Fresnel zone diffractive optics. The inherent low efficiency of the optics in this wavelength regime requires a very strong source such as the synchrotron. However, the use of such large-scale fascilities automatically limits the usefulness of the instrument for the ordinary biologist. Therefore, Trail and Byer (Stanford University) attempted to build a table-top soft X-ray microscope by using more efficient multilayer optics in combination with a laser-produced plasma as the soft X-ray source. The microscope operates in the 13.5 nm range in a scanning mode. The optics focus the soft X-rays from the approximately 50 μm plasma onto the studied

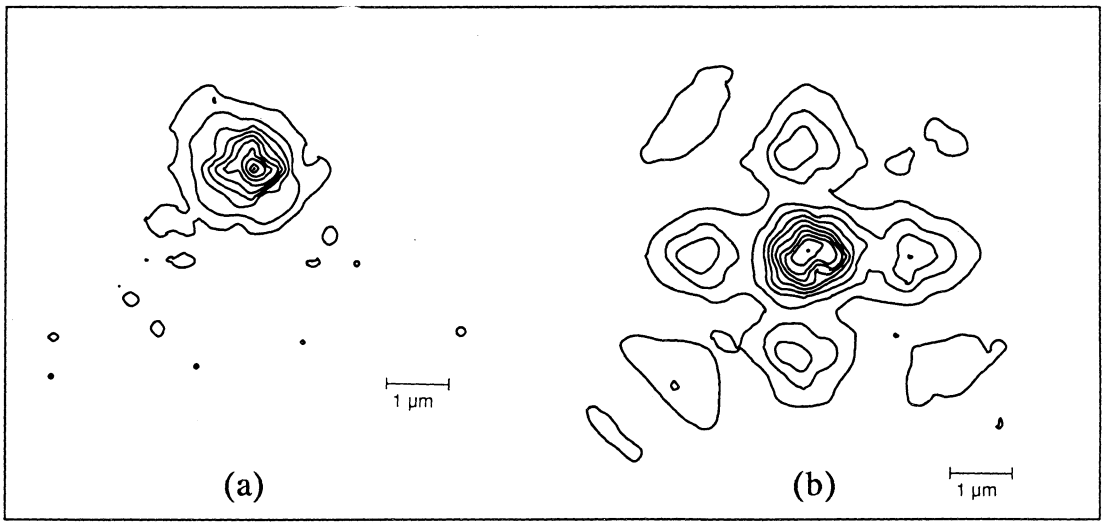

Fig. 6E.1. Intensity distribution at the focus of the Schwarzschild objective at (a) λ=13.5 nm and (b) λ=632.8 nm.

object with a demagnification of 1:100. The optics consist of an F1.7 Schwarzschild two-mirror objective coated with 40 layer pairs of Si and Mo for maximum reflection (approx. 50 %) at 13.5 nm.

The resolution of the Stanford scanning soft X-ray microscope is determined primarily by the size of the X-ray emitting plasma and the alignment of the two mirrors in the Schwarzschild objective. In order to optimize the latter, a tomographic method for the measurement of 2-D X-ray intensity distribution in the focal spot has been developed. The method utilizes a sharp edge that scans through the focal spot at different angles. The data obtained may after differentiation be used as input projections for tomographic reconstruction of the intensity distribution. Fig. 6E.1a depicts the reconstructed intensity distri-bution at $\lambda = 13.5$. The FWHM is 0.8 μm. Fig. 6E.1b shows the intensity distribution at $\lambda = 632.8$ nm. Note the strong diffraction side lobes due to the four-armed spider holding the central mirror in the Schwarzschild objective.

As mentioned above, the Stanford microscope operates at $\lambda = 13.5$ nm, thus making it unsuitable for biological studies. It is, however, an important demonstration that soft X-ray microscopy can be performed using a compact arrangement. We are currently working on the design of a $\lambda = 2.3$-4.4 nm compact microscope with a novel LPP source.

References

6.1. S. Andersson-Engels, J. Johansson, K. Svanberg and S. Svanberg Fluorescence Diagnosis and Photochemical Treatment of Diseased Tissue Using Lasers, Part I Analytical Chemistry **61**, 1367A, (1989), (Invited paper).

6.2. S. Andersson-Engels, J. Johansson, K. Svanberg and S. Svanberg Fluorescence Diagnosis and Photochemical Treatment of Diseased Tissue Using Lasers, Part II Analytical Chemistry **62**, 19A (1990), (Invited paper).

6.3. S. Svanberg: Medical Applications of Laser Spectroscopy, Physica Scripta **T26**, 90 (1989), (Invited paper).

6.4. S. Svanberg, Diagnostik och Behandling av Tumör- och Kärlsjukdomar Utnyttjande Laserteknik, Medicinska Riksstämman, Stockholm 1989, (Invited paper), (In Swedish).

6.5. S. Andersson-Engels, J. Johansson, K. Svanberg and S. Svanberg Laser-Induced Fluorescence in Medical Diagnostics, SPIE Vol. **1203**, 76 (1990), (Invited paper).

6.6. S. Andersson-Engels, J. Johansson, K. Svanberg and S. Svanberg Fluorescence Imaging and Point Measurements of Tissue: Applications to the Demarcation of Malignant Tumors and Atherosclerotic Lesions from Normal Tissue, Photochemistry and Photobiology **20** (1990), (Invited paper).

6.7. S. Andersson-Engels, J. Johansson, K. Svanberg and S. Svanberg proc. CLEO 1990, Anaheim, Calif.

6.8. S. Andersson-Engels, R. Berg, J. Johansson and S. Svanberg, Fluorescence and transillumination imaging for tissue diagnostics, proc. CLEO 1991

6.9. S. Svanberg, Laser Spectroscopy Applied to Energy, Environment and Medical Research, to appear in: **Photoionization Spectroscopy** *(Ed. N. Omenetto)* Plenum Press, to appear. (Invited paper).

6.10. K. Svanberg, The Interaction of Laser Light with Tissue - Fluorescence Diagnosis of Tumours and Atherosclerotic Lesions and Photochemical Treatment, Dissertation thesis, Lund University Hospital, Department of Internal Medicine and Department of Oncology (1989).

6.11. S. Andersson-Engels, Laser-Induced Fluorescence for Medical Diagnostics, Dissertation thesis, Lund Institute of Technology Lund Reports on Atomic Physics LRAP-108 (1989).

6.12. P. Hansson, Signal Processing Developments for a Mercury Lamp Based Filter Fluorescensor, Diploma Paper, Lund Institute of technology, Lund Reports on Atomic Physics LRAP-105, (1989).

6.13. N. Hildebrand, Prototype Temperature Control System For Combined Hyperthermia/PDT Treatment, Diploma Paper, Lund Institute of Technology, Lund Reports on Atomic Physics LRAP-115 (1990)

6A.1. S. Andersson-Engels, J. Ankerst, J. Johansson, K. Svanberg and S. Svanberg, Tumour Marking Properties of Different Haematoporphyrins and Tetrasulphonated Phthalocyanine - a Comparison, Lasers in Medical Science **4**, 115 (1989).

6A.2. S. Andersson-Engels, J. Ankerst, J. Johansson, K. Svanberg and S. Svanberg, Laser-Induced Fluorescence in Malignant and Normal Tissue of Rats Injected with Benzoporphyrin derivate, Submitted for publication

6A.3. S. Andersson-Engels, A. Brun, E. Kjellén, L.G. Salford, K. Svanberg and S. Svanberg, Laser-induced Fluorescence Detecting Brain Tumours in Rats, Lasers Med. Sci. **4**, 241 (1989).

6A.4. S. Andersson-Engels, R. Berg, J. Johansson, U. Stenram, K. Svanberg and S. Svanberg, Laser Spectroscopy in Medical Diagnostics, to appear in: **Photodynamic Therapy: Basic Principles and Clinical Aspects** *(Eds. Th. J. Dougherty and B.W. Hendersson)* (1990). (Invited book chapter).

6A.5. S. Andersson-Engels, J. Johansson and S. Svanberg, Multicolor Fluorescence Imaging System for Tissue Diagnostics, SPIE Vol. **1205** (1990).

6B.1. S. Andersson-Engels, Å. Elner, J. Johansson, S.-E. Karlsson, L.G. Salford, L.G. Strömblad, K. Svanberg and S. Svanberg, Clinical Recordings of Laser-Induced Fluorescence Spectra for Evaluation of Tumour Demarcation Feasibility in Selected Clinical Specialities, Lasers Med. Sci. (1989), (In press).

6B.2. S. Andersson-Engels, J. Ankerst, A. Brun, Å. Elner, A. Gustafson, J. Johansson, S.E. Karlsson, D. Killander, E. Kjellén, E. Lindstedt, S. Montán, L.G. Salford, B. Simonsson, U. Stenram, L.G. Strömblad, K. Svanberg and S. Svanberg, Laser Fluorescence Diagnostics of Tissue, Ber. Bunsen Gesellchaft **3**, 89 (1989), (Invited paper).

6C.1. S. Andersson-Engels, A. Gustafson, J. Johansson, U. Stenram, K. Svanberg and S. Svanberg, Laser-induced fluorescence used in localizing atherosclerotic lesions, Lasers Med. Sci. **4**, 171 (1989).

6C.2. S. Andersson-Engels, A. Gustafson, J. Johansson, U. Stenram, K. Svanberg and S. Svanberg, An investigation of possible fluorophores in human atherosclerotic plaque, submitted to Lasers in the Life Science

6C.3. S. Andersson-Engels, J. Johansson, U. Stenram, K. Svanberg and S. Svanberg, Time-Resolved Laser-Induced Fluorescence Spectroscopy for Enhanced Demarcation of Human Atherosclerotic Plaques, J. Photochem. Photobiol. B **4**, 363 (1990)

6C.4. S. Andersson-Engels, J. Johansson, U. Stenram, K. Svanberg and S. Svanberg, Malignant Tumor and Atherosclerotic Plaque Diagnosis Using Laser-Induced Fluorescence, IEEE J. Quant. Electr. November 1 (1990).

6C.5. S. Andersson-Engels, J. Johansson and S. Svanberg, The Use of Time-Resolved Fluorescence for Diagnosis of Atherosclerotic Plaque and Malignant Tumours, Spectrochimica Acta **46A**, 1203 (1990).

6D.1. R. Berg, Time-Resolved Studies of Light Propagation in Tissue, Diploma Paper, Lund Institute of Technology, Lund Reports on Atomic Physics LRAP-106, (1989).

6D.2. S. Andersson-Engels, R. Berg, O. Jarlman and S. Svanberg, Time-Resolved Transillumination for Medical Diagnostics, Opt. Lett. **15**, 1179-81 (1990)

6D.3. S. Andersson-Engels, R. Berg, J. Johansson, K. Svanberg and S. Svanberg, Medical Applications of Laser Spectroscopy, Invited paper to appear in Laser Spectroscopy IX, (Academic Press, New York 1989), (Invited paper).

6E.1. H.M. Hertz and R.L. Byer, Tomographic imaging of μm sized optical and soft X-ray beams, Opt. Lett. **15**, 396 (1990).

6E.2. H.M. Hertz and R.L. Byer, Tomographic imaging of focused soft X-ray beams, To appear in X-ray microscopy III, Springer series in optical sciences, Springer.

6E.3. H.M. Hertz and R.L. Byer, Tomographic determination of focused soft X-ray beams, Abstract for 3rd International Symposium on X-ray Microscopy, London, Sept. 1990 (summary of 6E.3).

7. INDUSTRIAL APPLICATIONS

Lennart Malmqvist, Willy Persson, Wilhelm Wendt

7A. Optical spectroscopy for process control

By combining modern optical techniques with spectroscopic know-how acquired in basic atomic spectroscopy we have, during the last few years, developed new methods for the control of smelt-metallurgical processes. The new technology has been applied to various processes, namely:
- the Pierce-Smith converter for copper
- the Noranda process for copper
- the HI-smelt process for direct reduction of iron ore
- the CLU converter for alloy steel
- the AOD converter for alloy steel
- the LD (LBE) converter for steel
- the EAF process for tool steel.

The degree of sophistication in the various studies varies from initial applicability tests to implementation of the technique in full-scale production units.

In the previous progress report we discussed in some detail the development related to the Pierce-Smith converter for copper. The first large-scale tests of the technology in the steel industry were performed at the CLU converter for alloy steel at Degerfors Järnverk.

The CLU process, which shows many similarities with the more commonly used AOD process, is based on the use of oxygen and superheated steam as refining agents. The process gases are introduced into the melt via tuyeres in the bottom of the converter (Fig. 7A.1). The oxygen and the steam react with the carbon in the bath to produce carbon monoxide and hydrogen. The hydrogen acts as a dilutant to the carbon monoxide which is necessary to limit chromium oxidation. The steam also acts as a coolant as the reaction between steam and carbon is strongly endothermic.

In order to maintain a low carbon monoxide partial pressure and thus counteract excessive chromium oxidation, the ratio between oxygen and steam is changed until pure steam is injected. When the carbon refining is completed the melt is purged with argon or a mixture of argon and nitrogen. Lime and ferrosilicon are added to reduce the chromium and manganese oxides in the slag.

The emission spectrum of the bright off-gas flame above the CLU converter has been recorded in the wavelength range 240-800 nm. A telescope focuses the light from the flame into an optical fibre about 30 m long. By using an optical fibre to transfer the light from the converter to the spectrometer it is possible to place the latter and the rest of the detection system in clean surroundings in the converter control room.

The observed spectrum is composed of a large number of discrete features emanating from atoms and molecules in the gas phase and a strong, continuous "background" radiated by the solid content of the flame. A survey of the atomic and molecular species identified in the

spectrum of the converter flame is given in Table I. During the first process step, i.e., with no steam content in the process gas, the discrete spectrum is of atomic origin. Strong emission is observed from iron and the alloying metals chromium, manganese and nickel and also from calcium and alkali metals. In addition, emission from impurities such as copper, lead and silver is observed.

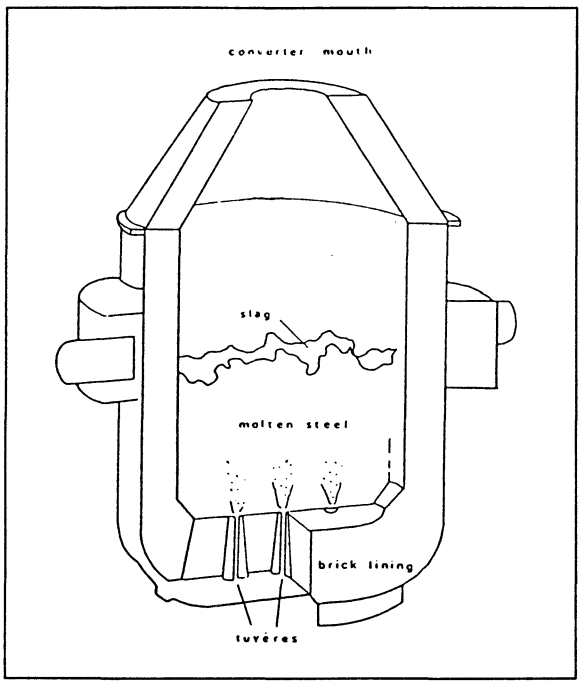

Fig. 7A.1. CLU converter

Element	Step 1	Step 2&3	Step 4
Fe	x	x	x
Cr	x	x	x
Mn	x	x	x
Ni	x	x	x
Ca		x	x
Ag	x	x	
Cu	x	x	x
Pb	x		
Na	x	x	x
K	x	x	x
Rb	x	x	x
CaF		x	
CaOH		x	
CuH		x	x
MnO		x	x
OH		x	
SiH		x	

Table I. Observed elements

During the subsequent process steps, i.e., when the steam content of the process gas is increased, a large number of molecular bands are observed in the spectrum. The more prominent bands stem from the OH radical and the CaOH and MnO molecules.

The intensity of the MnO spectrum decreases during the reduction step of the CLU process (Fig. 7A.2). At an MnO content in the slag below 1% the MnO spectrum is almost absent. Thus the MnO spectrum is well suited as an optical parameter for control of the MnO content in the slag during the reduction step. As there is a strong correlation between the MnO and the Cr_2O_3 contents in the slag, the progress of the reduction of Cr_2O_3 can be followed on-line by monitoring the intensity of MnO in the off-gas spectrum.

The spectroscopic technique can be applied to the reduction step with the view to determine the **optimum endpoint** of the reduction step and to facilitate an early prediction of the outcome of the reduction process by observing the **reduction rate.** The following are some of the benefits that can be obtained as a result of the on-line control of the reduction step:

- reduction in the time spent on the reduction step
  if the reduction is fast it can be interrupted before the preset time;
  if the reduction is slow measures can be taken before the preset

end of the step;
- reduction in consumption of inert gases
- reduction in consumption of furnace refractories
- reduction in consumption of alloying metals.

The technique has been implemented for permanent use at Degerfors Järnverk.

In the LD process for steelmaking an oxygen jet is blown at supersonic velocity from above onto the surface of the molten metal and the slag. The high velocity of the jet causes heavy turbulence and oxidation of

Fig. 7A.2. The decrease in the light emission from MnO during the reduction process

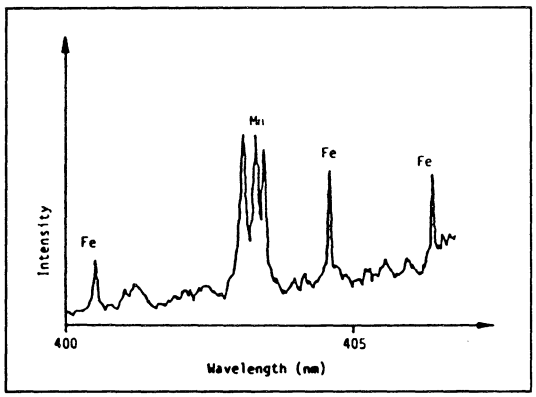

Fig. 7A.3. Emission spectrum in the 400 nm wavelength range

carbon in the melt takes place. In the LBE (Lance Bubbling Equilibrium) version of the LD process the melt is purged from below by an inert gas introduced via, e.g., porous plugs in the bottom of the converter, in addition to the oxygen jet from above. The blowing time is 15-20 minutes.

The spectroscopic studies at the SSAB Oxelösund converter (170 tons) have been performed during LBE as well as pure LD process modes. The light emission from two different locations has been analysed. In a first series of measurements a telescope focused light from the off-gas flame just above the converter mouth into an optical fibre, while in a second series of investigations an optical fibre inside the oxygen lance was used to collect light emitted by the mixture of gases,

liquid drops and particulate matter surrounding the lower end of the lance.

Qualitatively, the spectra observed during LD and LBE operation appear to be similar, though quantitatively there are distinct differences between them. Fig. 7A.3 shows the spectrum observed through the oxygen lance in the 400 nm wavelength range. The manganese triplet at 404 nm and some iron lines are present. To exemplify the potential of the technique to provide continuous on-line information the typical variation of the intensity of the manganese lines during a full process cycle is illustrated in Fig. 7A.4. The time resolution used is 15s. The intensity changes observed are not correlated with changes in, e.g., lance position or oxygen flow.

A number of optical parameters have been defined and their temporal

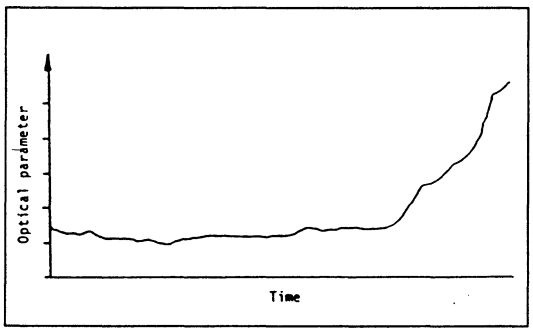

Fig.7A.4. Variation in Mn intensity during a heat

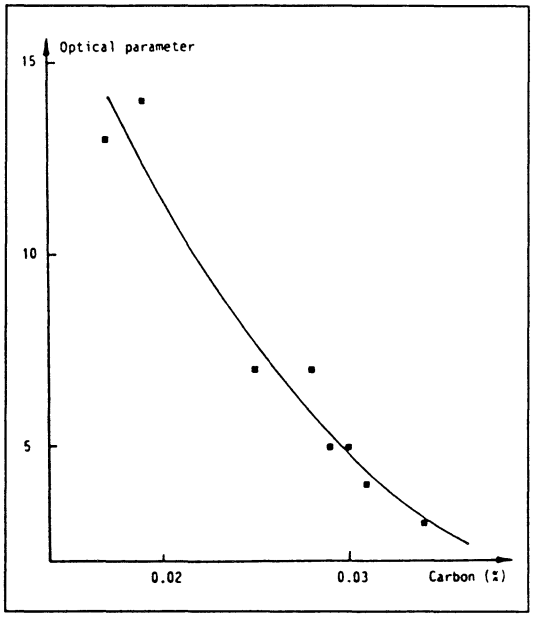

Fig.7A.5. Optical data vs carbon content in steel

behaviour has been studied over a large number of charges. The recorded material has been investigated for correlations between the endpoint values of the optical parameters and the composition of the metal and the slag, as determined by sampling and analysis. For instance, at low carbon contents there is a strong correlation between the carbon content in the melt and the observed spectrum (Fig. 7A.5). The results shown are from eight consecutive charges. Similarly, the optical spectrum seems to reflect the conditions in the slag, in particular, the basicity of the slag shows a good correlation with optical data.

7B. Mercury monitoring in natural and industrial processes

The Zeeman spectrometer developed for on-line monitoring of mercury emissions has been further improved as regards stability and ease of handling. It has been used for measurements in both natural and industrial processes.

In a collaboration with Department of Scientific and Industrial Research, New Zealand, the behaviour of mercury in geologically active

systems has been studied. Measurements have been performed at the Rotokawa geothermal fields in New Zealand and also on the active volcano island White Island off the coast of New Zealand. Extremely high mercury concentrations (1300 $\mu g/m^3$) were recorded at the upper end of deep boreholes at the Broadland power plant. In particular, interesting information has been obtained on the trapping of mercury in hydrothermal systems.

It has recently been pointed out (Nature **346,** 615 (1990)) that the increasing use of cremation could lead to problems in view of the thermal instability of mercury alloys and the volatility of the free metal. In a collaboration with the Department of Waste Management and Recovery at the Lund Institute of Technology we have performed real-time measurements of the mercury content in the off-gases during cremations. The study indicates that the mercury emission starts about ten minutes after the initiation of the cremation and lasts for about ten minutes (Fig. 7B.1). The mercury concentration varies between different cremations, the maximum concentration observed being 60 mg Hg/m^3. The effect of adding selenium during cremation to form the stable compound HgSe has been studied.

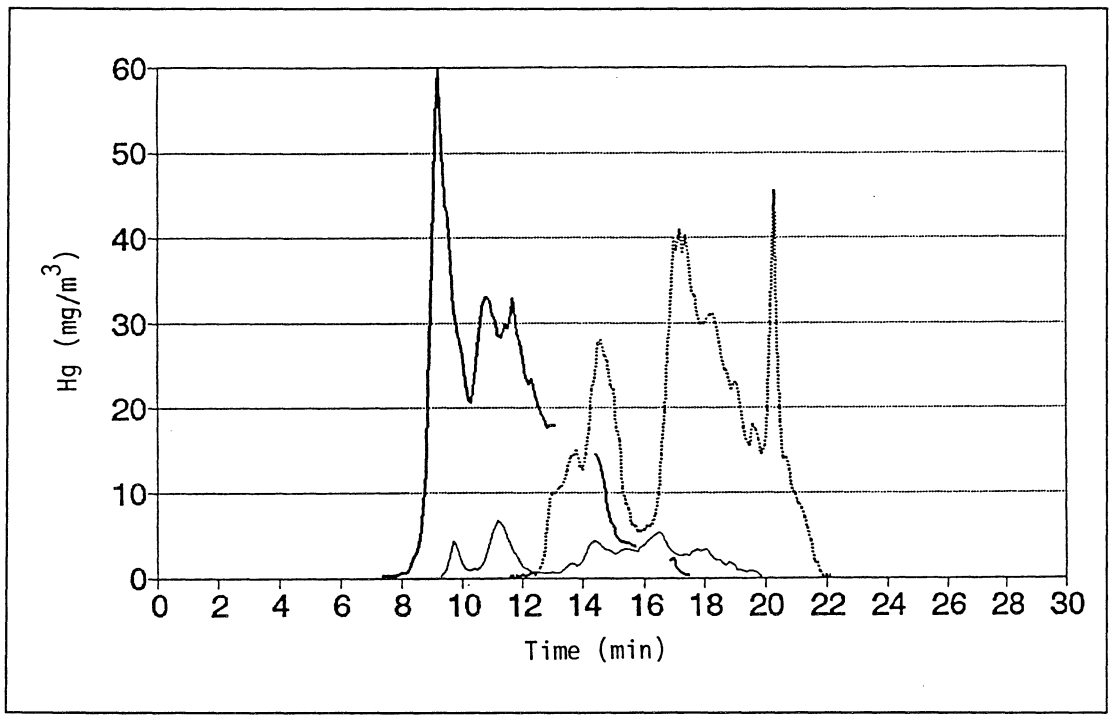

Fig. 7B.1. Mercury emission during three different cremations

7C. Trace element emissions from geothermal systems

In 1978 we started a program to try to find out if measurements of radon in the soil air close to the ground surface could give any useful information in prospecting for base metals. The results were very irregular and confusing. It was not possible to find stable radon levels, representative of the uranium content of different rock types, at any place tested. Often, high concentrations were found directly above known fractures and shear zones in the bedrock.

A radon transport model was proposed, assuming that radon was transported not only by ordinary diffusion but also by streaming; the radon atoms were assumed to be carried by a gas which moved slowly upwards through the bedrock towards the surface. If this upward transport system really existed, there was no reason not to suppose that other elements also could be transported by the same mechanism. Why should not metal particles from a concealed mineralization deep in the bedrock then be scavenged by passing bubbles and brought to the surface? If such matter carried by the bubbles could be collected and analysed it should reveal the existence and the position of the mineralization.

This transport hypothesis was the starting point for a series of investigations, aimed at the development of a new prospecting technique. The existence of a microflow of gas bubbles has been confirmed and also that gas bubbles passing through a mineralization can collect microscopic amounts of matter and lift it to the surface. The development is being pursued in a collaboration between the Departments of Nuclear Physics (Prof. K. Kristiansson) and Atomic Physics at the Lund Institute of Technology.

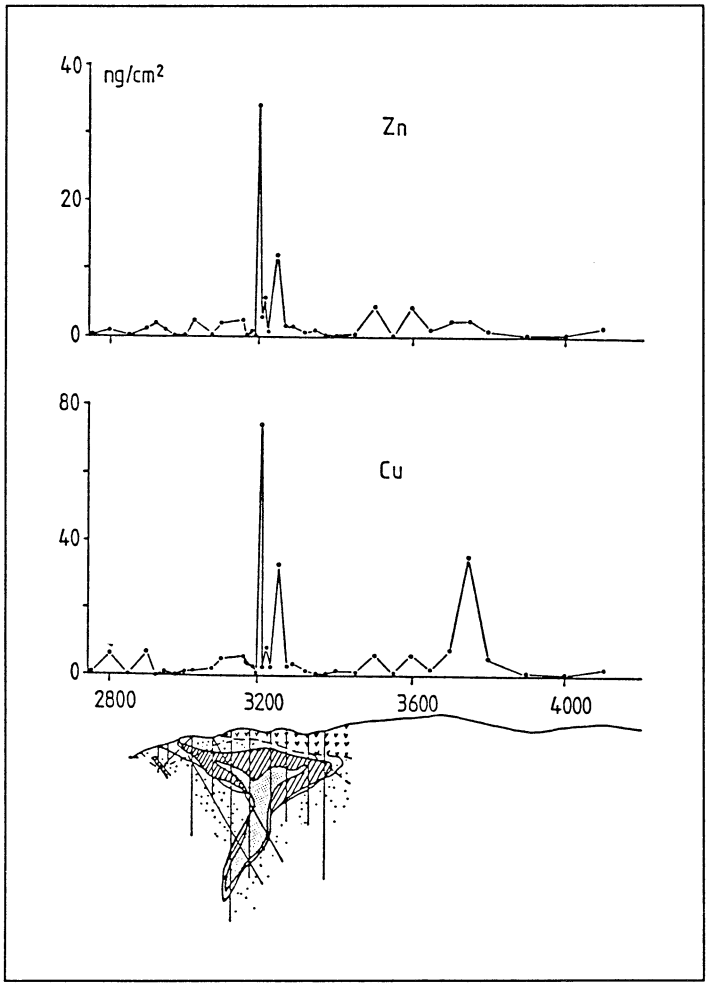

Fig. 7C.1. Zinc and copper emission from the Golden Cross deposit

During the last two years, special emphasis has been laid on the study of emissions from active geothermal areas and related ore-forming systems. Surprisingly high levels of, e.g., base metal emissions occur.

Epithermal gold prospects of various ages have been investigated,

ranging from ongoing ore formation to Precambrian deposits, in New Zealand, Japan, Finland and Sweden. Characteristic emission patterns have been found and a model for the appraisal of the gold potential has been formulated. In one case, namely at Golden Cross in New Zealand, the emission of gold has been recorded from a deposit covered by 75 m of younger volcanic rock (Fig. 7C.1).

Successful results have been obtained in the localization of deeply buried massive sulphide ore bodies. The project has proven the possibility of finding major ore bodies down to a depth of several hundred metres and in positions in which no other exploration technique can localize the deposits. Tests on different ore types and under different geological conditions have been made in Australia, Finland and Sweden.

On the technical side, analytical detection limits and technical evaluation and handling of the samples have been considerably improved. For some elements this improvement is of the order of a factor of 2 to 5, which is of great importance. The understanding of the geogas mechanism has also been improved. Special interest has been given to measurements on deep tectonic structures in Sweden, which have provided interesting geological information as well as improved understanding of the geogas mechanism.

References

7A.1. M. Aldén, W. Persson and W. Wendt, Swedish Patent SE 8703233-0.

7A.2. M. Aldén, W. Persson and W. Wendt, Australian Patent 593999.

7A.3. W. Persson, W. Wendt and H. Bertheussen, On-line Process Control in Steelmaking, JOM **41**, 17 (1989).

7A.4. W. Persson, On-line processkontroll i metallurgisk industri, Atom- och Molekylfysik i tillämpningar, Linköping, Nov. 16, 1989.

7A.5. W. Persson, W. Wendt and L. Malmqvist, Optical Spectroscopy for Control of Pyrometallurgical Processes, 22nd EGAS, Uppsala, July 10-13, 1990.

7A.6. W. Wendt and W. Persson, Optical Spectroscopy for the Characterization of an Alloy Steel Converting Process, Appl. Spectrosc. **44**, 987 (1990).

7A.7. W. Persson, W. Wendt and L. Malmqvist, Light Works for Process Control, Proceedings of the 6th International Iron and Steel Conference, Nagoya, Oct. 22-26, 1990.

7B.1. W. Hogland and W. Wendt, Mätningar av kvicksilverutsläpp från krematoriet på Norra kyrkogården i Lund, Internal Report 1990.

7C.1. B.W. Christenson, L. Malmqvist, K. Kristiansson and J.B. Finlayson, Soilgas trace metal transport - the geogas method applied to N Z epithermal and geothermal environments, Proceedings of Auckland University Geothermal Workshop, Vol. 10, 1989.

7C.2. L. Malmqvist, M. Isaksson and K. Kristiansson, Radon Migration through Soil and Bedrock, Geoexploration **26**, 135 (1989).

7C.3. K. Kristiansson, L. Malmqvist and W. Persson, Geogas Prospecting: A New Tool in the Search for Concealed Mineralizations, Endeavour **14**, 28 (1990).

TEACHING PROGRAM

1. UNDERGRADUATE TEACHING 1989-1990

Elvir Andersson, Jonas Bengtsson, Håkan Bergström, Stig Borgström, Jörgen Carlsson, Hans Hertz, Jonas Johansson, Bodil Jönsson, Gilbert Jönsson, Göran Jönsson, Per Jönsson, Rune Kullberg, Jörgen Larsson, Hans Lundberg, Göran Malmenryd, Nina Reistad, Anders Persson, Sven-Göran Pettersson, Rolf Petersson, Lennart Sturesson, Sune Svanberg + about 25 junior assistants.

At the Department of Physics, basic physics teaching is provided for the Schools of Engineering Physics (F), Electrical Engineering (E), Computer Science and Technology (D), Mechanical Engineering (M), Civil Engineering (V) and Chemical Engineering (K). Furthermore, specialised courses in atomic physics, laser physics, optics and spectroscopy are given.

The basic courses are, with one exception, given for students in their first year while the other more specialised courses are given in later years. It is also possible for students from other schools (mostly E, M and K) to follow these more specialised courses.

The courses contain both theory (lectures and problem solving) and laboratory practicals. The number of hours devoted to experimental work is, as a rule, about the same as the number of hours used for theoretical education (See Fig. 1). During experimental training on basic courses the students generally work in groups of two, and each supervisor teaches four such groups, i.e. 8 students at a time. For the specialised courses each supervisor can teach only 4 or 6 students at a time since the amount of equipment is limited, for economical reasons, to two sets. In the course on atomic and molecular spectroscopy, research equipment is used by the students in their experimental work.

A brief survey of the courses available and the attendance is given in the table on page 114. In the first column the name of the course is given, in the second the school and year, in the third the number of students, in the fourth the number of teaching hours (not including experimental instruction) and in the fifth, the number of hours of experimental work (the figures in parentheses give the number of students in each experimental group).

The greater part of the education for F1, E, D, M, V and BI is in the form of lectures to groups of 24 students. All other education is provided in the form of lectures and exercises in problem solving. The total number of teaching hours is about 6000. The teaching is performed by one professor, six senior lecturers, one junior lecturer, eight teaching assistants and about twenty-five assistants.

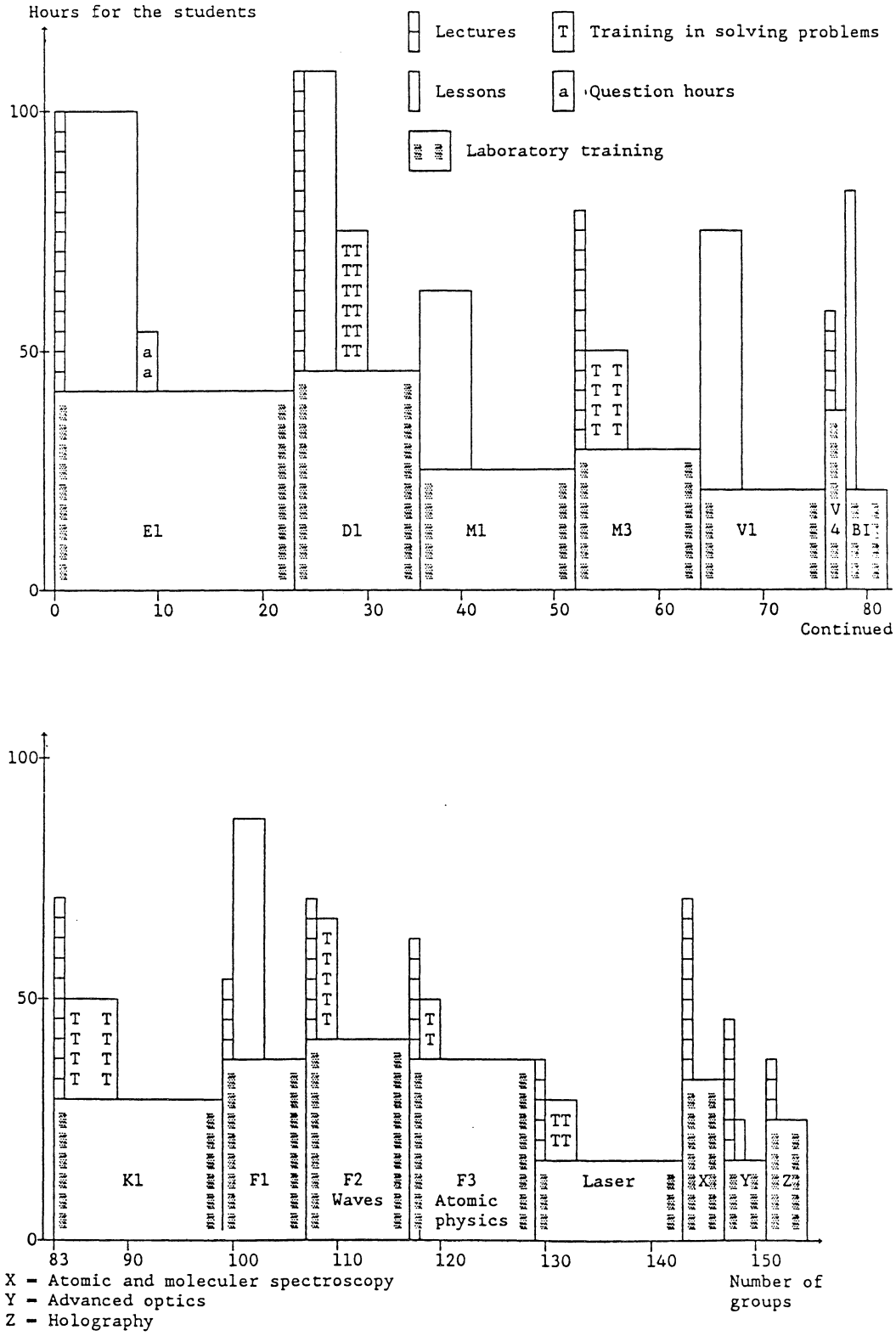

Fig. 1. Courses given by the Department of Physics. In the vertical direction the number of hours devoted to each student is given. In the horizontal direction the number of groups is specified. This means that the enclosed area is proportional to the number of teaching hours.

Table *Courses given by the Department of Physics*

		No. of students	Hours theory	Hours lab.
Physics course, E	E1	186	118	42(8)
Physics course, D	D1	90	132	46(8)
Physics course, M	M1	139	34	28(8)
" " , M	M3	92	70	28(8)
Physics basic course, V	V1	96	52	18(8)
Physics specialised course, V	V4	20	20	36(8)
Physics course, K	K1	128	38	28(8)
Physics course, BI	BI1	30	58	18(8)
Introductory course	F1	67	40	36(8)
Waves	F2	66	50	40(6)
Atomic Physics	F3	57	34	35(4)
Laser Physics	F4,E3,M3,D3	56	32	16(4)
Optical Techniques	F4	20	36	16(4)
Atomic and molecular spectroscopy	F3,F4	20	36	30(4)
Holography		16	10	15(10)
History of Science	F,E,M,V,A,K,D	100	35	-

2. BASIC COURSES

For the School of Engineering Physics the basic course *Physics, Extended course* is given. This consists of three parts, Introductory course, Waves and Atomic Physics, coupled with laboratory practicals of 36, 40 and 35 hours, respectively. *The Introductory Course* comprises experimental methods, gas physics, thermodynamics and geometrical optics. *The Wave physics course* makes the students well acquainted with phenomena in physical optics and acoustics. *Atomic physics* provides the students with basic knowledge on the structure of atoms and molecules and their properties. The course also gives some orientation in spectroscopic methods in different energy ranges.

For the Schools of Electrical Engineering and Computer Science and Technology the basic course *Physics course for E and D* is given. This comprises gas physics, thermodynamics, waves and modern physics combined with 42 (E) or 46 (D) hours of laboratory practicals.

For the School of Civil Engineering (course V1) and Fire Defence Engineering (course BI1) the basic courses *Physics basic course for V* and *basic course for BI* are given. These consist of gas physics with ther-

modynamics and fundamental electricity combined with 18 hours of laboratory practicals. For the course V4 the specialised course *Physics continued course* is given, which is directed towards physical measuring techniques with 36 hours of laboratory practicals. This course is attended by about 20 students.

For the School of Chemical Engineering the basic course *Physics course for K* is given. This consists of electricity, wave physics, geometrical optics and nuclear physics combined with 28 hours of laboratory practicals.

The course on the *History of Science* is available to all sections of the Institute of Technology. This course, given in collaboration with teachers from the Faculty of Humanities, illuminates the impact of science in relation to the development of society.

3. SPECIALIZED COURSES

The specialised course *Laser Physics* is designed to provide the students with knowledge concerning the physical principles of laser physics and to teach them about the most general types of lasers and their most important fields of application. In laboratory practicals the students learn to make simple adjustments and measurements with different types of lasers. This year, the course will be followed by about 60 students from the Schools of Engineering Physics (F), Electrical Engineering (E), Mechanical Engineering (M) and Computer Science and Technology (D).

The specialised course *Atomic and Molecular Spectroscopy* is intended to provide knowledge about modern atomic and molecular spectroscopy with special emphasis on technical applications. About 20 students follow this course. Together with the laser physics course this course forms the natural introduction to post-graduate studies at the Department.

A course in *Holography* is also available to those interested in photography, imaging techniques and optical measurements. The course starts with lectures in ray optics and wave optics and, together with laboratory practicals, the fundamentals of holography and related topics are discussed and different types of holograms are made.

A specialised course in *Optical Techniques* has been established at the Department. This course, emphasising Fourier optics, interferometry, fibre-optics, holography and phase-conjugation techniques was given for the first time in the autumn of 1985.